

General Disclaimer

One or more of the Following Statements may affect this Document

- This document has been reproduced from the best copy furnished by the organizational source. It is being released in the interest of making available as much information as possible.
- This document may contain data, which exceeds the sheet parameters. It was furnished in this condition by the organizational source and is the best copy available.
- This document may contain tone-on-tone or color graphs, charts and/or pictures, which have been reproduced in black and white.
- This document is paginated as submitted by the original source.
- Portions of this document are not fully legible due to the historical nature of some of the material. However, it is the best reproduction available from the original submission.

NASA Contractor Report 168008

COMPARISON OF MODERN ICING CLOUD INSTRUMENTS

(NASA-CR-168008) COMPARISON OF MODERN ICING
CLOUD INSTRUMENTS Final Report (Meteorology
Research, Inc.) 133 p HC A07/MF A01

N83-18720

CSCD 01D

Unclas
G3/06 02807

D. M. Takeuchi, L. J. Jahnsen, S. M. Callander, and M. C. Humbert

Meteorology Research, Inc.

Altadena, California 91001



January 1983

Prepared for

NATIONAL AERONAUTICS AND SPACE ADMINISTRATION
Lewis Research Center

Under Contract NAS3-22760

CONTENTS

	<u>Page</u>
1. INTRODUCTION	1
2. IRT INSTRUMENTATION AND DESCRIPTIONS	3
Axially Scattering Spectrometer Probe (AASSO-100) and Forward Scattering Spectrometer Probe (FSSP-100)	6
Optical Array Cloud Particle Spectrometer Probe (OAP-200X)	11
Leigh Ice Detector Set	14
Johnson-Williams (J-W) Liquid Water Content Indicator	16
Rosemount Model 102 Total Temperature Sensor	17
Dew Point Hygrometers (E.G. & G. Model 137-C3 and General Eastern Model 1011)	18
3. DATA SET DESCRIPTION	20
Data Recovery Percentages	20
Tunnel Settings	24
Data Selection	25
Data Reduction Procedures	28
Data Volume Description	32
4. RESULTS AND DISCUSSION	37
IRT Cloud Repeatability	37
IRT Cloud Uniformity	43
Effect of Steam Tube Wraps	49
Effects of Temperature and Velocity on Probe Performance	53
Instrument Intercomparisons	55
Drop Size Distribution Form	80
5. CONCLUSIONS	104
6. RECOMMENDATIONS	106
7. REFERENCES	107
APPENDIX A TEST POINT SUMMARY	108

1. INTRODUCTION

During January 1981 the U.S. Air Force (USAF) Flight Test Center (AFFTC) at Edwards Air Force Base, California, conducted a test program at the NASA Lewis Research Center (LeRC) Icing Research Tunnel (IRT) aimed at documenting and improving the performance of the USAF A-10 inlet Icing Protection System. While inlet testing was the primary objective, the testing period and schedule provided a unique opportunity for additional icing instrumentation studies. These additional studies were focused on comparisons between modern state-of-the-art droplet/icing measurement systems and those systems and techniques already in use for some years. In addition, documentation and investigation of the characteristics of the IRT itself could be accomplished with both types of systems.

These studies were beyond the scope of interest to the USAF A-10 group. However, they were of vital interest to NASA, FAA, the U.S. Army and Air Force and indeed to the entire icing and cloud physics community. In August 1981, MRI was awarded a contract (NAS3-22760) from NASA LeRC to perform the analyses of the data obtained during USAF test program in January. The primary objectives of the contract were to provide the following:

- Descriptions of the "modern" icing instrumentation installed in the IRT.
- Data listings for each tunnel test condition.
- Analyses of the data including information investigations into:
 1. The repeatability of the tunnel and tunnel uniformity,
 2. Instrument comparisons with other instruments and comparison of tunnel droplet spectra with natural cloud conditions, and
 3. Velocity effects on spectrometers and temperature effects on accretion instruments.

This final report serves to accommodate these objectives in fulfillment of the report requirements of the contract. Section 2 presents descriptions of the instruments in addition to the instrumentation setup in the IRT. Documentation of the data reduction procedures for the data listings which are presented in a separate data volume is given in Section 3. Data recovery information and problems encountered during testing are also discussed. The results of the analyses are presented in Section 4 with conclusions and recommendations following in Section 5.

2. IRT INSTRUMENTATION AND DESCRIPTIONS

Figure 2-1 presents a schematic of the instrumented IRT. In addition to the instruments for recording of tunnel air speed, air temperature, and dew point temperature, the test section was equipped with a specially fabricated test stand for mounting of the cloud droplet instrumentation. The test stand was equipped with a Johnson and Williams hot wire device and a Leigh ice detection meter and was capable of mounting two of the Particle Measurement Systems, Inc. (PMS) cloud particle spectrometers as shown in Figure 2-2. The PMS probes tested included four Axially Scattering Spectrometer Probes (ASSP), two Forward Scattering Spectrometer Probes (FSSP), and two Cloud Particle Spectrometers (CPS). Probes belong to the following organizations were used in the IRT:

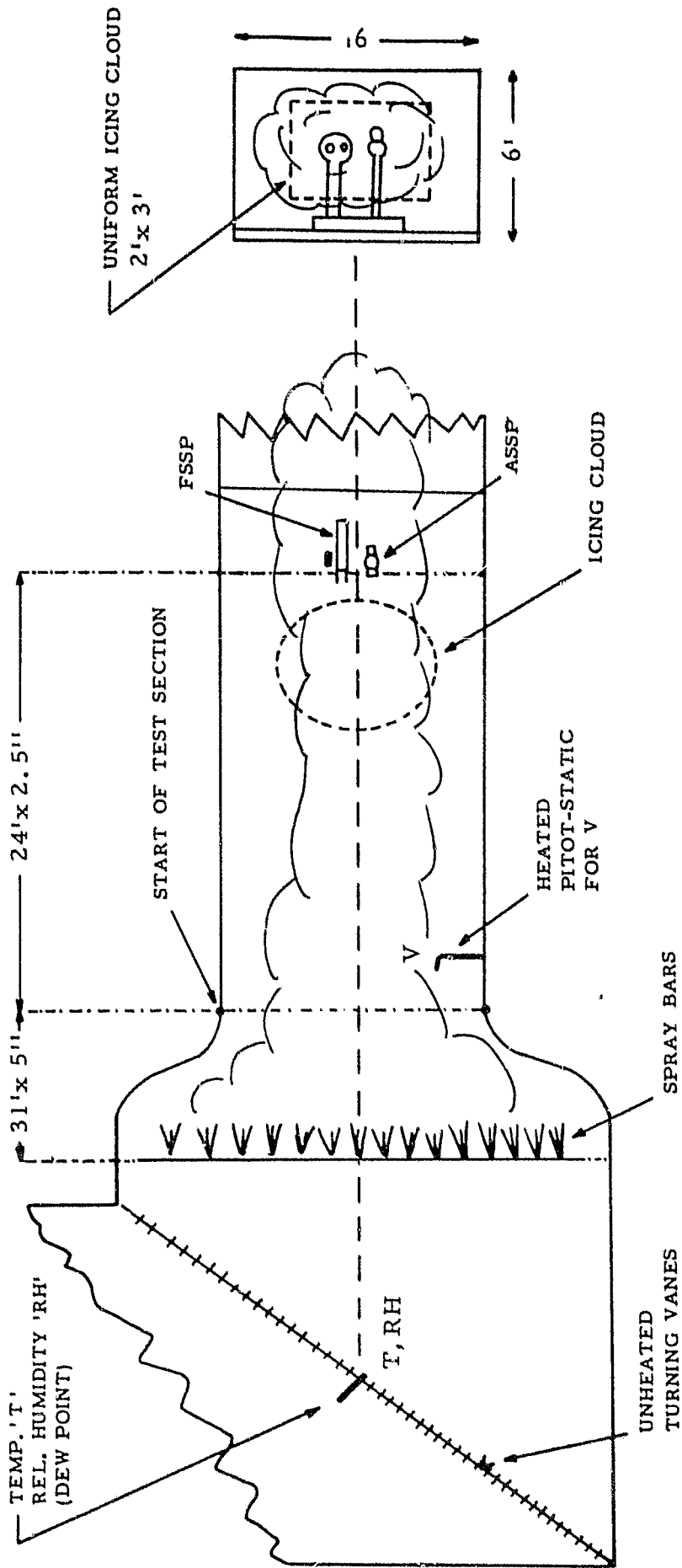
- U.S. Air Force Geophysical Laboratory (AFGL).
- Meteorology Research, Inc. (MRI).
- Particle Measurement Systems, Inc. (PMS) (leased by MRI).
- Leigh Instruments, Limited.

The FSSP's and CPS's were interchanged at the location shown for the CPS in Figure 2-2. The ASSP's were always mounted as shown in the figure. Data were recorded onto digital tape at a rate of once per second.

Since the heaters provided with the PMS probes were not able to de-ice the probes adequately at the cold temperatures, the PMS probes were wrapped with steam tubes. Special tests revealed that the steam tubes did not alter the air flow through the probes' sample tubes. Also, for given test conditions, near identical estimates of the cloud properties were determined from the measurements with and without the steam tube wrappings as will be discussed in a later section.

The following subsections present descriptions of the probes installed on the test stand.

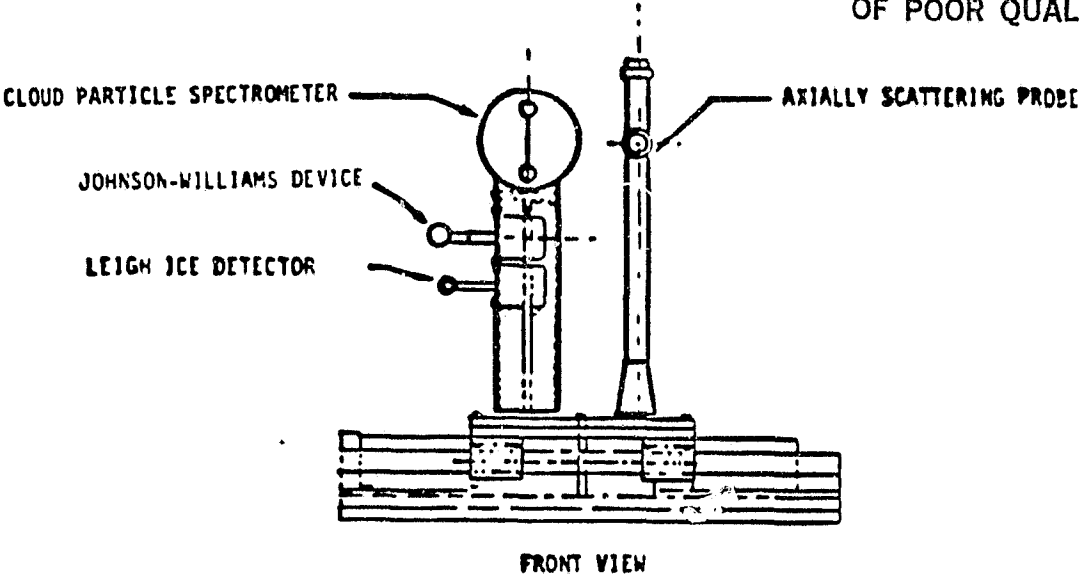
ORIGINAL PAGE IS
OF POOR QUALITY



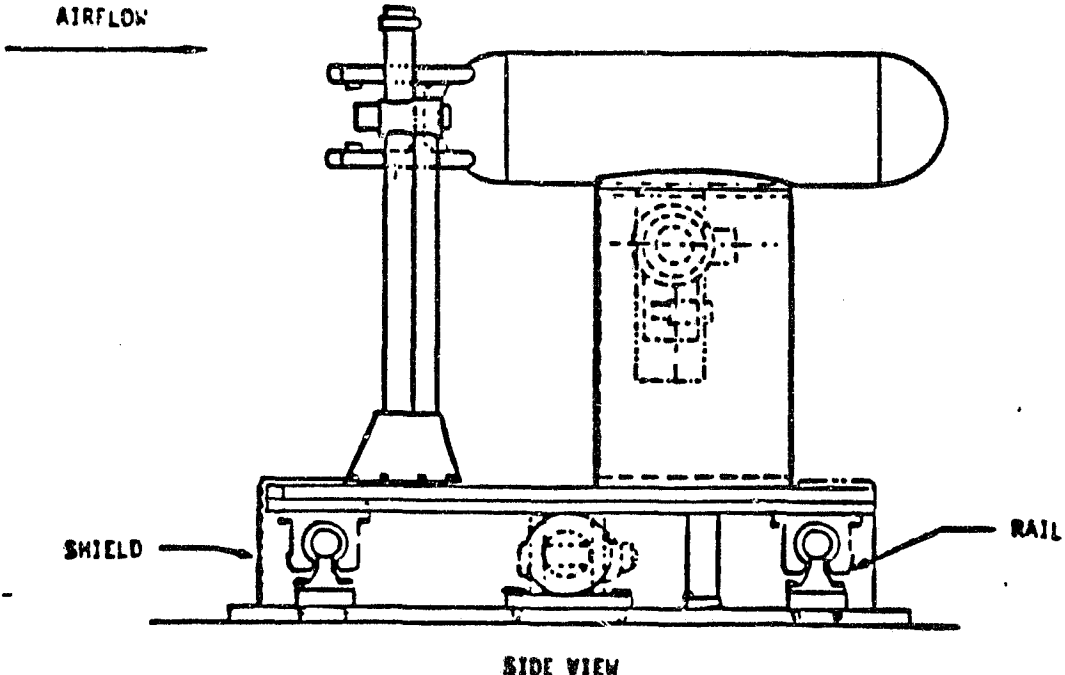
81/214

Figure 2-1. TOP VIEW OF IRT SHOWING INSTRUMENT LOCATIONS

ORIGINAL PAGE IS
OF POOR QUALITY



79-515a



79-515b

Figure 2-2. INSTRUMENTED TEST STAND ASSEMBLY

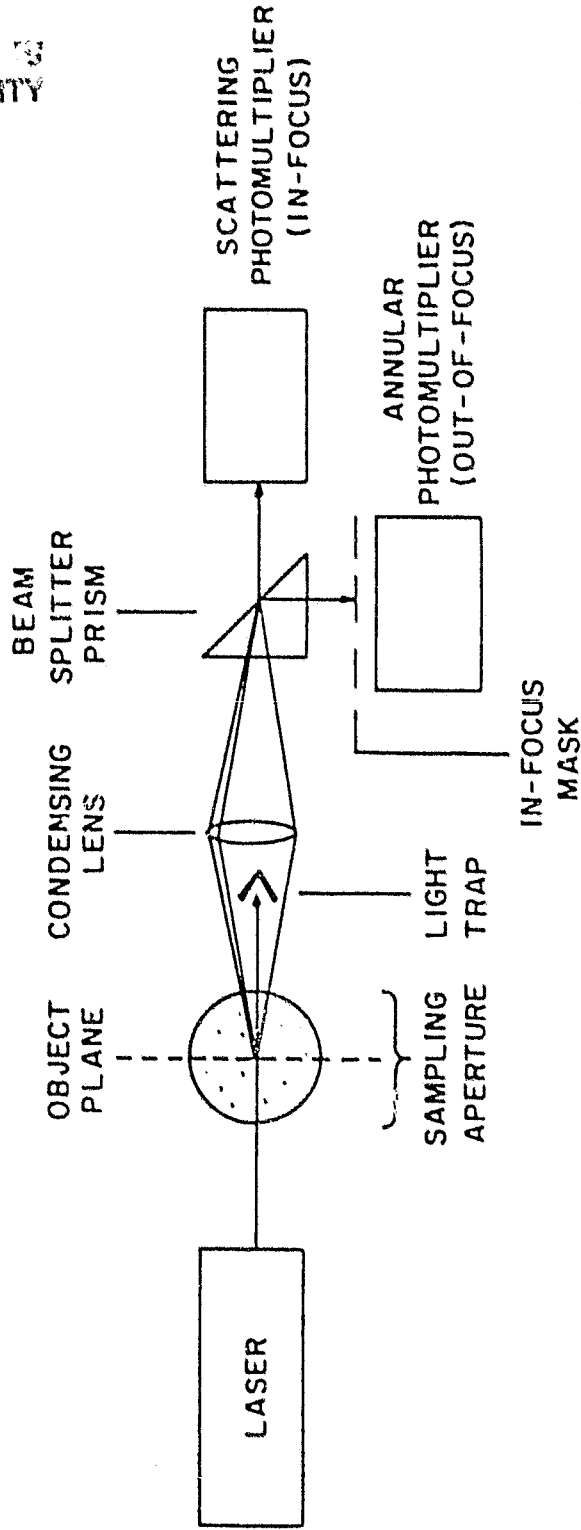
2.1 Axially Scattering Spectrometer Probe (ASSP-100) and Forward Scattering Spectrometer Probe (FSSP-100)

The Particle Measurement Systems, Inc. (PMS) ASSP-100 is a droplet sizing device developed in the early 1970's. Droplet sizes are estimated on a particle-by-particle basis from measurements of the amount of forward scattered light as droplets pass through a focused laser beam. Figure 2-3 presents a block diagram of the optical system. Particles intercepting the laser beam scatter light through the optics. The scattered light is received at a beam-splitting prism where one half of the beam is deflected 90° and focused onto a detector (annular) which is masked at the center while the other half is focused onto an unmasked (or signal) detector.

Since the intensity of light scattered from a given size droplet is a function of its position within the focused beam, it is necessary to establish if the particle is contained within the desired depth-of-field and if the particle passes through the central part of the beam where the intensity is uniform. The depth-of-field is defined as that region along the beam axis where the signal received by the unmasked detector exceeds that of the masked detector by a factor of 2.5. A droplet is rejected if the pulse pair comparisons indicate a smaller value. The transient time (or pulse width) of the particle as it passes through the laser beam is analyzed to determine its chordal transect through the beam. Particle transit times are measured and compared with a stored running mean of approximately 1,000 accepted pulse widths. Pulses exhibiting transient times greater than the average are accepted. This edge effect discrimination is performed to eliminate undersizing of particles as they pass through the outer and weaker intensity regions of the beam and is based upon the decrease in chordal transit distances from the center through the edge of the beam.

For a particle accepted as being within the depth-of-field and in the central region of the beam, the peak intensity is measured by a pulse height analyzer to determine particle size. Since Mie theory for spherical particles indicates that scattering intensity is near proportional to the square of particle size, the signal from the pulse height analyzer is gated to provide a count in one of 15 equally spaced size channels by a series of voltage comparators having square weighted voltage thresholds.

ASSP
(AXIAL SCATTERING SPECTROMETER PROBE)



81/221

Figure 2-3. AXIAL SCATTERING SPECTROMETER PROBE OPTICAL SYSTEM DIAGRAM

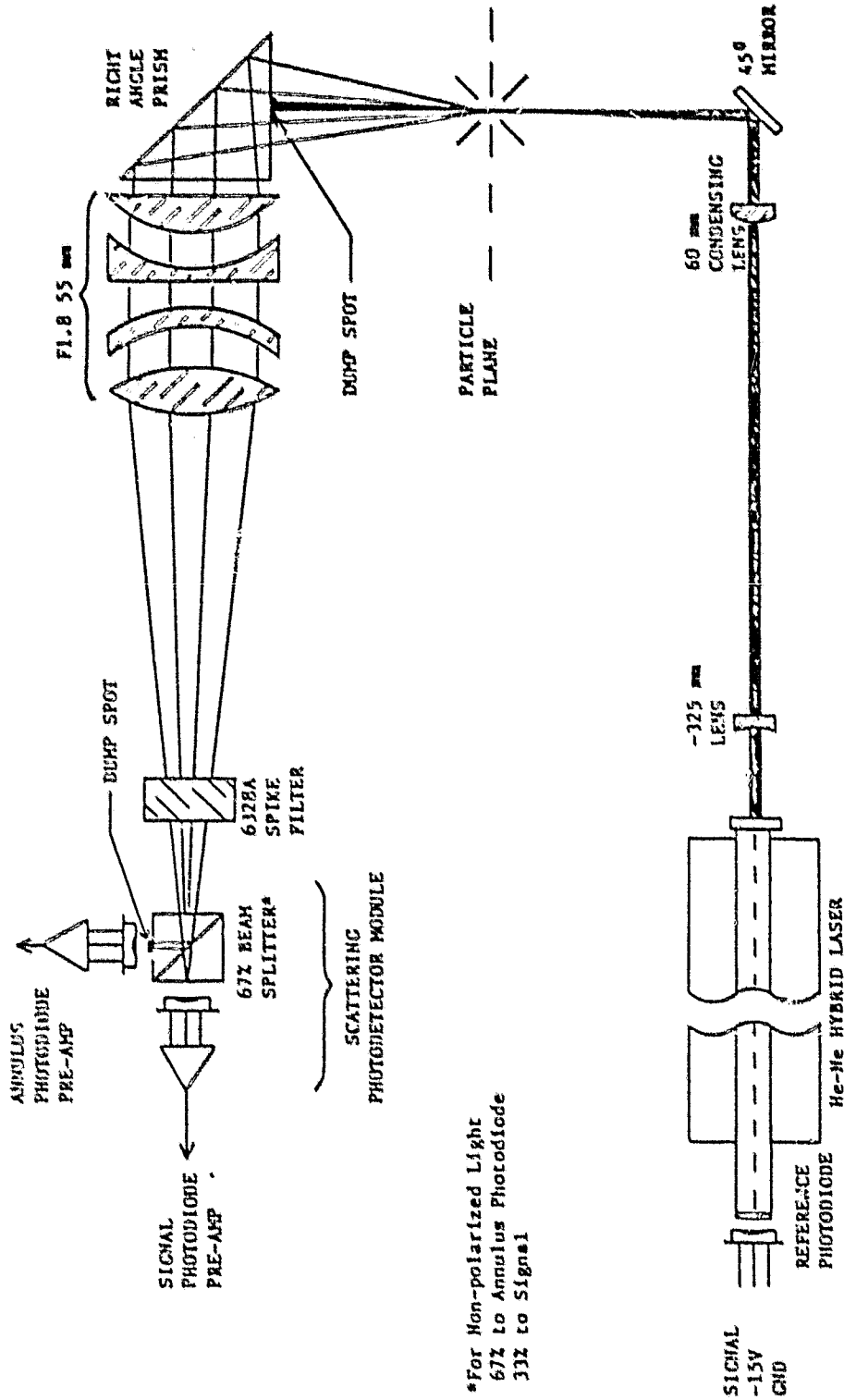
Each particle sized and counted by the ASSP causes a latch to be set and inhibits the measurement of other particles for a period of 4 μ s. This finite time period insures sufficient time for quantification and transfer of information without interference from subsequent particles entering the sampling aperture.

The FSSP was designed and built as an improved successor to the ASSP. The modifications included refinements to its optical and electronic subsystems rather than in basic operating principles. As compared to the ASSP, the FSSP analyzes light scattered at wider angles of 4-18° as opposed to the 7-16° in the ASSP. The FSSP also generally has a shallower depth of field which results in sharper size discrimination and a smaller sampling area. The physical construction of the FSSP is also different as shown in the block diagram of the optical system in Figure 2-4.

Both probes are capable of sizing particles from 0.5 to 47 microns diameter in four size ranges (2-47 μ m, 2-32 μ m, 1-16 μ m, and 0.5-8 μ m) and resolves them into 15 equally spaced size intervals. They are also normally designed for airborne sampling velocities of 20 to 125 m/sec (~250 kts) and can be modified for use at lower or higher velocities. For measurements conducted at higher speeds, pulse height distortion leads to under estimation of particle size. The characteristics of the ASSP and FSSP are summarized in Tables 2-1 and 2-2. As an option, the total number of pulses or strobes sensed through the beam width and within the depth-of-field can be recorded. Hence, an acceptance ratio (or efficiency) based on the total particle counts in the 15 size channels and total strobes provides a more accurate value for the effective beam diameter. Early versions of the ASSP did not have this velocity reject feature and, therefore, assumed an effective diameter of approximately one half the beam width.

Another option on probe activity serves to provide information on possible errors in the counting efficiency of the probes. Since particles which are sensed as entering the beam (outside as well as within the depth of field) require finite time periods in the acceptance/rejection logic, they are also counted and processed to provide outputs on probe activity from which the "busyness" of the probe is inferred. High (as opposed to low) activity indicates that a large (small) portion of the particles entering within the effective sampling area (effective beam width x depth of field)

ORIGINAL PAGE IS
OF POOR QUALITY



81/220

Figure 2-4. FORWARD SCATTERING SPECTROMETER PROBE OPTICAL SYSTEM DIAGRAM

Table 2-1

AXIALLY SCATTERING SPECTROMETER PROBE CHARACTERISTICS

Number of size channels	15
Size range	3 to 45 microns
Size resolution	3 microns
Maximum particle rate	100 k Hz
Coincidence errors	Less than 10% with concentrations of 10^3 cm^{-3}
Maximum particle velocity	125 m/sec
Power	115v, 60 Hz, 1.0 amp plus required de-ice power (300 W using 28 v heaters)
Environmental	Temperature: -40°C to $+40^\circ\text{C}$ Altitude: 0 to 40,000 ft msl
Mechanical	Probe: 24-inch long airfoil
Weight	Probe: approximately 6 lb

Table 2-2

FORWARD SCATTERING SPECTROMETER PROBE CHARACTERISTICS

Number of size channels	15
Size range	3 to 45 microns
Size resolution	3 microns
Maximum particle rate	100 k Hz
Coincidence errors	Less than 10% with concentrations of 10^3 cm^{-3}
Maximum particle velocity	125 m sec ⁻¹
Power	115v, 60 Hz, 1.0 a plus required de-ice power (300 W using 28 v heaters)
Environmental	Temperature: -40°C to $+40^\circ\text{C}$ Altitude: 0 to 40,000 ft msl
Mechanical	Probe: 34-inch long, 7-inch diameter cylinder
Weight	Probe: approximately 45 lb

would not be processed since a large (small) fraction of a given time period is lost in rejecting particles. Laboratory experiments at PMS show that the counting efficiency (probe count/true count) decreases exponentially from a value of 1 starting at an activity of about 40 percent to approximately 0.6 as activity increases to 80 percent. Hence bulk parameters such as liquid water content (LWC) and total number concentrations are usually underestimated at the higher activities. This type of coincidence error is thought not to affect the resulting size distribution shape or form from which medium volume diameter (MVD) is estimated since it applies equally to all particles. Although PMS provides empirical correction factors from their laboratory tests, it is felt that since scattering intensity is dependent upon particle size, the corrections would not necessarily apply to clouds having different particle size distributions. This contention is partially verified in Section 4 where LWC estimates from probes having this option are compared.

2.2 Optical Array Cloud Particle Spectrometer Probe (OAP-200X)

The Cloud Particle Spectrometer counts and sizes particles from 20 to 300 μm by imaging the shadow of each particle on a linear array of photodiodes as shown in Figure 2-5. A helium-neon laser (6238 \AA) is used with condensing and imaging optics to focus the shadow of a particle lying within the sample volume. The beam is vertical between sampling arms, and the focal plane is centered between the two sampling arms. The particle may shadow one or more of the photodiode elements. Each active element of the photodiode array contains its own amplifying and logic circuit (PC). If the shadowing of an element causes at least a 50 percent reduction in light level to PC (this is an electronic truncation of depth of field and minimum size), a flip-flop circuit is triggered. Two end photodiode elements are used in logic to reject particle shadows extending over the end of the active part of the photodiode array.

Information from each PC of the array is acquired by an accumulator. The particle is sized in the BMS by accumulating flip-flop information from the PC, and converting this into a particle size. The unit particle size results from a determination of the number of elements set, the size of each array element, and the magnification of the optical system. Each second of particle information collected by the BMS is dumped in proper form for recording.

ORIGINAL PAGE IS
OF POOR QUALITY.

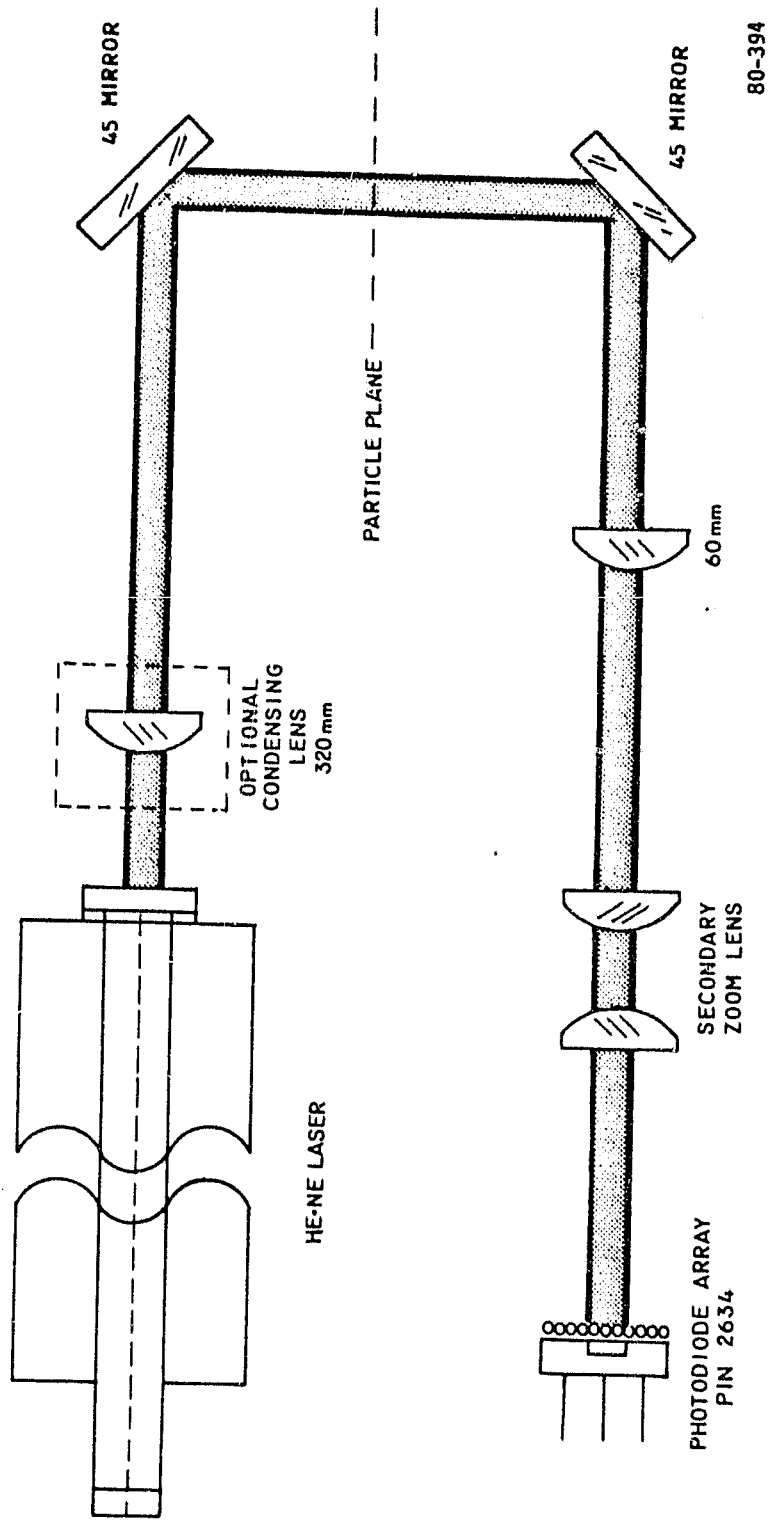


Figure 2-5. CLOUD PARTICLE SPECTROMETER PROBE OPTICAL SYSTEM DIAGRAM

These probes are equipped to size into 15 equal size channels. There are two basic size ranges currently in use. The cloud probe range is 20 to 300 μm , and the precipitation size range generally over 200 to 4500 μm . In the precipitation size range, some models size 200 to 3000 μm , and others 300 to 4500 μm , each divided into 15 equal size channels. Detailed specifications of these probes taken from PMS handbooks appear in Table 2-3.

Table 2-3

CLOUD PARTICLE SPECTROMETER CHARACTERISTICS

Number of array elements	24
Number of size channels	15
Size range (basis system)	20 to 300 microns
Maximum particle velocity	250 knots
Maximum aperture	6.5 cm
Power	115v, 50 to 400 or 60 Hz, 60 W De-ice: 28v DC, 70 W
Dimensions	Cylinder: 18 in (length); 6-1/2 in (diameter); Optical Extensions (two): 20 in (length); 1 in (diameter)
Weight	45 lb
Environmental	Temperature: -60°C to +50°C Humidity: 10% to 100% Altitude: 0 to 40,000 ft msl

Of importance to users of these probes is their sampling volumes. Knollenberg (1970) used glass beads and opaque discs of various diameters placed on glass slides to determine their shadow size and light intensity distribution in a parallel plane as a function of distance. Using coherent illumination, he found that at close distances, the particle was in sharp focus and all of the decrease in light intensity was measured to be in a distance equal to the particle diameter. One would expect this from basic optics (Stone, 1963) and for non-spherical solid articles one would expect that at close distances all of the decrease in light intensity would be in an area equivalent to the cross sectional area of the particle. At distances far from the particle diameter, the decrease in intensity was found to be

distributed over a much wider distance than the particle diameter. The depth of field DF for the measured shadow size to be within ± 10 percent of the actual particle size, which corresponded to a 40 percent reduction in light intensity, was found in non-dimensional units to be $DF = \pm 3$. The detection threshold of a 50 percent reduction in light level before the circuits are triggered was derived from this criteria. The depth of field in dimensional units as a function of particle radius R and illumination wavelength λ is therefore, $DF = \pm 3R^2/\lambda$. For a He-Ne laser where $\lambda = 0.6328 \mu\text{m}$, for a 200 μm diameter particle $DF = 9.4 \text{ cm}$, and for a 1000 μm diameter particle, $DF = 948 \text{ cm}$.

The sampling volume is the product of the depth of field, the effective array width (which is related to the width of the array minus the diameter of the particle) and the true air speed. If the depth of field for a given particle diameter is wider than the separation between sampling arms, then the depth of field is equal to the arm width of 6.1 cm. This is true for the drops having diameters larger than 160 μm .

2.3 Leigh Ice Detector Set

The Leigh Ice Detector Set (IDS) aspirator features an annular ejector nozzle which when powered by compressed air is used to entrain ambient air and thereby induce high-velocity air flow over the ice-collecting probe (Figure 2-6). The air flow is maintained relatively constant despite variations in the freestream velocity vector. Thus, the IDS is designed to continuously sample the air for supercooled liquid water.

The ice-collecting probe which is located crosswise in the ejector duct takes the form of a small-diameter thin-wall tube (Figure 2-7). It has an ice-collecting efficiency close to unity as calibrated in the Canadian National Research Council's icing tunnel. The thin-wall tube has sufficient resistance to serve as its own heater with no internal filament required. The thermal inertia of the probe is therefore very low. In response to heat generated by probe de-icing, the ice interface at the probe is melted and the ice is shed out the tailpipe of the duct. The photodetector senses restoration of the beam to full strength at shedding and turns the probe de-ice power off. Continued cyclic icing and de-icing occurs

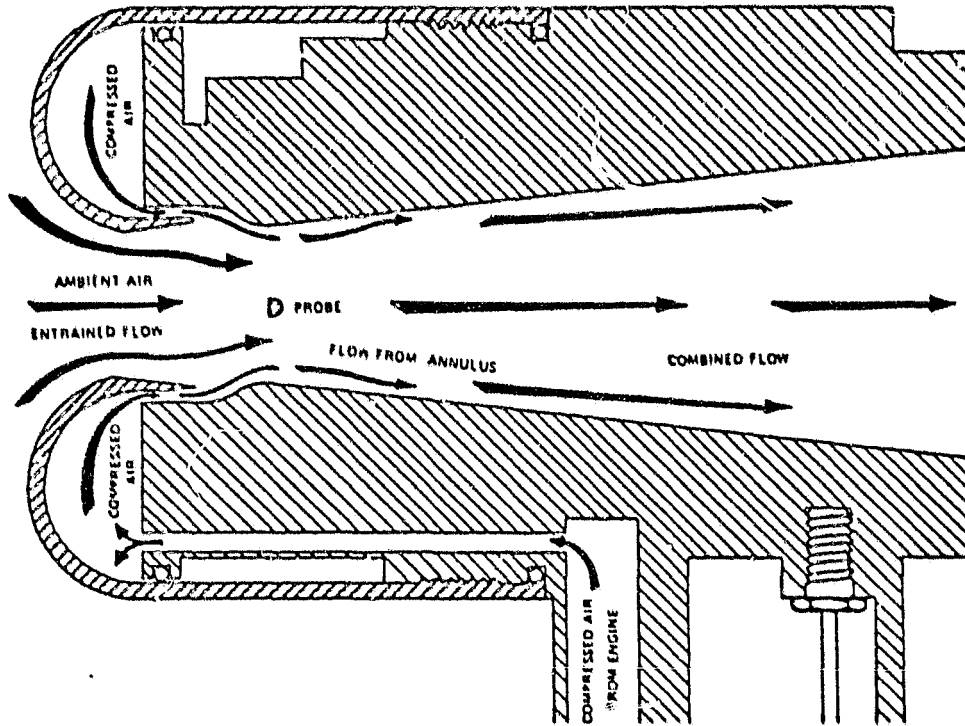


Figure 2-6. ASPIRATOR OF THE LEIGH ICE DETECTOR SET

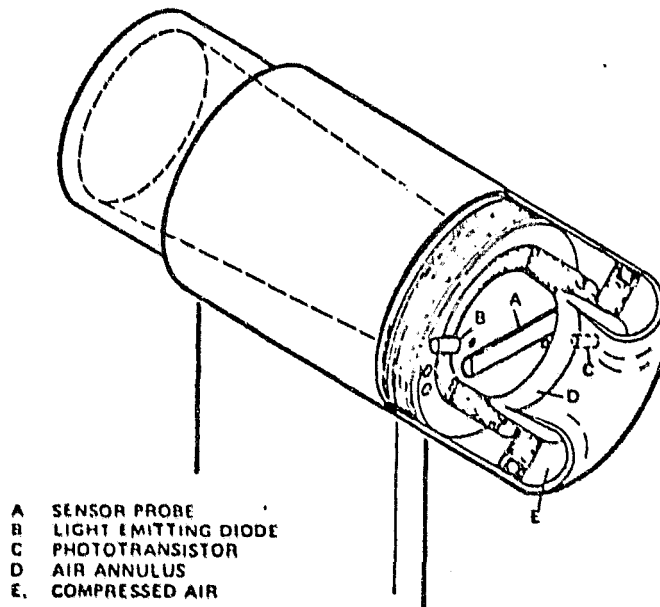


Figure 2-7. LEIGH ICE COLLECTING PROBE AND OPTICAL ICE THICKNESS SENSOR

until no further ice is encountered. It is notable that the presence of supercooled droplets is determined from icing of the supercooled water and not just the atmospheric conditions under which ice can but might not form.

Crosswise in the duct and at a 45° angle to the probe axis is located a solid-state soft infra-red emitter and a photo transistor (Figure 2-7). The oblique light path ensures that a large ice catchment area on the sensor probe face is monitored for ice growth thereby accommodating minor variations in probe ice formations. Once a given thickness of ice is accreted on the probe, the IR beam is occluded and logic circuits within the unit turn on electric current to de-ice the probe.

The sawtooth output signal from the photo transistor resulting from the cyclic buildup of ice on the probe is then electronically processed to provide an initial ice warning signal and a computation of rate of formation of ice in terms of ambient liquid water content (LWC).

The ice detector unit provides a voltage signal that is proportional to the liquid water content being measured. This signal is used to drive a standard aircraft type instrument scaled in liquid water content (LWC). The signal can also be recorded for data gathering purposes.

2.4 Johnson-Williams (J-W) Liquid Water Content Indicator

The Johnson-Williams (J-W) liquid water content indicator is a hot-wire aircraft instrument designed to measure the liquid water content (LWC) of droplets having diameters of less than about 40 μm and is an adaptation of the hot-wire anemometer. The device uses a nickel-iron wire of a known temperature coefficient of resistance and is heated at a constant current above the boiling point of water. In dry air, the sensing wire is balanced in a bridge circuit at a steady-state temperature between the electrical heat supplied and the heat removed by dry airflow. Droplets impinging the sensing wire evaporate, cool the wire, and thereby cause changes in wire resistance. The resulting imbalance in the bridge circuit is proportional to the liquid water content. Since larger drops tend to be sliced by the wire and not totally evaporated, LWC is underestimated when significant concentrations of large drops exist in the clouds.

The external probe houses two calibrated resistance wires which are mounted in a 1.1 inch diameter tube. The sensing wire is exposed perpendicular to the airstream and bisects the tube while the second wire is mounted with its axis parallel to the airstream direction and at the base of the tube where it is not subject to water drop impingement. The base mounted wire serves to compensate for variations in air speed, altitude, and air temperature and is connected as part of the bridge circuit. At times, water or ice collected at the compensating wire causes changes and variations in the zero offset of the device and results in unreliable estimates of LWC. Characteristics of the J-W device are presented in Table 2-4.

Table 2-4

SPECIFICATIONS OF THE JOHNSON-WILLIAMS
LIQUID WATER CONTENT INDICATOR MODEL LWH

Liquid water content range	0-3 g/m ³ or 0-1 g/m ³
Droplet diameter response range	<~40 μm
Time response	1 second at 100 mph;
Accuracy	0.25 gm ⁻³
Precision	0.1 gm ⁻³
Power	27 VDC; 15 amperes
Environmental	Temperature: totally compensated Altitude: 0-30,000 ft Speed: 100-400 mph
Mechanical	Cylindrical probe: 1.1 in diameter 2.1 in long
Weight	Probe with electronics: approximately 12 lbs

2.5 Rosemount Model 102 Total Temperature Sensor

The Rosemount temperature sensor makes use of a recessed platinum resistance element and a flow duct which is designed to achieve a consistently high ram recovery and to reduce the effect of droplet impingement by inertial separation. Flow within the duct is controlled by boundary layer bleed ports to improve time response and a right-angle baffle for separation of water

droplets from the sensing element. The housing is equipped with de-icing heaters without appreciable increase in sensing error. The sensing element is connected to a bridge circuit where a high gain operational amplifier converts changes in resistance to a voltage analog of temperature. The sensor specifications are listed in Table 2-5.

Table 2-5

ROSEMOUNT MODEL 102 TOTAL TEMPERATURE SENSOR SPECIFICATIONS

Type	Platinum resistance thermometer: 50 Ω at 0°C
Recovery factor	0.99
Range	-50°C to +50°C
Output	0 to 5 v DC
Resolution	0.02°C
Linearity	0.02°C
Time constant	2 seconds
Power (heater)	260 watts nominal

Qualified to MIL-P-277230 (ASG)

2.6 Dew Point Hygrometers (E.G. & G. Model 137-C3 and General Eastern Model 1011)

Both devices when used in conjunction with a water separator is capable of measuring dew point from an aircraft at speeds up to 300 knots and at altitudes up to 25,000 Kft. The instruments utilize the thermoelectric or Peltier cooling effect to cool a mirror to the saturation temperature or dew point. A focused light on the mirror is reflected onto a photodetector which in turn drives the thermoelectric cooler when changes in the reflected light are sensed. The mirror is cooled when a decrease of condensate occurs. The system stabilizes on and controls about a particular dew layer thickness. The measurement of the mirror temperature under stabilized conditions is thus taken as the dew frost point temperature. Table 2-6 presents specifications of the two sensors.

Table 2-6
 SPECIFICATIONS OF DEW POINT HYDROMETER

E. G. & G. 137-C3

	<u>Control Unit</u>	<u>Sensor</u>
Range	+50°C to -50°C	+70°C to -55°C
Accuracy	±0.5°C above 0°C ±1.0°C below 0°C	±0.5°C
Response	2°C/sec	2°C/sec
Power	115 VAC 50/1000 cps 20 watts	

General Eastern Model 1011

	<u>Sensor</u>
Range	-75°C to +50°C
Accuracy	±0.2°C above 0°C ±0.4°C between 0°C to -40°C ±1.0°C between -40°C to -75°C
Response	2°C/sec
Power	115 VAC 50/500 Hz 50 watts

3. DATA SET DESCRIPTION

A total of 209 tests were conducted during the January 1981 testing program at the NASA LeRC IRT. For each test point, cloud measurements were taken in the IRT test section from a J-W device, a Leigh IDS, and two of the PMS probes. Eight additional test points obtained on June 8, 1981, supplement the data set. The testing in June was conducted to evaluate possible effects of the steam tube wrappings on the PMS probe measurements. The Leigh IDS was not available for these tests. Measurements were taken under a variety of tunnel conditions and included variations in tunnel airspeed, temperature, cloud LWC and cloud median volume diameter (MVD). Airspeeds ranged from 50 to 285 mph while temperatures varied from about -20°F (-29°C) to 68°F (20°C). Based on early tunnel calibrations with rotating cylinders, the clouds produced in the IRT were characterized by LWC and MVD ranging from about 0.5 to 5 g/m³ and 10 to 30 μm, respectively. Due to the large matrix of testing conditions and to time constraints of the program, each test condition was not measured by all of the available PMS probes.

3.1 Data Recovery Percentages

Table 3-1 presents a summary of the various PMS probe configurations in the IRT and data recovery information for each of the indicated cloud measurement devices. The test points are identified in chronological order for convenience. The eight test points (210-217) are listed separately since the two PMS probes and J-W device used in June were not identical to the probes used in January. The PMS probes are identified by type and a number from 1 to 4 for reference purpose. In this report the PMS probes will not be identified by organization since it is not pertinent to the analyses.

As shown, a large portion (~66 percent) of the J-W measurements from January were judged unacceptable and resulted from a loose wire connection in its control box which rendered the device as being either inoperative or intermittent. Measurements from the Leigh IDS were judged unacceptable if the device was not operating, operating intermittently, or operating beyond its full scale range. It is noted that seven of the tests were conducted at temperatures warmer than freezing on 21 January. Hence, since the Leigh device does not provide LWC estimates at these warm temperatures, these test points are not counted in the totals.

Except for FSSP 2, sufficient numbers of test points were recovered from the remaining PMS probes. Glass bead calibrations performed prior to each test day and review of the measurements revealed that FSSP 2 was not calibrated to the manufacturer's specifications. Calibrations performed with four different batches of bead sizes revealed that instead of peak counts being found at four different and widely spaced channel numbers, counts from two of the intermediate sized batches peaked at an identical channel number. Hence although three of the sized batches (10-15 μm , 25-35 μm , and 35-45 μm) had peak counts in their appropriate channel numbers (3, 8 and 13), the counts from the intermediate sized batch (15-25 μm) peaked in channel 8 instead of the nominal channel 5. The consequence of this problem resulted in bimodal mass distributions with a mode always found in channel 3 and with the second mode ranging between channels 6 to 8. Measurements from the remaining PMS probes under identical tunnel conditions displayed single mode distributions.

An example of a typical bimodal distribution from FSSP 2 is presented in Figure 3-1. For comparison purposes, an acceptable measurement from ASSP 2 for the same test point and a rejected measurement from FSSP 1 are also included. The example of the rejected data point is presented since the exponential form of the distribution is characteristic of practically all of the rejected measurements from the remaining ASSP and FSSP probes. For all of the rejected data from ASSP 4 on January 19 (test points 141-209), the pre-test calibrations revealed significant changes in their measurement capability from the earlier tests. Whereas the counts from the bead lots of given size ranges peaked in their nominal probe channels early in the test program, they later fell in corresponding smaller numbered channels; thus indicating a broadening of channel band width and decrease in probe sensitivity. Calibrations performed on both of these probes with sized glass beads between 35-45 μm revealed peak counts falling from probe channels 12-13 down to channels 8-9 during the later tests. The apparent broadening of channel band width of from 3 to about 4.5 μm resulted in distributions of exponential form which were characterized by number or mass density decrease with channel number (or particle size) increase. Although not verified, experience strongly suggests that probe deterioration in both these instances resulted from water being lodged in the optical lenses of both probes.

82/C04

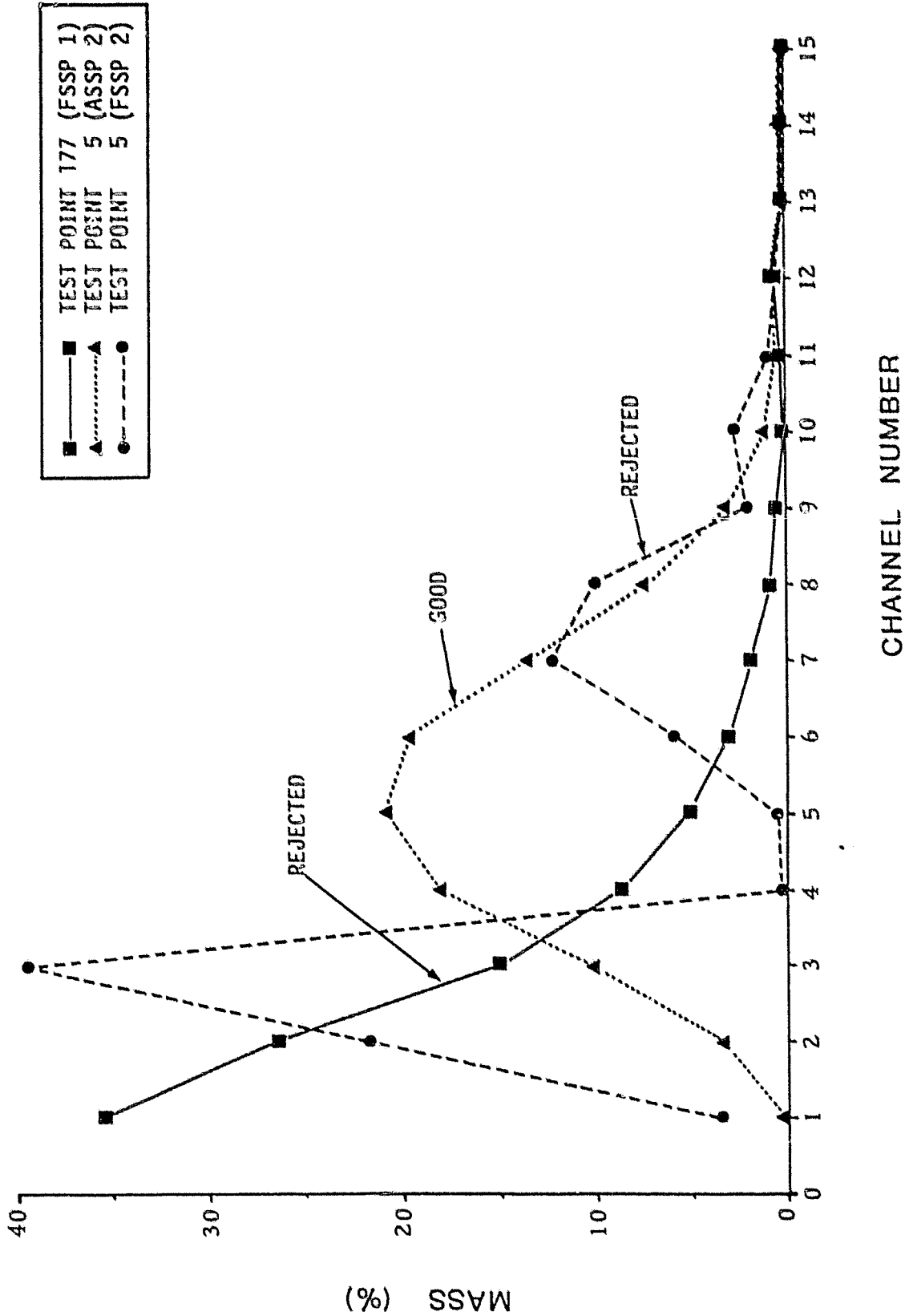


Figure 3-1. EXAMPLES OF GOOD AND BAD DROP SIZE DISTRIBUTIONS FOR INDICATED TEST POINTS AND PROBES

The remaining rejected PMS probe measurements resulted from probe deterioration due to problems associated with their optical system. Rapid heating from about -4 to 29°F for the last test point (217) after the probes were "cold socked" in the IRT for several hours caused lense "fogging" in both FSSP 1' and ASSP 2'. As for the remaining rejected samples, ice build up within the sampling tubes was observed to have obstructed the laser beam and thereby affected the measurements. These problems were readily detected by the operator in real time from noting the characteristic exponential distributions on the display console.

Subsequent review of the reduced data lead to rejecting an additional 4 test points and was based upon noting that both the estimated LWC and MVD for a given tunnel test condition (given air speed and tunnel pressure settings) differed significantly from the other measurements taken with the same probe. For these rejected samples, the LWC estimates were lower by a factor of 2 to 3 while the MVD was also lower by about 4 to 6 μm.

3.2 Tunnel Settings

Cloud conditions (LWC and MVD) within the test section were controlled by separate air and water pressure settings of the spray system and by the air velocity through the enclosed and refrigerated IRT. The following empirical equations which were based on early work with rotating cylinders show these relationships.

$$\text{LWC}(\text{g/m}^3) = \frac{6.545 \sqrt{38.7 (P_w - P_a)}}{V}$$

$$\text{MVD}(\mu\text{m}) = \frac{1.09(43.9 - \sqrt{3.48V}) \sqrt{38.7(P_w - P_a)}}{\left(\frac{P_a}{1.13} + 10\right)} + 0.0052V + 4$$

where

P_a = air pressure setting, psig
 P_w = water pressure setting, psig
 V = tunnel air speed, mph
 $20 < P_a < 75$
 $P_w < 110$
 $5 < (P_w - P_a) < 65$

ORIGINAL PAGE IS
OF POOR QUALITY

Table 3-2 presents a summary of the IRT cloud conditions which shows the number of test points as functions of given air and water pressure settings and tunnel air speeds. As shown, the greatest majority (212 test points) of the tests were conducted at 24 primary pressure (fixed air and water) settings where a minimum of at least 2 test points were obtained. Five of the remaining tests were conducted at five different pressure settings (ID 25). In four of the fixed pressure settings (ID 15, 18, 19, and 20), tunnel air velocity was also varied systematically. Hence it is indicated that probe testing was subject to 54 different cloud conditions for which each is listed information on the control parameters, P_a , P_w , and V .

Temperatures are also tabulated and serve merely to present ranges over which each of the cloud conditions were run. Further information on the number of test points as function of temperature range is summarized in Table 3-3. Here it is shown that the majority of tests were conducted at temperatures between -20 to 19°F and that the largest number (89) of test points were obtained at temperatures between 10 to 19°F . Had all of the measurements been judged acceptable, it becomes quite apparent that it was not possible to obtain measurements from each of the PMS probes for all test conditions (fixed cloud and temperature).

3.3 Data Selection

Measurements taken over periods ranging from about 20 to 300 seconds were processed to obtain representative estimates of each test condition which was maintained in the IRT test section for durations ranging from about 2 to 15 minutes. The sampling periods were chosen to represent the early steady state cloud conditions as revealed by time plots of key cloud parameters (LWC and MVD). Possible measurement deterioration with time increase due to ice buildup on the probes was the primary reason for selecting data early (as opposed to late) in the total spray period. Steady state conditions were usually measured at the test section some 40 to 60 seconds after the nozzles were turned on and properly adjusted. The nozzles were turned on after cooling (or heating) the IRT to a desired temperature and after increasing the tunnel air speeds from idle velocity to a designated velocity.

Table 3-2
SUMMARY OF IRT TEST CONDITIONS

Pressure Setting ID	Air Pressure (PSI)	Water Pressure (PSI)	IRT TAS (mph)	IRT LWC g/m ³	IRT MVD (μm)	Number of test points	Temperature	Pressure Setting ID	Air Pressure (PSI)	Water Pressure (PSI)	IRT TAS (mph)	IRT LWC g/m ³	IRT MVD (μm)	Number of test points	Temperature
1	20.5	30.5	230	0.56	17.1	4	-11 to 16	19e	50.0	75.0	220	0.93	15.3	1	-11
2	24.0	75.0	235	1.24	28.9	3	16	19f	50.0	75.0	230	0.89	15.0	1	-10
3	25.0	32.5	200	0.56	15.2	2	14	19g	50.0	75.0	240	0.85	14.6	1	-10
4	26.0	42.0	100	1.63	25.3	5	5 to 15	19h	50.0	75.0	250	0.81	14.3	1	-11
5	30.0	55.0	200	1.02	21.3	2	16	19i	50.0	75.0	260	0.78	14.0	2	-10
6	30.0	63.0	194	1.19	23.9	7	13 to 14	19j	50.0	75.0	270	0.75	13.7	1	-10
7	31.0	41.0	200	0.64	15.1	4	13 to 14	19k	50.0	75.0	283	0.72	13.3	1	-10
8	32.0	39.0	100	1.08	16.3	12	13 to 54	20a	50.0	90.0	50	5.15	28.5	3	-20 to -11
9	35.0	57.0	235	0.81	17.1	3	16	20b	50.0	90.0	100	1.58	24.5	5	-20 to -11
10	36.0	62.0	220	0.94	18.5	11	4 to 58	20c	50.0	90.0	150	1.78	21.4	5	-20 to -11
11	36.0	70.0	260	0.91	18.4	10	4 to 62	20d	50.0	90.0	200	1.29	18.9	5	-20 to -11
12	36.0	73.0	270	0.92	18.5	6	4 to 16	20e	50.0	90.0	220	1.17	18.0	2	-15 to -9
13	36.0	76.0	285	0.90	18.2	10	5 to 68	20f	50.0	90.0	230	1.12	17.5	2	-11 to -10
14	41.0	58.0	100	1.67	19.7	5	4 to 15	20g	50.0	90.0	240	1.07	17.1	2	-11 to -10
15a	42.5	56.0	150	1.00	15.7	20*	-9 to 53	20h	50.0	90.0	250	1.03	16.7	2	-11 to -9
15b	42.5	56.0	200	0.79	14.8	6	13 to 14	20i	50.0	90.0	260	0.99	16.3	2	-9
16	44.0	75.0	240	0.94	16.8	6	4 to 16	20j	50.0	90.0	270	0.95	15.9	2	-12 to -8
17	46.0	78.0	228	1.01	17.1	2	-11	20k	50.0	90.0	285	0.90	15.3	2	-11 to -8
18a	50.0	60.0	50	2.58	16.4	2	-14 to -13	21	53.0	76.0	173	1.13	16.0	3	5
18b	50.0	60.0	100	1.29	14.5	2	-14 to -13	22	53.0	91.0	250	1.00	15.9	8	4 to 60
18c	50.0	60.0	150	0.86	13.1	2	-14 to -11	23	64.0	69.0	100	0.91	10.3	5	4 to 15
18d	50.0	60.0	200	0.64	12.0	3	-14 to 16	24	65.0	100.0	100	2.41	19.5	5	4 to 16
18e	50.0	60.0	220	0.59	11.6	2	-9	25a	13.5	42.5	150	1.46	39.8	1	-11
19a	50.0	75.0	50	4.07	23.5	2	-18 to -11	25b	30.0	46.0	228	0.76	16.9	1	-11
19b	50.0	75.0	100	2.04	20.3	2	-18 to -11	25c	23.0	69.0	228	1.21	29.0	1	-11
19c	50.0	75.0	150	1.36	17.9	2	-18 to -11	25d	36.0	67.0	220	1.03	19.8	1	9
19d	50.0	75.0	200	1.02	16.0	17	-12 to 56	25e	50.0	57.0	235	0.46	10.3	1	16

*Includes the 8 test points taken on June 8, 1981.

ORIGINAL PAGE IS
OF POOR QUALITY

Table 3-3

NUMBER OF TEST POINTS AS FUNCTION
OF TEMPERATURE RANGE

<u>Temperature Index</u>	<u>Temperature Range</u>	<u>Number of Test Points</u>
1	-20 to -11	51
2	-10 to -1	23
3	0 to 10	44
4	11 to 20	89
5	20 to 32	3*
6	>32	<u>7</u>
	Total	217

*Points taken from June 8 only.

ORIGINAL PAGE IS
OF POOR QUALITY

Figure 3-2 presents a time plot of measurements taken at the test stand during the conduct of a typical test (211). After initiating the spray nozzles (0 sec), the spray cloud is shown to arrive at about 20 seconds and to reach near steady state at about 50 to 55 seconds. After approximately 90 seconds and for times to approximately 320 seconds into the run, the PMS probe estimates are shown to decrease while the J-W trace remains at a nearly constant value. Although the largest decrease appears in the LWC trace of the ASSP, estimates of the FSSP on other occasions decreased at faster rates. The spray cloud was turned off after a five minute (at 300 sec) testing period and was sensed approximately 25 seconds later (325 sec) at the test stand as evidenced by the rapid decline of the indicated probe traces.

3.4 Data Reduction Procedures

Procedures employed in the reduction of the PMS probe measurements consisted of initially converting the raw counts in each of the 15 size channels to a number density N_i by the following equation:

$$N_i = \frac{C_i}{A_i \times V \times \text{EFF} \times \Delta t}$$

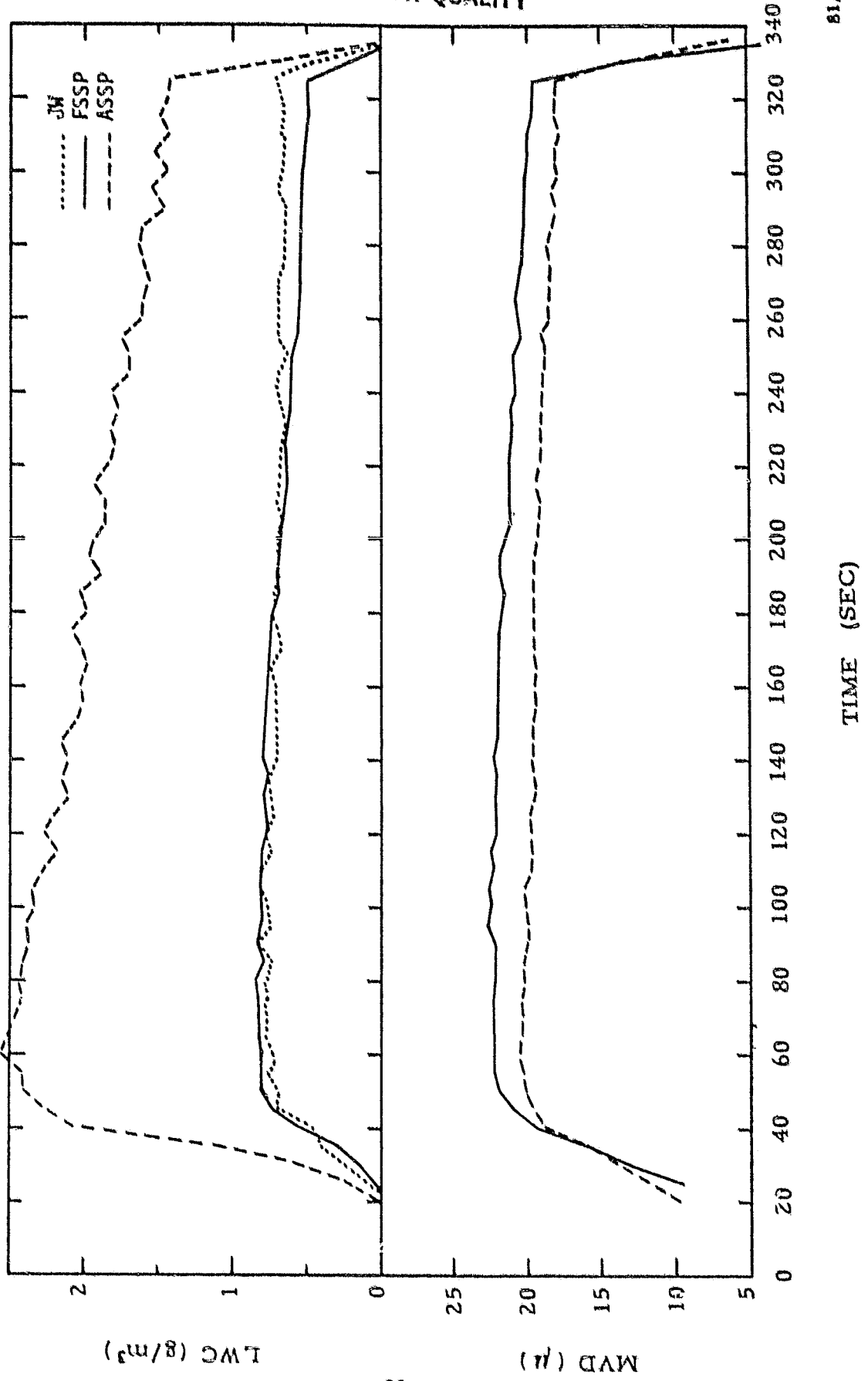
where

- C_i = raw counts recorded in each channel number, i , in a time interval, Δt .
- A_i = sample area for each channel number.
- V = true air speed.
- EFF = efficiency factor

For the ASSP and FSSP devices, A_i remains constant for all 15 size channels, while the constant EFF is determined from the ratio of the sum of the raw counts in 15 size channels and the separately recorded total strobe counts (ST) during the time interval Δt .

$$\text{EFF} = \frac{\sum_{i=1}^{15} C_i}{\text{ST}}$$

ORIGINAL PAGE IS
OF POOR QUALITY



81/171

TIME (SEC)

Figure 3-2. TIME PLOT OF INDICATED PARAMETERS TAKEN AT 23°F WITH STEAM TUBE WRAPS

For probes without the velocity reject feature, EFF is assumed to be equal to one.

The constant EFF also maintains a value of 1 for data from the OAP. However, in these optical array devices, the sample area varies with channel number as:

$$A_i = \Delta D \times (K - i) \times L$$

where

- ΔD = channel width.
- K = $N-1$.
- N = number of sensitive elements in the photodiode array.
- L = depth of field.

For the larger channels (8-15), L is larger than the probe aperture distance of 6.1 cm and hence remains fixed to it. Depth of field compensation for the smaller channels (1-7) is thus computed from the following equation:

$$A_i = A_i \times \left(\frac{i}{8}\right)^2, i = 1,7$$

where A_i to the right of the equal sign is computed from the previous equation.

Once determined, the number density values provide means for computation of the following bulk parameters from integration of the data.

1. Total number density, N_T

$$N_T = \sum_{i=1}^{15} N_i$$

2. Liquid water content, LWC

$$LWC = \frac{\pi}{6} \rho_w \sum_{i=1}^{15} N_i D_i^3$$

**ORIGINAL PAGE IS
OF POOR QUALITY**

where

D_i = midpoint size of each channel, $D_i = i \times \Delta D$
 ρ_w = density of water.

3. Median volume diameter, MVD

$$MVD = \frac{D = MVD}{D = D_i} \sum_{D = D_i} N_i D_i^3 = \frac{1}{2} \sum_{i = 1}^{15} N_i D_i^3$$

Table 3-4 presents a summary of the sampling characteristics of the PMS probes tested in the IRT. The band widths listed were determined from the glass bead calibrations performed prior to each test.

Table 3-4
PMS PROBE SAMPLING CHARACTERISTICS

<u>Probe</u>	<u>ΔD (μm)</u>	<u>A_i (mm^2)</u>	<u>N</u>	<u>Velocity Reject</u>
FSSP 1	3.0	0.243	-	No
FSSP 2	3.0	0.254	-	No
ASSP 1	3.5	0.672	-	Yes
ASSP 2	3.0	0.811	-	Yes
ASSP 3	3.5	0.459	-	No
ASSP 4	3.0	0.614	-	No
FSSP 1 ¹	3.9	0.547	-	Yes
ASSP 2 ¹	3.3	0.653	-	Yes
OAP 1	2.0	eq	22	-
OAP 2	2.0	eq	22	-

All cloud data were corrected for local velocity differences from bockage effects from the probe supports and traverse hardware in tunnel test section without the probes in place. Although no significant velocity differences were measured at the sampling points of the PMS probes, pitot-static pressure measurements disclosed overspeeding at the Leigh IDS and J-W hot wire by factors of 1.18 and 1.13, respectively, and have been appropriately handled in the data reduction software.

3.5 Data Volume Description

Data listings in the form of a drop size distribution report for each test condition and PMS probe measurements are presented in a separate data volume as part of the contract requirements. An example is presented in Figure 3-3. Table 3-5 presents a summary of the information listed and identifying keys for the computer generated listings. It is noted that the IRT cloud expectations were computed from the equations given in Section 3.2 for which the independent variables are also listed. Air and water pressure settings, temperature, and air speed for each test point were obtained from the tunnel operator's log sheet. In addition to the written comments, negative values are also listed for some of the data judged unacceptable. For measurements from the J-W and Leigh devices, a default value of -0.88 g/m^3 is listed if they were inoperative while a negative sign is assigned to the estimate if they functioned intermittently. Missing relative humidity information for the test period is indicated by a default value of -99 percent.

To complement the distribution reports, the data volume also includes a computer generated test point summary for each of the data tapes listed in Table 3-1. The summaries precede the distribution reports. Figure 3-4 presents an example of a summary for Tape 3. Identifying keys for information summarized appear in Table 3-6. The test point summaries are also presented in Appendix A.

DROPLEY SIZE DISTRIBUTION
TEST POINT 70

DATE 1/14/81 RUN ID 5861
 START TIME(LST) 2016: 5 DURATION(SEC) 30
 IRT TEST CONDITIONS: TAS(MPH)= 230 TEM(F)= -10 RH(X)=.99
 SPRAY PRESSURE SETTINGS: AIR(PSIG)= 50.0 H₂O(PSIG)= 90.0
 IRT CLOUD EXPECTATIONS: LWC(G/M3)= 1.12 MVD(U)= 18

SUPPORTING LWC(G/M3) MEASUREMENTS: JWC =.88 CV(X)= 0 LEIGH= 1.15 CV(Z)= 1

AVERAGE SPECTRA INFORMATION
PROBE ASSP 3

DI (U)	DI/MVD	HI (/CC)	HD (/CM4)	MI (G/CC)	MD (G/CM4)	MI/LWC (Z)	MD/LWC (Z)
3.5	.14	.5025E+01	.1436E+05	.1128E-09	.5223E-06	.01	.01
7.0	.29	.5693E+02	.1055E+06	.6653E-08	.1895E-04	.61	.63
10.5	.43	.7095E+02	.2027E+06	.4301E-07	.1229E-03	5.99	4.61
14.0	.57	.7323E+02	.2092E+06	.1052E-06	.3006E-03	9.75	14.37
17.5	.71	.5086E+02	.1453E+06	.1427E-06	.4078E-03	13.23	27.00
21.0	.86	.5365E+02	.9614E+05	.1632E-06	.4662E-03	15.13	42.72
24.5	1.00	.1992E+02	.5691E+05	.1534E-06	.4382E-03	14.22	56.94
28.0	1.14	.1184E+02	.3382E+05	.1361E-06	.3888E-03	12.61	69.55
31.5	1.28	.6958E+01	.1988E+05	.1139E-06	.3254E-03	10.56	80.11
35.0	1.43	.3242E+01	.9262E+04	.7278E-07	.2079E-03	6.75	86.86
38.5	1.57	.4717E+00	.1548E+04	.1409E-07	.4027E-04	1.31	88.16
42.0	1.71	.1156E+01	.3303E+04	.4484E-07	.1281E-03	4.16	92.32
45.5	1.85	.6609E+00	.1888E+04	.5260E-07	.9314E-04	3.02	95.34
49.0	2.00	.4646E+00	.1328E+04	.2662E-07	.8178E-04	2.65	98.00
52.5	2.14	.2853E+00	.8151E+03	.2161E-07	.6176E-04	2.00	100.00

PROBE LWC(G/M3)= 1.08 CV(X)= 4
 PROBE MVD(U) = 24.5 CV(Z)= 1
 PROBE RT(/CC) = 316. CV(X)= 3

COMMENTS
 RELATIVE HUMIDITY MEASUREMENTS NOT TAKEN
 Jm INACTIVE

Figure 3-3. EXAMPLE OF DROPLEY SIZE DISTRIBUTION REPORT

ORIGINAL PAGE IS
OF POOR QUALITY

Table 3-5

KEY FOR TEST POINT LISTING

Information	Key	Units
Test point number	TEST POINT	-
Date	DATE	MO/DA/YR
Run number	RUN ID	-
Start time	START TIME	LST
Sample duration	DURATION	sec
IRT Settings		
Air speed	TAS	mph
Temperature	TEM	F
Relative humidity	RH	°
Air pressure	AIR	psig
Water pressure	H2O	psig
MVD	MVD	microns
LWC	LWC	g/m ³
LWC from J-W device	JW	g/m ³
Coefficient of variation*	CV	%
LWC from Leigh device	LEIGH	g/m ³
Coefficient of variation	CV	%
Probe identifier	PROBE	name
Size distribution/per channel		
Mid-point diameter, Di	DI	microns
Normalized size, Di/MVD	DI/MVD	-
Number density, Ni	NI	/cm ³
Number density per band width, N _D	ND	/cm ⁴
Mass density, M _i	MI	g/cm ³
Mass density per band width, M _D	MD	g/cm ⁴
Percent mass, Mi/LWC	MI/LWC	%
Cumulative percent, mass, $\sum_{i=1}^i$ Mi/LWC	SMI/LWC	%
Probe LWC, $\sum Mi$	PROBE LWC	g/m ³
Coefficient of variation	CV	%
Probe MVD	PROBE MVD	microns
Coefficient of variation	CV	%
Probe total number density, N _T	NT	/cm ³
Coefficient of variation	CV	%
Data quality comments	COMMENTS	-

*The coefficient of variation is defined as the ratio of the standard deviation to the mean of the parameters computed from the one-second data recordings; CV = σ /mean.

IRT TEST POINT SUMMARY
JANUARY 1981

TAPE 8

TEST PT	RUN ID	DA	TIME	DT LST	TAS SEC	TEM MPH	PAIR F	RH X	PH20 PSIG	T=0 G/M3	DV U	J=0 G/M3	L=0 G/M3	PROBE ID	G	U /CC	PROBE / CV(%)	NT RCT	ALP LAM	AC	EFF	REMARKS						
120	5863	16	181435	60	100	14	-99	65.0	100.0	2.41	20	-88	1.46	0	2	ASSP	1	3.37	20	1428	193	7.6	564	0	44	JM INACTIVE		
121	5863	16	181835	60	100	14	-99	64.0	69.0	.91	10	-88	.67	0	4	OAP	1	.02	228	0	0-10.	0	0	0	9	1	JM INACTIVE	
122	5863	16	182245	60	100	13	-99	41.0	58.0	1.68	20	-88	1.44	0	2	OAP	1	.18	53	3	2-10.	0	0	0	1168	0	JM INACTIVE	
123	5863	16	1827	5	60	100	13	-99	26.0	42.0	1.63	25	-88	1.40	0	3	OAP	1	.33	66	4	3-10.	0	0	0	45	0	JM INACTIVE
124	5863	16	1832	0	60	100	13	-99	32.0	39.0	1.08	16	-88	.02	0	2	OAP	1	.04	54	0	0-10.	0	0	0	46	0	JM INACTIVE
125	5863	16	1839	0	60	150	14	-99	43.0	56.0	.98	15	-88	.02	0	0	OAP	1	.01	131	0	0-10.	0	0	0	45	0	LEIGH INACTIVE
126	5863	16	1844	5	60	200	14	-99	50.0	75.0	1.02	16	-88	.01	0	0	OAP	1	.04	124	0	0-10.	0	0	0	35	1	LEIGH INACTIVE
127	5863	16	185435	30	220	14	-99	36.0	62.0	.94	19	-88	.01	0	0	OAP	1	.05	86	0	0-10.	0	0	0	34	2	LEIGH INACTIVE	
128	5863	16	1900	0	30	240	15	-99	44.0	75.0	.94	17	-88	.27	0	120	OAP	1	.03	98	0	0-10.	0	0	0	31	1	JM INACTIVE
129	5863	16	190455	30	250	14	-99	53.0	91.0	1.00	16	-88	.01	0	0	OAP	1	.05	139	0	0-10.	0	0	0	29	0	LEIGH INTERMITTENT	
										.92	20	510	114	5.0	436	26	29	1	4	0	0	0	0	0	0	1	JM INACTIVE	
										.92	20	510	114	5.0	436	26	29	1	4	0	0	0	0	0	0	0	1	LEIGH INACTIVE

ORIGINAL PAGE IS
OF POOR QUALITY

Figure 3-4. EXAMPLE OF TEST POINT SUMMARY

ORIGINAL PAGE IS
OF POOR QUALITY

Table 3-6

KEY FOR IRT TEST POINT SUMMARIES

Information	Key	Units
Data tape	TAPE	-
Run number	RUN ID	-
Day	DA	-
Start time	TIME	Local
Sample duration	DT	sec
Tunnel air speed	TAS	mph
Tunnel temperature	TEM	F
Tunnel relative humidity	RH	%
P _a	PAIR	psig
P _w	PH20	psig
Tunnel LWC expectation	T-Q	g/m ³
Tunnel MVD expectation	DV	microns
J-W LWC*	J-Q	g/m ³
Leigh LWC	L-Q	g/m ³
PMS probe		
Probe name	PROBE	-
LWC	Q	g/m ³
MVD	DV	microns
N _T	NT	/cm ³
Total raw counts/sec	RCT	x10 ⁻²
Gamma distribution coefficient, α	ALP	-
Gamma distribution coefficient, λ	LAM	x10 ⁻³ /micron
Average probe activity	ACT	%
Average probe efficiency	EFF	%
Data quality comments	REMARKS	-

*The coefficient of variation (CV) for the cloud measurements are listed beneath the probe estimates.

4. RESULTS AND DISCUSSION

Test point measurements judged acceptable serve as the basic data set for the analyses. The following subsections present the results of the following analyses tasks.

- IRT cloud repeatability.
- IRT cloud uniformity.
- Effect of steam tube wraps on spectrometer measurements.
- Temperature and velocity effects on spectrometer measurements.
- Instrument intercomparisons.

4.1 IRT Cloud Repeatability

For obvious reasons, demonstration of cloud repeatability is essential to the remaining analyses tasks. For the purpose of obtaining quantitative estimates of cloud repeatability, the analyses evaluates the sample to sample variations with respect to the mean by the following standard statistical equations.

$$\bar{x} = \frac{\sum_{j=1}^n x_j}{n}$$

$$s^2 = \frac{\sum_{j=1}^n (x_j - \bar{x})^2}{(n - 1)}$$

$$CV = \frac{s}{\bar{x}} \times 100\%$$

where

- x_j = a sample variable
- \bar{x} = sample average or mean
- n = number of samples
- s = estimate of the standard deviation
- CV = coefficient of variation

Hence low values computed for the coefficient of variation indicate high repeatability and vice versa.

Table 4-1 presents information on averages and on the temporal variation (CV) of the various measurements for given tests from data collected (1) during the time when the spray cloud passed through the test section (spray) and (2) during the initial time period of the spray (sample). Both of these corresponding data sets had identical starting times. The statistics were based upon samples computed for each second of recorded data and for the indicated durations (n = number of seconds). For a given instrument and a given test, the following observations are made.

- Based on the statistics given for the accretion (Leigh and J-W) devices, temporal variations in cloud LWC during a given spray remains small; typically between 4-8 percent.
- Although the statistics from the accretion devices indicate higher absolute variations with increase in average cloud LWC amounts, their percentages are relatively constant and hence considered not affected by different airspeed or temperature settings in the IRT.
- The sampling durations chosen are sufficient to provide precise estimates of the average spray conditions as evidenced by the near identical values listed for the spray and sample averages of the accretion devices. Of the five test conditions presented, four of the sample estimates are within about 1 percent while the fifth (test point 61) is within 7 percent of their corresponding spray average values. Based upon sampling considerations and the relatively small CV shown, it is quite apparent that the 20 to 50 second periods are more than sufficient to provide precise estimates of the average spray conditions.
- The PMS probe estimates of the average spray LWC show significantly wider percent variations than those from the accretion devices and thus indicate that they are less reliable rather than that the cloud conditions varied widely during the course of the spray. Aside from the steady conditions indicated from the two accretion devices, support is provided from the sample values which generally show higher estimated averages having significantly smaller CV values. These differences between the spray and sample statistics reflect decreases in measurement precision during the course of the spray which resulted from ice buildup within the sampling tubes as indeed were confirmed by inspection after test conclusion.

Table 4-1
IRT REPEATABILITY
VARIATION DURING GIVEN SPRAY

Test Point	TEM (F)	V (mph)	Duration (sec)	Leigh LWC (g/m ³)		J-W LWC (g/m ³)		FSSP LWC (g/m ³)		ASSP LWC (g/m ³)		FSSP MVD (μ)		ASSP MVD (μ)	
				AVE	CV(%)	AVE	CV(%)	AVE	CV(%)	AVE	CV(%)	AVE	CV(%)	AVE	CV(%)
3	14	200	575	0.99	4	-	-	-	-	0.06	64	-	-	15.8	1
61	7	100	265	1.78	4	-	0.34	28	2.30	10	22.7	7	20.8	3	
183	-11	220	260	0.63	6	-	0.05	23	0.04	84	14.5	5	18.2	17	
210	29	150	300	-	-	0.72	8	0.55	27	2.53	5	20.1	5	20.3	1
213	-4	150	720	-	-	0.79	6	0.65	25	1.18	74	8	17.2	20	
Average				1.13	5	0.76	7	0.40	23	1.22	47	19.9	6	18.5	8
<u>SPRAY</u>															
3	14	200	30	1.00	4	-	-	-	-	0.14	8	-	-	16.5	2
61	7	100	30	1.91	4	-	0.50	14	2.83	5	25.3	4	22.5	2	
183	-11	220	40	0.63	4	-	0.07	9	0.09	5	15.5	3	18.6	1	
210	29	150	55	-	-	0.71	8	0.71	3	2.61	3	21.8	1	20.5	1
213	-4	150	30	-	-	0.80	5	0.77	3	2.26	4	22.1	1	20.8	1
Average				1.18	4	0.76	7	0.51	7	1.98	5	21.2	2	19.8	1
<u>SAMPLE</u>															

**ORIGINAL PAGE IS
OF POOR QUALITY**

- Based on the near identical CV values listed for the PMS sample estimates of cloud LWC and those from the accretion devices, it is indicated that the PMS probe measurements taken early during given tests are valid. Hence it is inferred from the sample estimates that the temporal variations in cloud MVD were also small and for these test points in the range of from 1 to 4 percent.
- Measurement deterioration due to ice buildup in the PMS probes results in a larger percentage decrease in estimating LWC than in estimating MVD as is inferred by the corresponding sample and spray averages and is as expected since LWC is proportional to the cube of particle size.

Table 4-2 presents additional information on the repeatability of the IRT spray clouds. Summarized information on both cloud LWC and MVD from measurements from each of the cloud instruments listed include:

Table 4-2
IRT REPEATABILITY SUMMARY FOR A GIVEN SPRAY CLOUD

Instrument	Variation (%) in LWC				Variation (%) in MVD		
	Given Spray	Given Day	Test Period	Yearly	Given Spray	Given Day	Test Period
Leigh	4	10	12	-	-	-	-
J-W	6	21	15	12*	-	-	-
FSSP 1	15	36	19	-	3	4	4
ASSP 1	6	20	24	-	2	3	3
ASSP 2	10	15	-	-	3	3	-
ASSP 3	6	20	33	-	2	7	7
ASSP 4	9	37	-	-	3	7	-

*One tunnel setting.

1. Variation during a given spray is determined from the average of the CV values of all accepted test points.
2. Variation during a given day which represents an evaluation of test point averages taken under identical tunnel conditions (fixed air and water pressure and airspeed settings) at different times on a given day.

**ORIGINAL PAGE IS
OF POOR QUALITY**

3. Variation over the test period which represents an evaluation of test point averages taken under identical tunnel conditions on different days.
4. Yearly variations which represent an evaluation of the year to year variations in the IRT spray clouds of a given set of tunnel settings.

Information presented for items 2-4 above represents a normalized form of the coefficient of variation (NCV) which is based upon (1) normalizing the sample to sample variations of the estimates (x_i = LWC or MVD) taken at a given tunnel condition, s , to their average, \bar{x}_s , and 2) pooling the normalized squared deviations of all possible given tunnel conditions, k , as follows:

$$NCV = \left[\frac{\sum_{s=1}^k \sum_{i=1}^{n_s} \left(\frac{x_i - \bar{x}_s}{\bar{x}_s} \right)^2}{\sum_{i=1}^k n_s - 1} \right]^{1/2} \times 100\%$$

$$\bar{x}_s = \frac{\sum_{i=1}^{n_s} x_i}{n_s}$$

$$n_s > 1$$

For evaluating item 2 above:

- x_i = sample estimate taken at a given tunnel condition on a given day.
 n_s = number of samples taken at a given tunnel condition on a given day.

For evaluating the test period on daily variation:

- x_j = average of all sample estimates taken at a given tunnel condition on a given day.
 n_s = number of different days when samples were taken at a given tunnel condition.

For evaluating the yearly variation:

- x_j = average of all sample estimates taken at a given tunnel condition during a season.
- n_s = number of different test periods (e.g., January and June 1981) when samples were taken at a given tunnel condition.

Based on this procedure, the samples were normalized to account for absolute cloud differences at the various tunnel settings and pooled to lend confidence to the variation estimates since in most cases with the PMS probes, only 1 to 3 tests were conducted at a given tunnel condition over a two day period. Hence all of the accepted samples from a given instrument were not necessarily used in evaluating the effects listed under each column of the table.

Prominent features of the summary table include the following observations:

- Larger LWC variations exist between sprays taken at fixed tunnel settings than during given sprays. Measurements from the accretion devices show average temporal deviations of 4 to 6 percent and normalized test point to test point variations of 10 to 20 percent.
- Generally larger LWC variations are indicated from the PMS probe measurements and infers that their estimates of LWC are less reliable than those of the accretion devices. Larger variations are also found between sprays of fixed tunnel conditions than during given sprays.
- Although slightly larger MVD variations are also shown to exist between sprays, the variations of between 3-7 percent are small and not significantly different than the averages of 2 to 3 percent shown for given sprays. For a MVD of $25 \mu\text{m}$, these percentages translate to absolute variations of less than about $1 \mu\text{m}$.
- Cloud variations among tests conducted at given tunnel settings were similar irregardless of whether the tests were conducted on a given day or on different days as indicated by similar values listed beneath the given day and test period headings.
- Although a 12 percent yearly variation is listed, it is noted that the estimate is based only on one tunnel setting ($k = 1$) and on measurements taken with the J-W device in January and June 1981 ($n_s = 2$) and therefore does not present a representative estimate of the yearly variation.

Based on these observations it is concluded that the IRT clouds are quite homogeneous (± 5 percent in LWC and $\pm 2-3$ percent in MVD) during given tests and are highly reproducible ($\pm 10-15$ percent in LWC and $\pm 3-7$ percent in MVD). These estimates are considered not to be inconsistent with estimates provided by NASA which are based upon errors due to pressure and velocity settings of the IRT operating equations given in a previous section.

NASA curves on drop size (MVD) error as functions of maximum errors of air and water pressure settings (± 2 PSI) and of tunnel velocity (± 2 mph) are presented in Figures 4-1 to 4-3, respectively. Percentage error curves in LWC are presented in Figure 4-4 for maximum air and water pressure setting errors of ± 2 PSI. Distinguishing features of the NASA error curves include the following:

- The drop size error due to an error in air pressure setting increases with decrease in air pressure and in tunnel velocity, and with increase in the absolute difference between the water and air pressure and amounts to less than $\pm 2 \mu\text{m}$ for a ± 2 PSI setting error.
- The drop size error due to an error in the water pressure setting increases with decrease in air pressure setting and in tunnel velocity but with decrease in the absolute difference between the water and air pressures and amounts to less than $\pm 2 \mu\text{m}$ for a ± 2 PSI setting error.
- The drop size error due to an error in the velocity setting increases with decrease in air pressure setting and in tunnel velocity, and with increase in the absolute difference between the water and air pressure settings and amounts to less than $\pm 0.3 \mu\text{m}$ for a ± 2 mph setting error.
- For a ± 2 PSI error in either the air or water pressure setting, the percentage error in LWC increases exponentially with decrease in the absolute difference between water and air pressure settings. For this setting error, a LWC error of ± 5 percent is indicated for a 20 PSI pressure difference (PD) and increases exponentially to ± 20 percent at a PD of 5 PSI. The effect of a ± 2 mph velocity setting error has a negligible influence on cloud LWC and MVD.

4.2 IRT Cloud Uniformity

Cloud uniformity is concerned in this analysis task with cloud variations along a direction perpendicular to the air flow in the IRT test section

ORIGINAL PAGE IS
OF POOR QUALITY

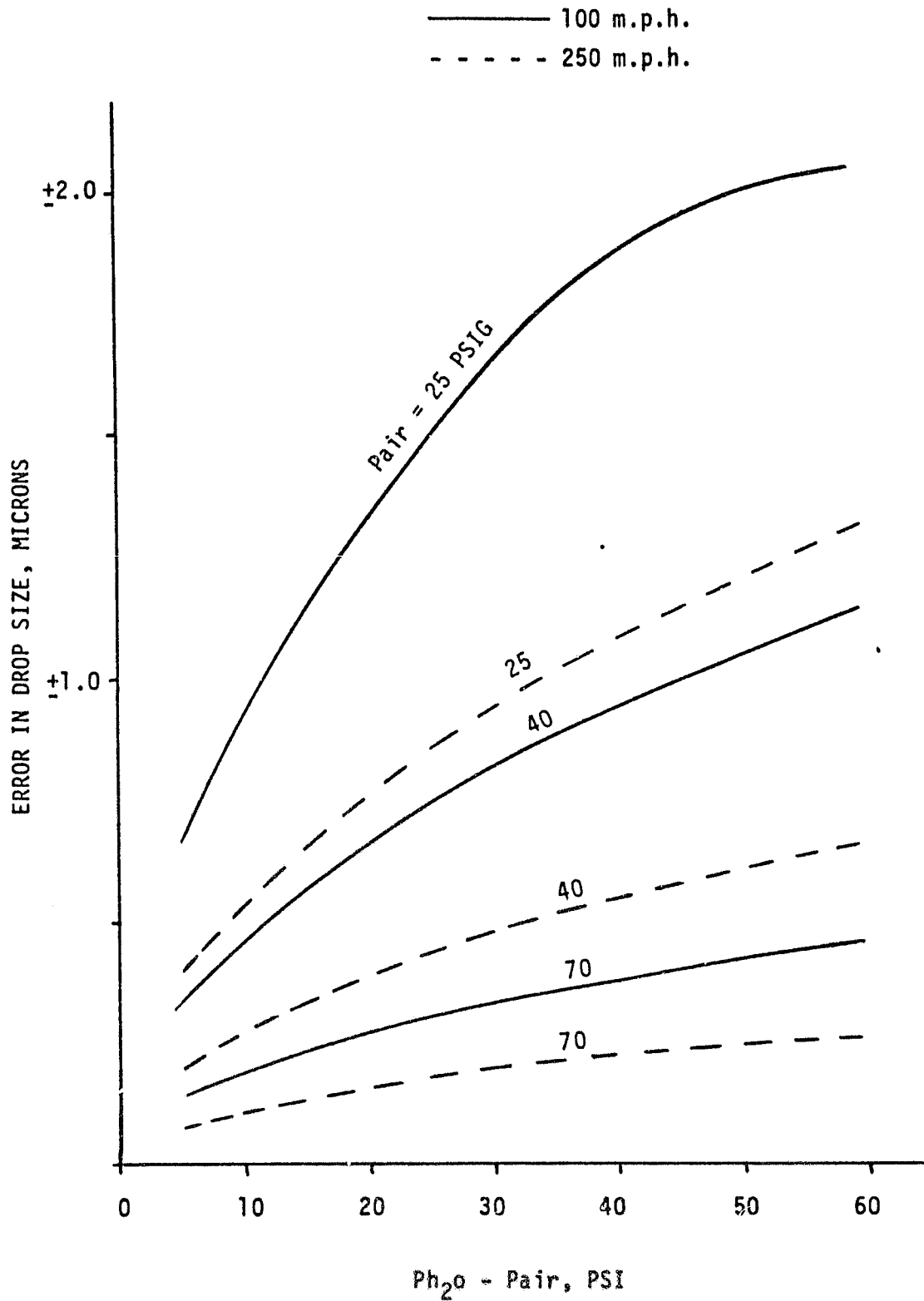


Figure 4-1. DROP SIZE ERROR IN IRT DUE TO PRESSURE SETTING ERROR
ERROR IN PAIR of ± 2 PSI (MAX ERROR)

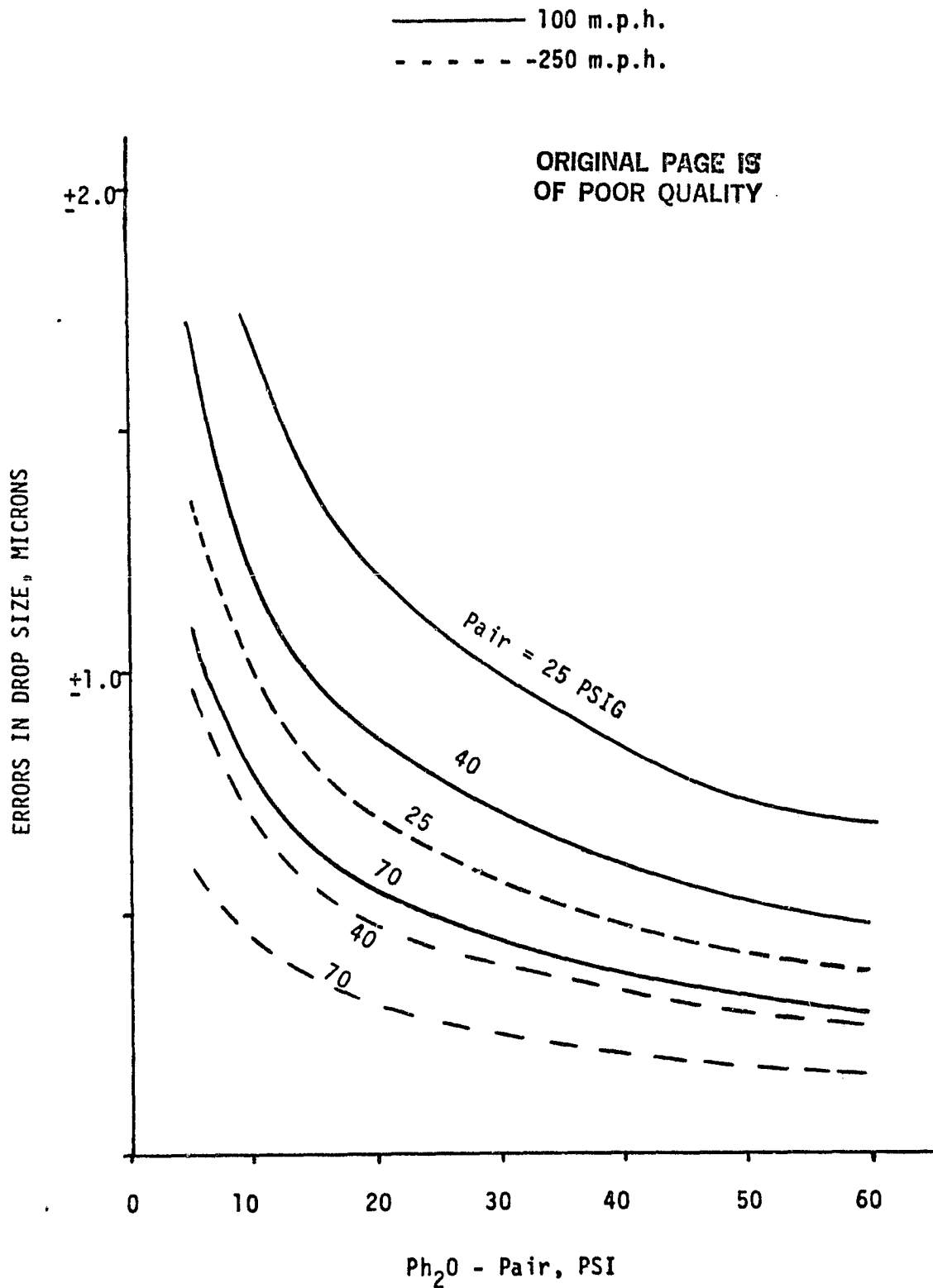


Figure 4-2. DROP SIZE ERROR IN IRT DUE TO PRESSURE SETTING ERROR
ERROR IN PWATER of ± 2 PSI

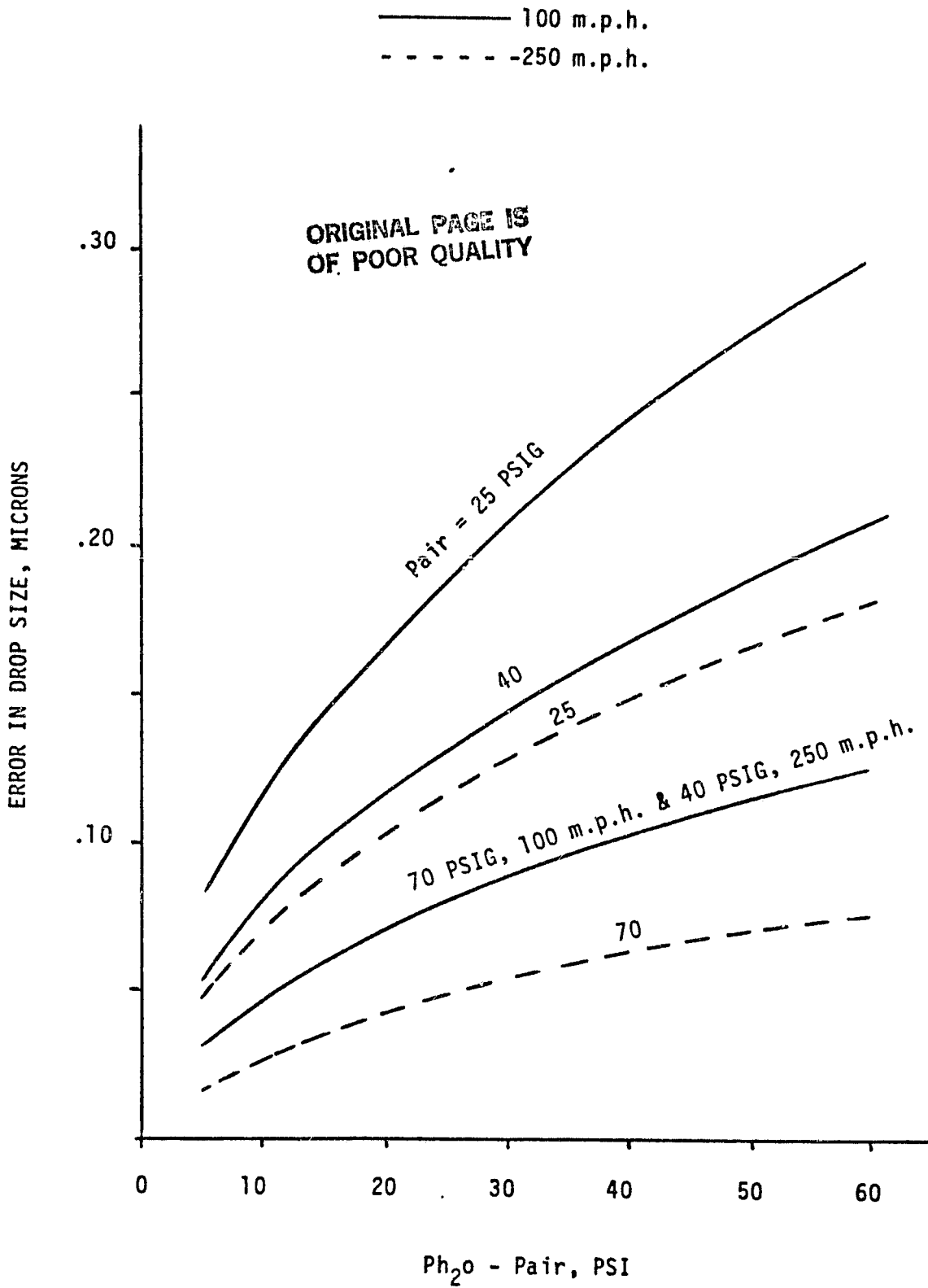


Figure 4-3. DROP SIZE ERROR IN IRT DUE TO VELOCITY SETTING ERROR
 ERROR IN VELOCITY of ± 2 M.P.H. (MAX ERROR)

ORIGINAL PAGE IS
OF POOR QUALITY

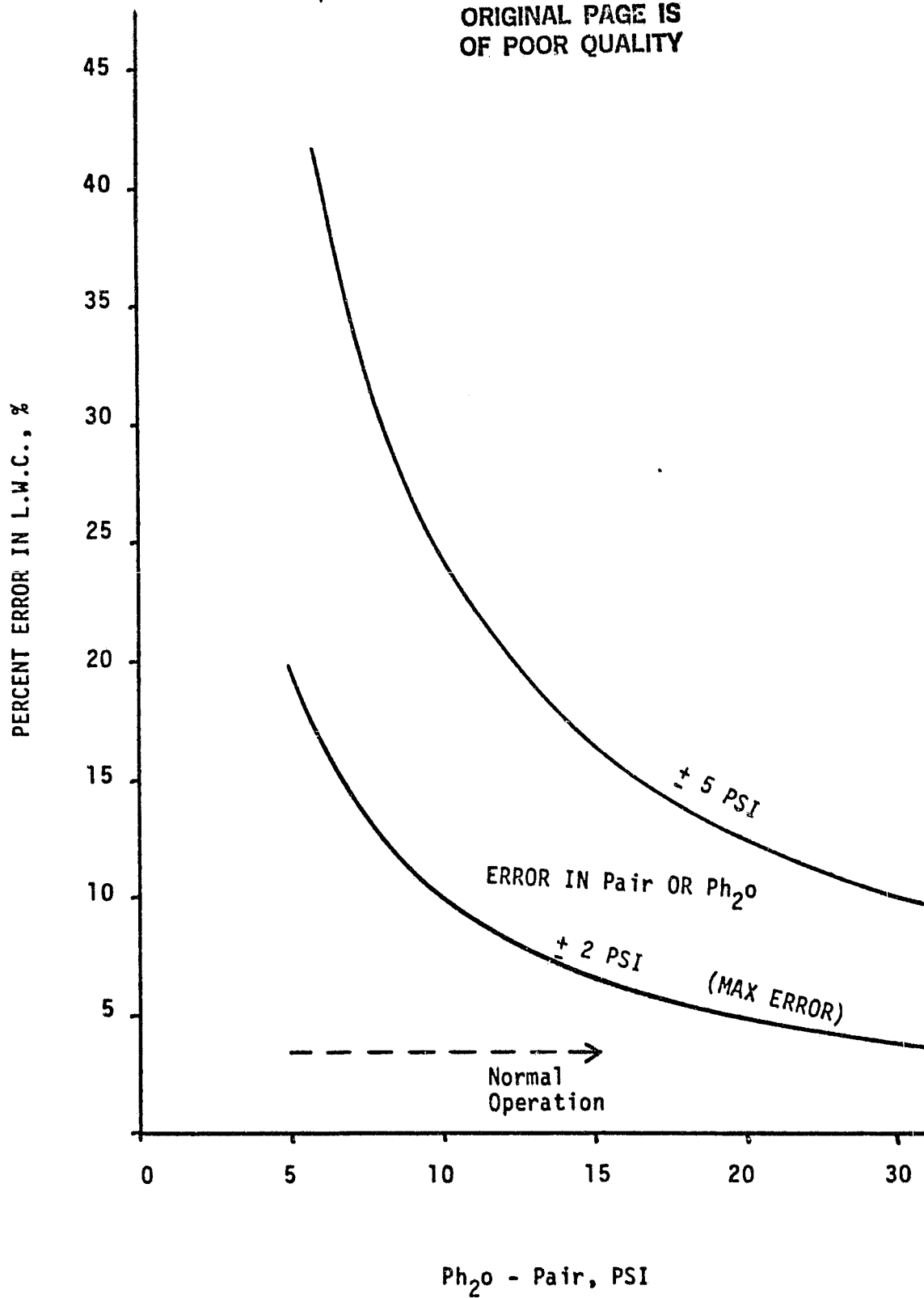


Figure 4-4. LWC ERROR IN IRT DUE TO PRESSURE SETTING ERROR

and serves to determine whether or not cloud (LWC and MVD) differences existed between the sampling locations of the two PMS probes. The probes were separated by approximately 8 inches. To attain this objective, measurements were taken at fixed and known distances from the center of the test section by moving the test stand along the cross-wind direction. For the evaluation, measurements made at fixed tunnel conditions on 8 January 1981 and on 30 October 1979 (Boeing-Vertol tests) serve as the data base. Unfortunately, both the Leigh and J-W devices were inoperative during this segment of testing in January and were not installed during the Boeing-Vertol tests.

Table 4-3 presents comparisons of the cloud measurements for these tests which were conducted at two different but fixed tunnel conditions. From the 95 percent confidence interval (CI) given for the five centered measurements and from the approximate 10 percent CV determined for the two off-centered estimates, it can be concluded statistically that the given cloud was not significantly different at $\pm 12''$ from tunnel center on 8 January. Since only one test point measurement for a given tunnel condition was obtained at each of the test stand positions in the Boeing-Vertol tests, no statistical

Table 4-3

TUNNEL UNIFORMITY COMPARISONS OF
CLOUD LWC AND MVD AT GIVEN DISTANCES FROM
TUNNEL CENTER FOR FIXED TUNNEL CONDITIONS

Date	Test Stand Position	No. of test points	$\overline{\text{LWC}}$ (g/m ³)	95% CI (g/m ³)	$\overline{\text{MVD}}$ (μm)	95% CI (μm)
<u>ASSP 2 ESTIMATES</u>						
1/8/81	12" North	1	0.09	-	21	-
	Center	5	0.17	0.10-0.25	23	19-27
	12" South	1	0.11	-	19	-
<u>BOEING VERTOL - ASSP ESTIMATES</u>						
10/30/79	24" North	1	0.60	-	17	-
	Center	1	0.88	-	19	-
	24" South	1	0.87	-	19	-

conclusions can be given. However, based on the statistics given for the PMS probe measurements on cloud repeatability, it is strongly inferred that the LWC and MVD estimates at the given test stand positions were also not significantly different. These inferences are strongly substantiated by a large number of tests conducted by NASA IRT engineers during February 1981. In these independent tests, vertical bars (2 inch cylinders, 6 ft long) were placed at nine locations across the 9 ft width of the tunnel. Ice accretion was measured on these bars at a number of heights for several cloud and air speed settings. Since tunnel velocity remains essentially constant in the test section except for distances within 6 inches of the walls, cloud uniformity can be determined from contour plots of ice accretion. Based on these test results, NASA engineers concluded that the clouds remain uniform ($\pm 10\%$) in an approximate 2 ft high by 3 ft wide center section of the tunnel.

4.3 Effect of Steam Tube Wraps

The series of tests (210-217) conducted on 8 June 1981 were specifically designed to determine whether or not the steam tube wraps (STW) had any significant effects on the measurement precision of the PMS scattering probes. A total of eight tests were conducted at a given cloud condition and included five test points with the wraps on and three without them. The tests were conducted at two tunnel temperatures; warm (23 to 29°F) and cold (-4°F). Test point 217 which was made without the wraps at the warm condition was rejected from the analysis. Subsequent rapid heating of the tunnel after an approximately two hours operation at the cold temperatures resulted in severe underestimating of particle sizes by both PMS probes due to fogging of the optics.

Table 4-4 presents a summary of the measurements. For a given probe, the LWC estimates from measurements made without the STW are shown to be within the range of those made with the STW and therefore the small differences (± 5 percent) in the averages shown are considered insignificant. In comparing the estimates of MVD, no difference is indicated in the FSSP measurements while only a one micron or 5 percent difference is indicated in the

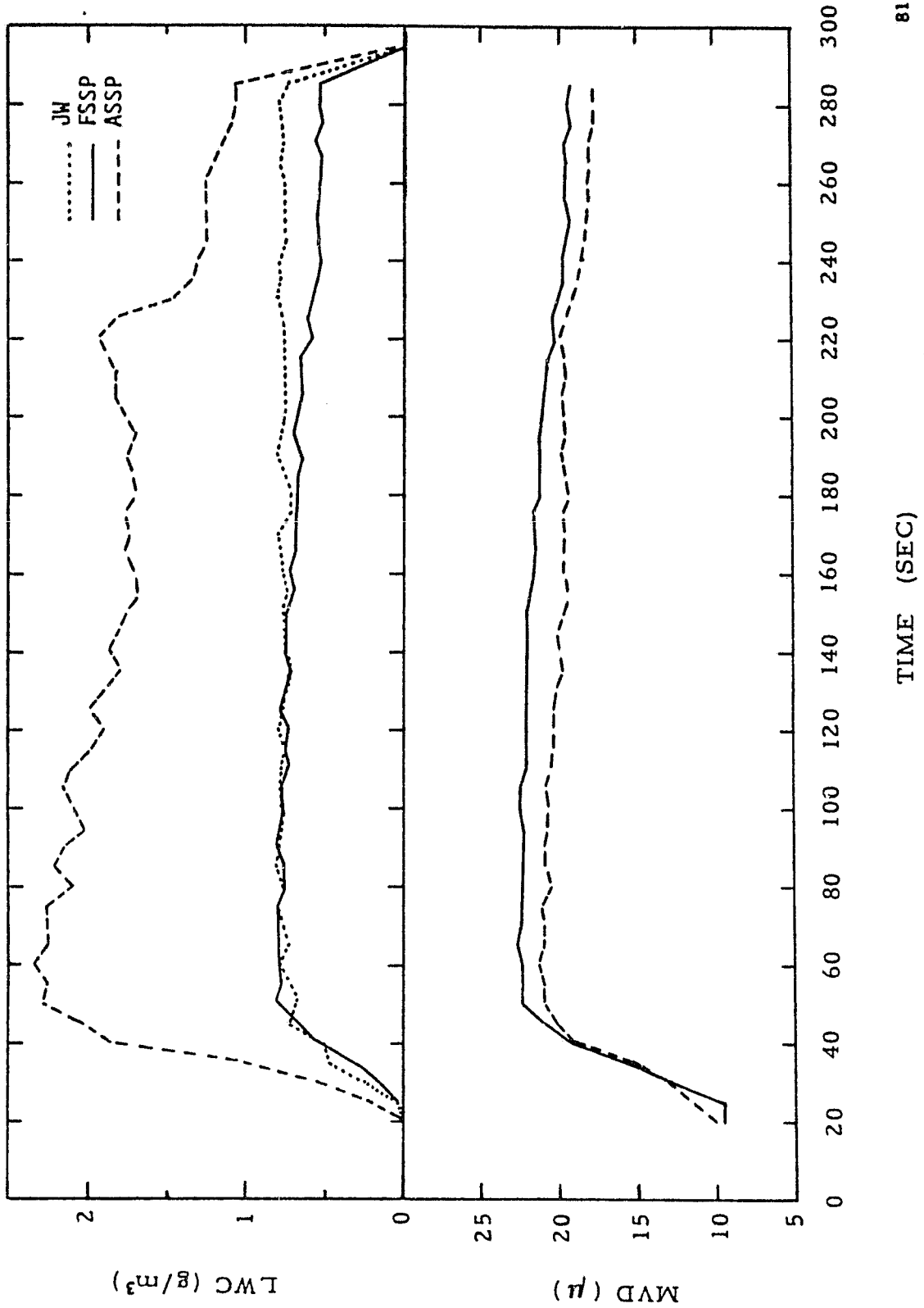
ASSP measurements. Since this 5 percent difference in MVD is similar in magnitude to the test point to test point variations given in Table 4-2, it is also considered insignificant. It is therefore concluded that the STW did not affect the measurement accuracy of these scattering probes as expected.

Table 4-4

SUMMARY OF PMS PROBE MEASUREMENTS
WITH AND WITHOUT STEAM TUBE WRAPS

Test Point Number	Temperature (°F)	Steam Tube Wrap	J-W LWC (g/m ³)	FSSP1' LWC (g/m ³)	ASSP2' LWC (g/m ³)	FSSP1' MVD (μm)	ASSP2' MVD (μm)
210	29	ON	0.71	0.71	2.61	22	21
211	23	ON	0.77	0.82	2.39	22	20
212	-4	ON	0.77	0.78	2.19	22	21
213	-4	ON	0.80	0.77	2.26	22	21
214	-4	ON	<u>0.83</u>	<u>0.76</u>	<u>2.17</u>	<u>22</u>	<u>21</u>
Average			0.78	0.77	2.32	22	21
215	-4	OFF	0.77	0.73	2.48	22	22
216	-4	OFF	<u>0.75</u>	<u>0.72</u>	<u>2.41</u>	<u>22</u>	<u>22</u>
Average			0.76	0.73	2.45	22	22
% Diff = $\left(\frac{\text{ON-OFF}}{\text{ON}}\right) \times 100$			4	5	-5	0	-5

Time plots of probe estimates of LWC and MVD for tests conducted at -4°F with and without the STW are presented in Figures 4-5 and 4-6, respectively. Although degradation is shown in the ASSP measurements in both tests, the adverse effect of not having the STW is shown (Figure 4-6) at approximately 240 seconds into the run when ice buildup practically disabled the probe. For the FSSP probe, no apparent change (compared to the J-W trace)



81/172

Figure 4-5. TIME PLOT OF INDICATED PARAMETERS TAKEN AT -4°F WITH STEAM TUBE WRAPS

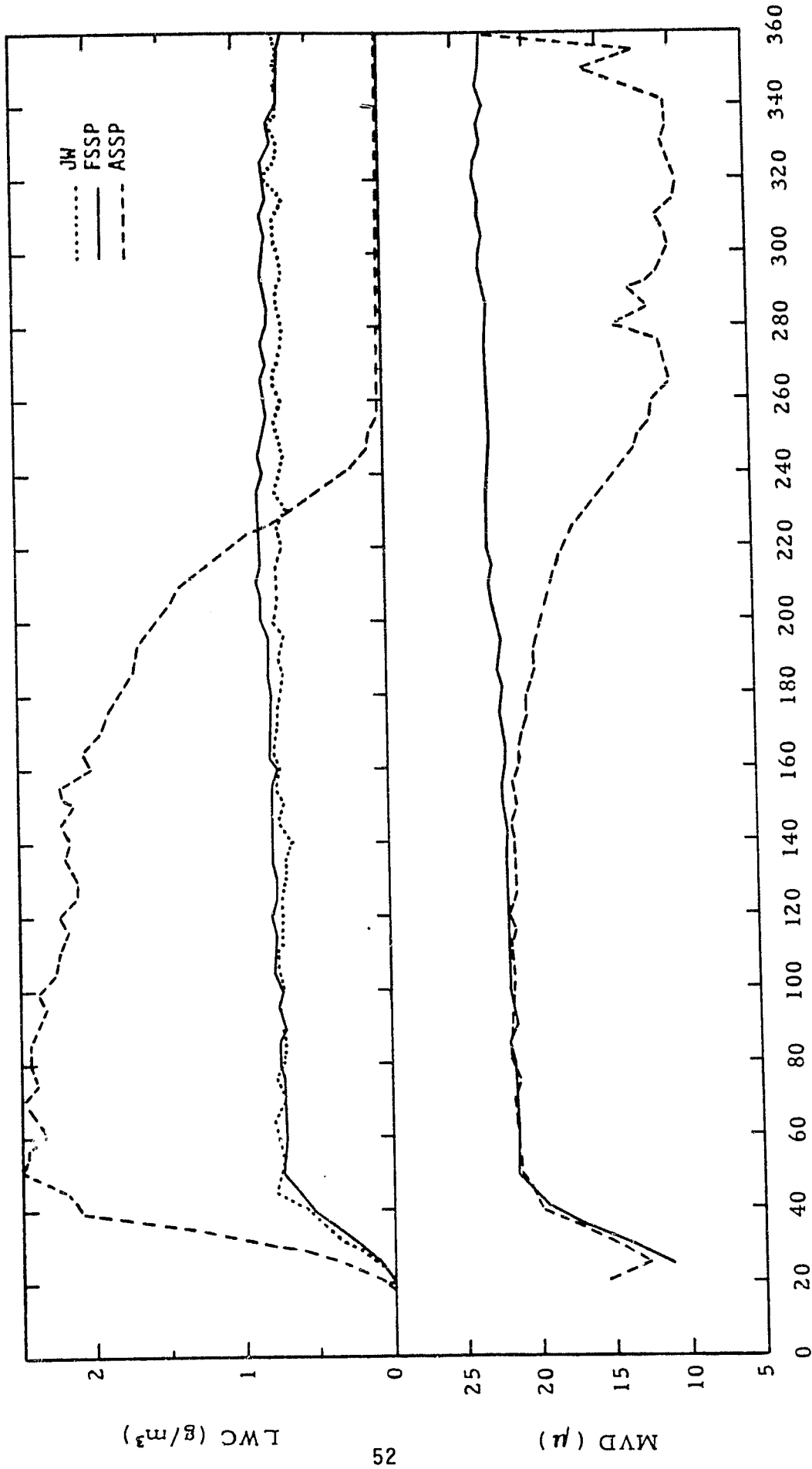


Figure 4-6. TIME PLOT OF INDICATED PARAMETERS TAKEN AT -4°F WITHOUT STEAM TUBE WRAPS

is indicated with time in the test without the STW. However, some deterioration is shown in the measurements with the STW. The far greater deterioration in the ASSP was caused by interference to the laser beam from icing over of the water deflector protrusion which was located near the tip of the laser and within its sampling tube. The FSSP devices do not have these obstructions in the sampling tube. To relieve this problem in some of the ASSP devices, the deflector pieces have since been removed and replaced functionally by warm air flow through a purge line terminating at the base of the sampling tube.

As expected, since mass is proportional to the cube of particle size, probe icing is shown to result in greater underestimations of LWC than of MVD. In the extreme case shown of the ASSP measurements in Figure 4-6, a decrease of more than one order of magnitude is indicated (~270 sec) in the LWC estimate for a factor of two underestimation in MVD. For the FSSP estimates shown in Figure 4-5, the 2 μm or 10 percent change in MVD corresponds to a reduction in LWC of about 30 percent. Hence, during normal use and especially during moderate to severe natural icing conditions, it is indicated that the probe estimates of particle sizes or MVD would tend to be more precise than of the higher moment related parameters such as LWC.

4.4 Effects of Temperature and Velocity on Probe Performance

Of concern to users is knowledge of the measurement accuracy of the various cloud instruments under various operating and environmental conditions. The IRT provided opportunities to investigate two possible problem areas; namely the effects of temperature and velocity on instrument performance. Studies by NASA LeRC personnel suggest that all ice accretion instruments including the Leigh IDS systematically underestimated LWC at temperatures near the freezing point of water. This decrease in accuracy has been attributed to the Ludlam Limit which is associated with a condition where less than 100 percent of the supercooled deposits freeze upon impact as a result of heating caused by the release of the latent heat of fusion. Primary factors which determine the Ludlam Limit on the device are the ambient temperature, collection rate and perhaps droplet sizes. Since higher numbers of observations were taken during the January program, it seemed appropriate to further examine this effect. Unfortunately, the tests were conducted at temperatures

which were either much warmer than the operating limit (<32°F) of the device or much colder (<17°F) than the temperature range of 20 to 32°F where instrument accuracy was suspect.

For users with turbojet aircraft, information on the accuracy of the spectrometer measurements at airspeeds close to and beyond the upper limit set for by the manufacturer of about 250 Kts (~285 mph) is also desired. Of particular interest is to what degree are the particles undersized at or beyond the upper velocity limit. Unfortunately, tunnel blockage by the test stand and associated hardware limited top airspeeds to approximately 285 mph. Nevertheless it was still felt worthy of investigation.

In order to evaluate both of these effects on measurement precision, absolute standards must first be known. In both of these investigations, the cloud LWC and MVD set forth by the tunnel operating equations (Section 3.0) were chosen as references. Since the operating equations indicate that the cloud LWC and MVD are also dependent on tunnel velocity, and since only a few runs were made at a fixed cloud condition but with varying temperature, the ratios of the estimates to those given by the operating equations were stratified into given velocity and temperature ranges for evaluation. Table 4-5 presents the stratification intervals used in the evaluation with accompanying index values.

Table 4-5
DATA STRATIFICATIONS

Index	TEM (F)	TAS (MPH)
1	≤-16	50
2	-15 to -6	100
3	-6 to 0	150
4	0 to 10	200
5	10 to 20	225 to 275
6	20 to 30	>275
7	>30	-

The results of this evaluation procedure are presented in Figure 4-7 for measurements taken with the Leigh and J-W devices. The means and standard deviations (error bars) are plotted against the corresponding index values. For the Leigh measurements, no systematic change with temperature increase is shown in the mean ratio values as expected. Except for the observations made at a tunnel velocity of 50 mph, the remaining average ratio values display no apparent dependency on velocity. At the lowest tunnel velocity, the Leigh device consistently underestimated the tunnel values. The random fluctuations of the means also indicate that the J-W estimates were not affected by the tunnel temperatures. Although a general increase in the values of the means is shown with speed increase, the wide error bars indicate that the effects of tunnel velocity were insignificant. These observations are consistent with the few runs made at fixed temperature and pressure settings but at varying tunnel velocities. Plots of these test point estimates for both these devices appear in Figure 4-8.

In the MVD evaluations (Figure 4-9) of the PMS probe measurements, the means also remain fairly constant indicating that temperature changes did not bias these estimates. However, the means are shown to increase systematically with increases in tunnel velocity. This dependency is further exemplified in Figure 4-10 from the test series conducted at fixed temperature and pressure settings and show that while the tunnel values based on the operating equations gradually decrease with speed increase, the probe estimates remain fairly constant for speeds exceeding about 100 to 150 mph. Although these comparisons may perhaps suggest possible bias in the probe estimates, they may likewise infer possible errors in the operating equations. Discussions on these comparisons are presented in the following section.

4.5 Instrument Intercomparisons

Of primary interest to the total analyses effort is perhaps the comparability of the measurements from the various instruments. Aside from establishing the comparability of the measurements from given clouds, the measurements also lend means to reevaluate the calibrations performed with the rotating cylinders. Table 4-6 presents regression analysis results (by the method of test squares) for the various instruments listed and includes the following information:

ORIGINAL PAGE IS
OF POOR QUALITY

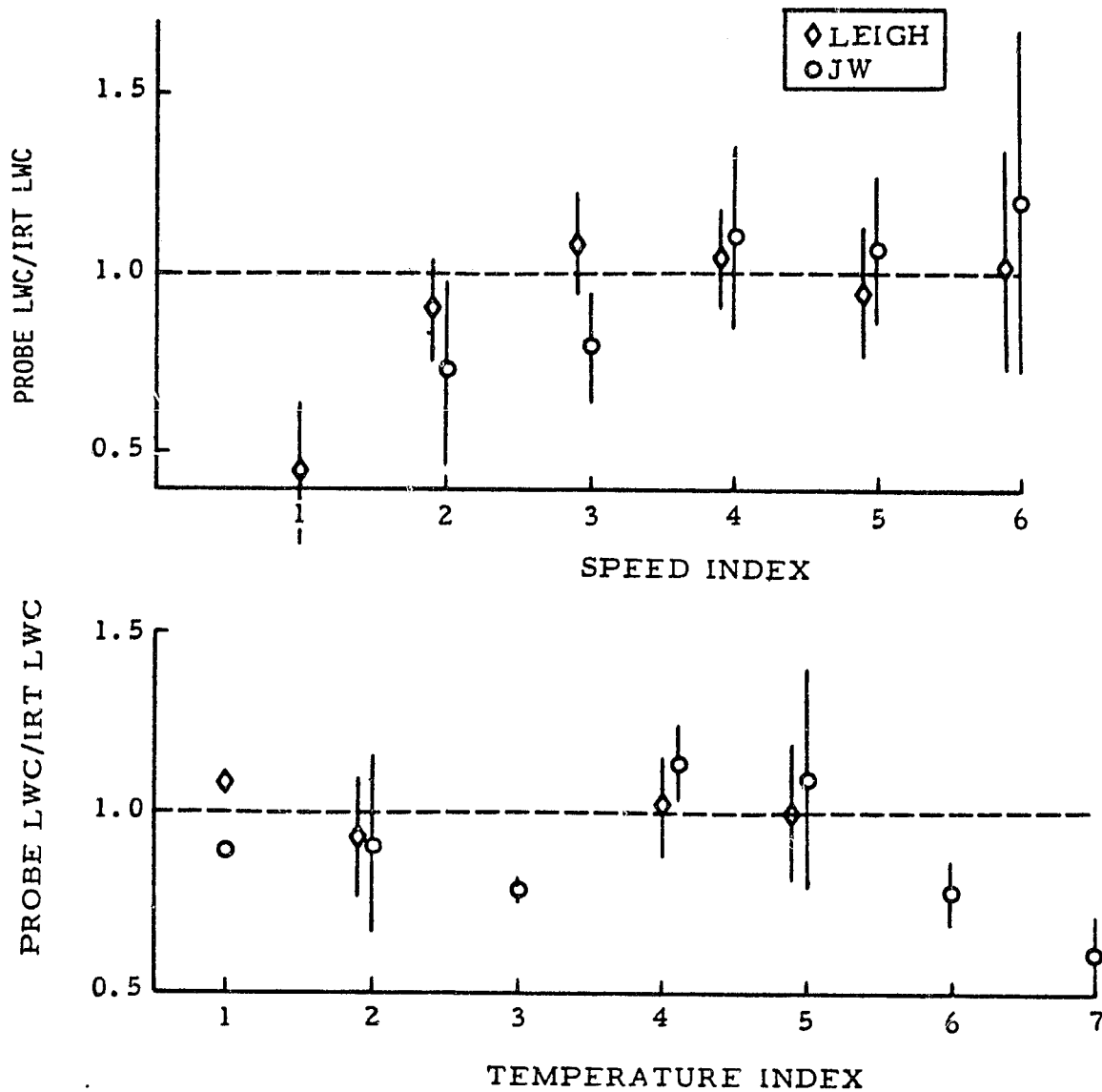


Figure 4-7. AIR SPEED AND TEMPERATURE EFFECTS ON PROBE ESTIMATES OF LWC

ORIGINAL PAGE IS
OF POOR QUALITY

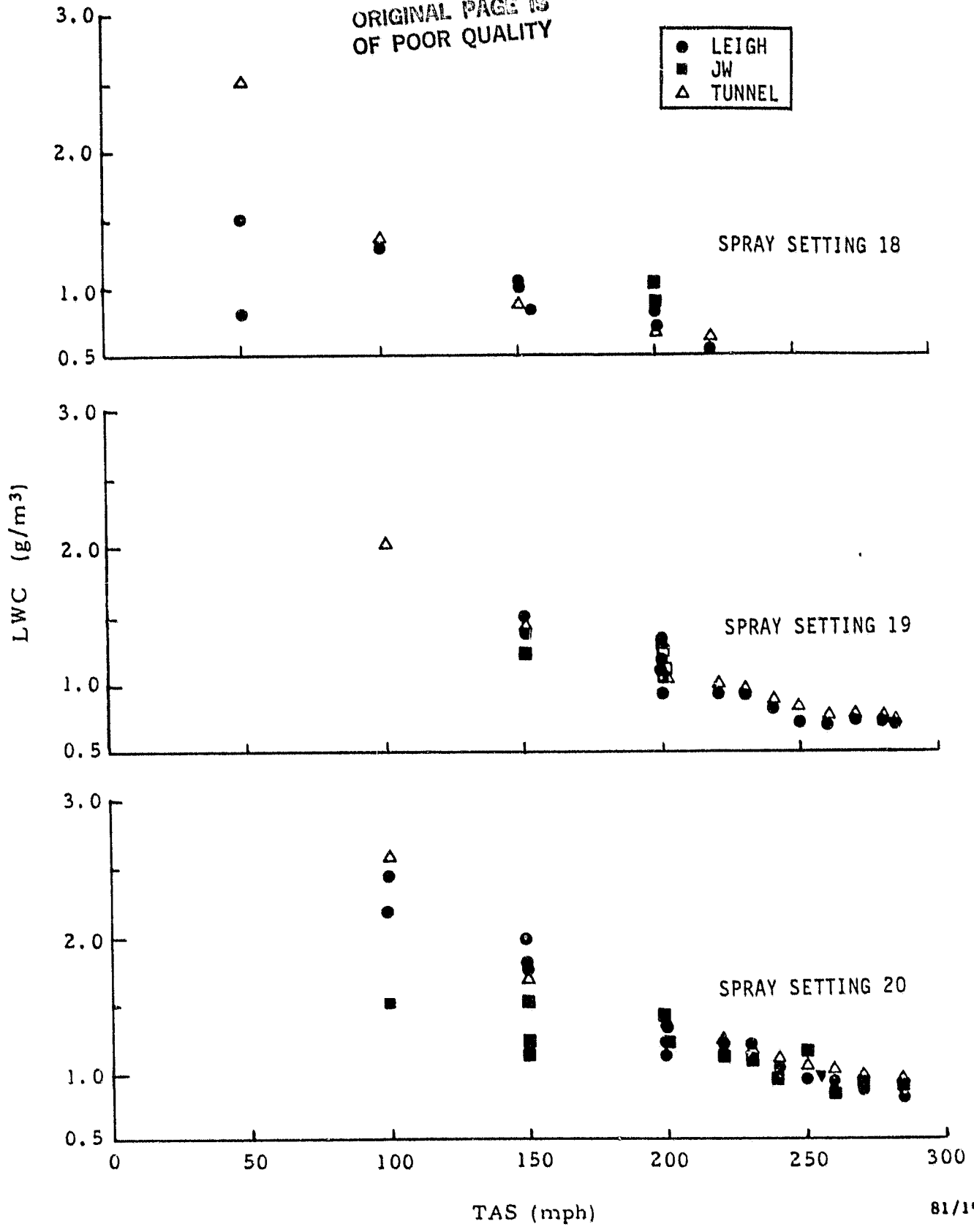
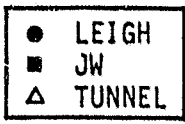


Figure 4-8. VELOCITY EFFECTS ON PROBE ESTIMATES OF LWC FOR GIVEN SPRAY SETTINGS

ORIGINAL PAGE IS
OF POOR QUALITY

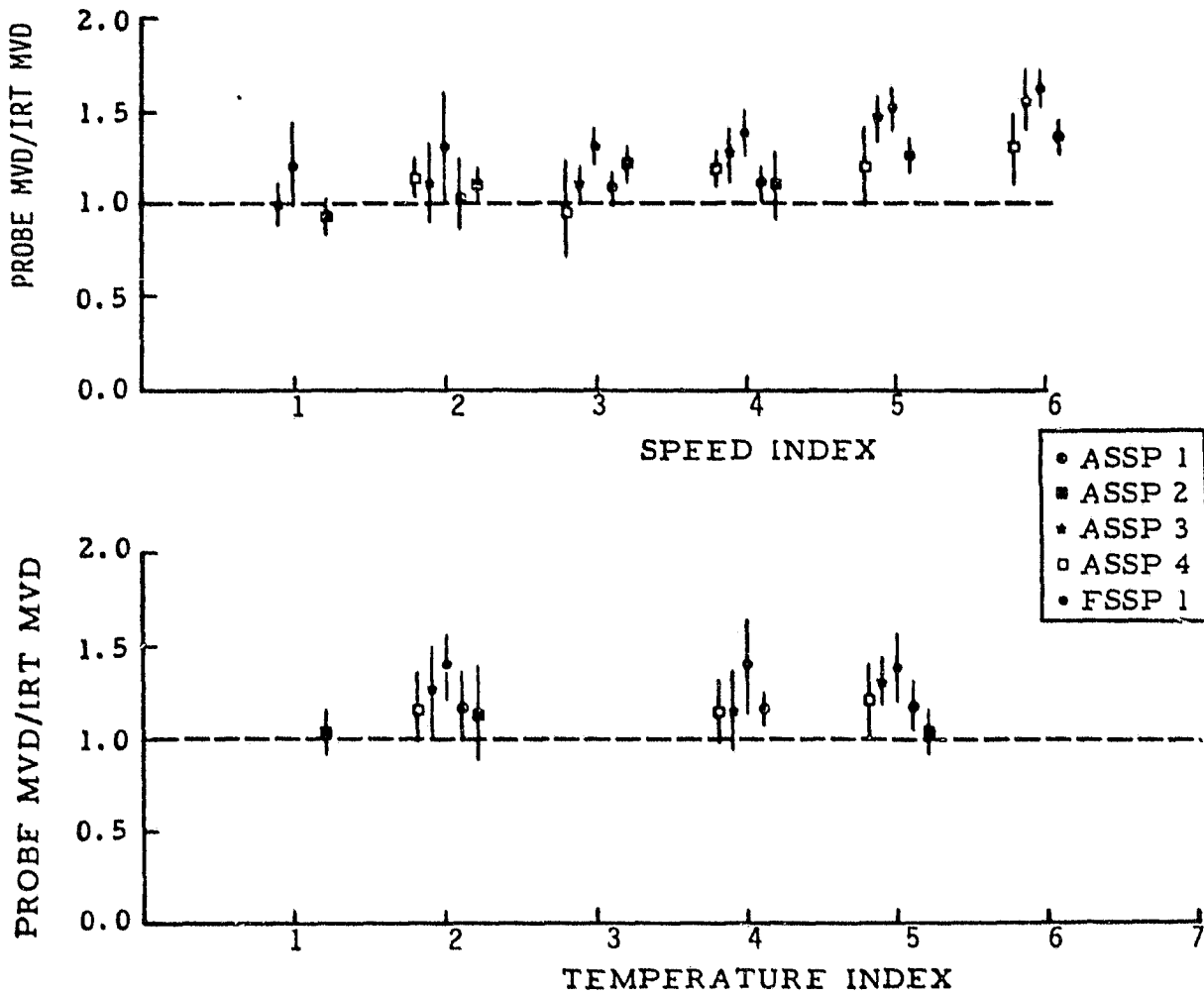


Figure 4-9. AIR SPEED AND TEMPERATURE EFFECTS ON
PROBE ESTIMATES OF MVD

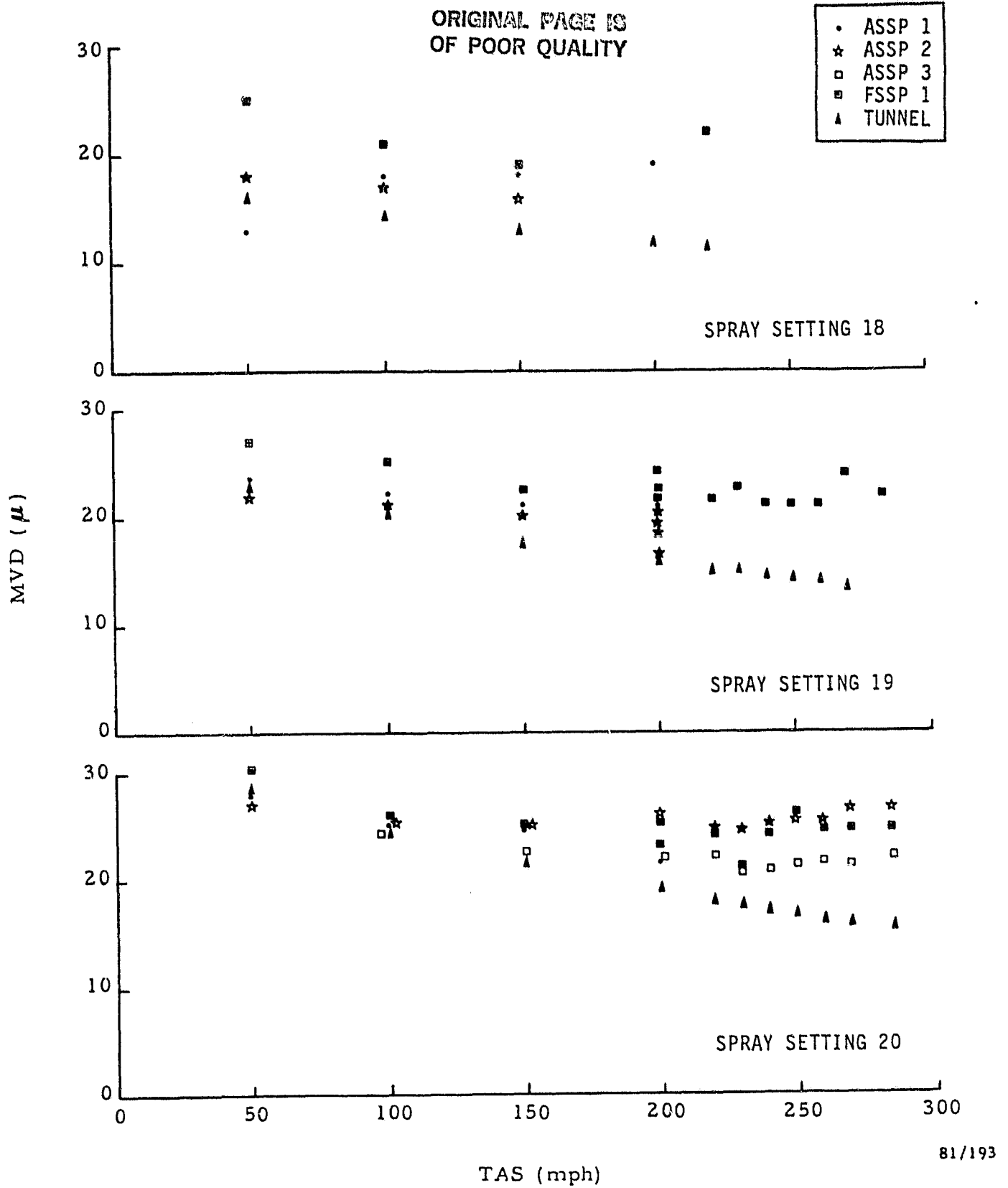


Figure 4-10. VELOCITY EFFECTS ON PROBE ESTIMATES OF MVD FOR GIVEN SPRAY SETTINGS

ORIGINAL PAGE IS
OF POOR QUALITY

Table 4-6

INSTRUMENT COMPARISONS
LINEAR REGRESSION ANALYSIS SUMMARY
 $y = a + bx$

Instruments	n	a	b	r	e	Comparisons
J-W vs Tunnel*	80	0.75	0.24	0.28	0.26	LWC
Leigh vs Tunnel	154	0.39	0.60	0.79	0.21	LWC
Leigh vs J-W	57	0.45	0.61	0.51	0.25	LWC
PMS vs Tunnel	121	0.17	0.55	0.58	0.72	LWC
FSSP 1 vs Tunnel	37	0.21	0.09	0.65	0.09	LWC
ASSP 1 vs Tunnel	22	0.02	1.28	0.87	0.37	LWC
ASSP 2 vs Tunnel	10	-0.01	0.57	0.95	0.27	LWC
ASSP 3 vs Tunnel	29	0.34	0.81	0.87	0.51	LWC
ASSP 4 vs Tunnel	23	-0.51	0.81	0.89	0.21	LWC
PMS vs \overline{PMS}	121	0.0	1.00	0.65	0.66	LWC
PMS vs Tunnel	121	13.1	0.50	0.57	2.6	MVD
FSSP 1 vs Tunnel	37	15.6	0.47	0.69	1.8	MVD
ASSP 1 vs Tunnel	22	12.8	0.39	0.62	1.8	MVD
ASSP 2 vs Tunnel	10	10.2	0.60	0.96	0.9	MVD
ASSP 3 vs Tunnel	29	13.4	0.50	0.50	3.3	MVD
ASSP 4 vs Tunnel	23	8.7	0.70	0.78	1.8	MVD
PMS vs \overline{PMS}	121	0.0	1.00	0.79	1.9	MVD

*The tunnel estimates are based on the IRT operating equations.

1. n = number of data pairs.
2. a = intercept of the linear equation of the form $y = a + bx$.
3. b = slope of linear equations.
4. r = correlation coefficient.
5. e = standard deviation of regression.

It is noted that for a given comparison, the estimates from the instrument listed first represent the dependent variables, while the estimates of the instrument listed second represent the independent variables. Hence, for the listed instruments, Leigh versus J-W, y and x are represented, respectively by the measurements from the Leigh and J-W devices. For these comparisons, the tunnel values were determined from the IRT operating equations.

Comparisons with the Leigh and J-W devices included all of the accepted test point estimates. The PMS scattering probe comparisons, however, included only those measurements from given tunnel conditions (fixed airspeed and pressure settings) where the measurements from at least two different probes were deemed acceptable. This compromised data selection was used since comparisons between probes should be made of clouds having common microphysics properties and since only a few (four) sets of acceptable measurements from all five of the PMS probes were obtained under the same tunnel or cloud conditions. Based on this data selection criteria, measurements from 37 different tunnel conditions were compared. In addition, for each tunnel condition, the data from each probe is represented by the average of the corresponding test point estimates.

Scatter diagrams comparing the LWC measurements from the Leigh and J-W devices against the tunnel estimates (IRT LWC) and against each other are presented in Figures 4-11 to 4-13 and show that the measurements are generally in agreement with the calibrations performed with the rotating cylinders. As compared to the tunnel values, the measurements from both instruments are shown to fall on either side of the one-to-one line for IRT LWC of less than about 2 g/m^3 . Larger scatter is also evident of the J-W measurements in this range as is also indicated from the larger values of e listed in Table 4-6. For IRT LWC exceeding 2 g/m^3 , the measurements from both instruments fall below

ORIGINAL PAGE IS
OF POOR QUALITY.

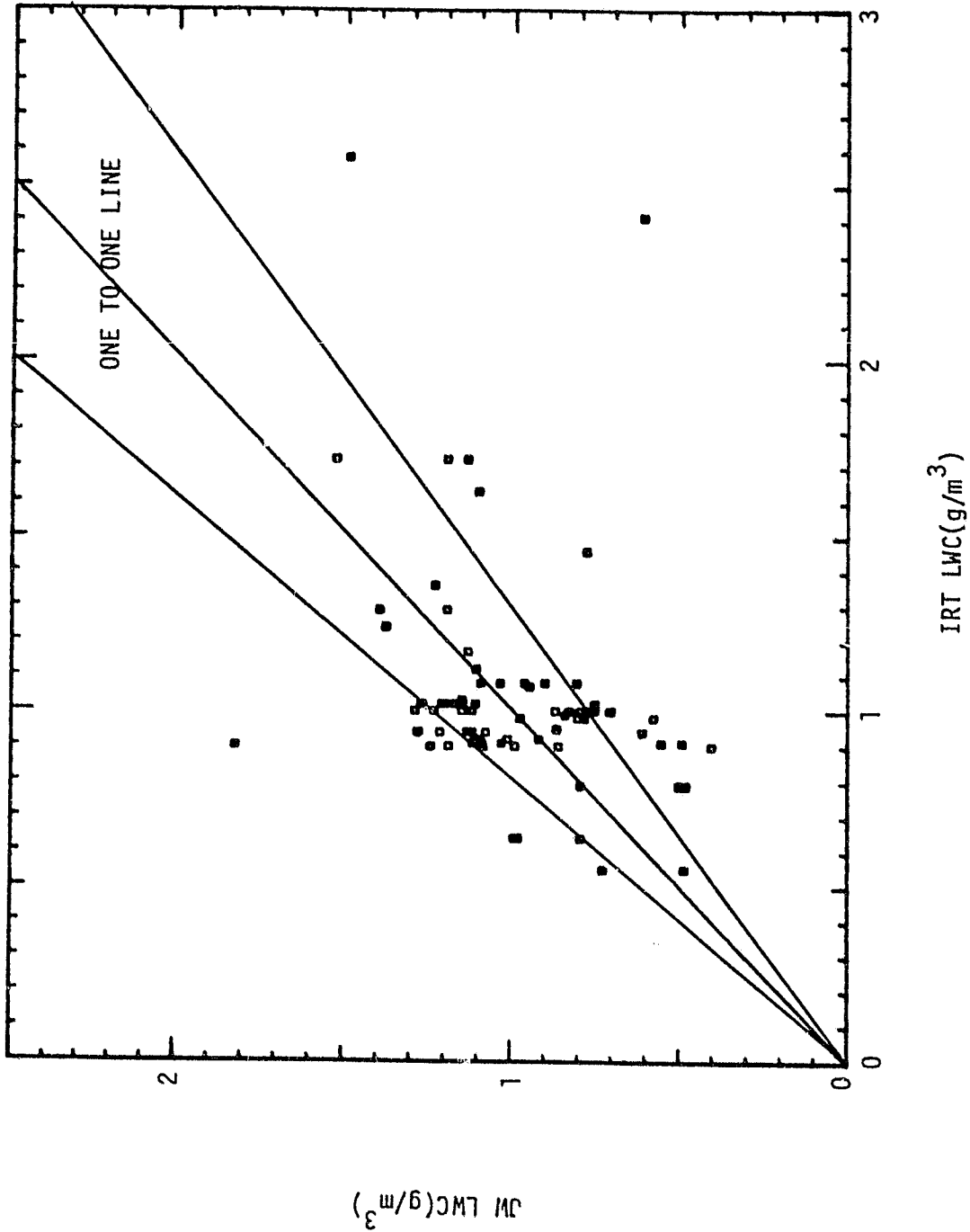


Figure 4-11. SCATTER DIAGRAM OF J-W LWC VERSUS IRT LWC

ORIGINAL PAGE IS
OF POOR QUALITY

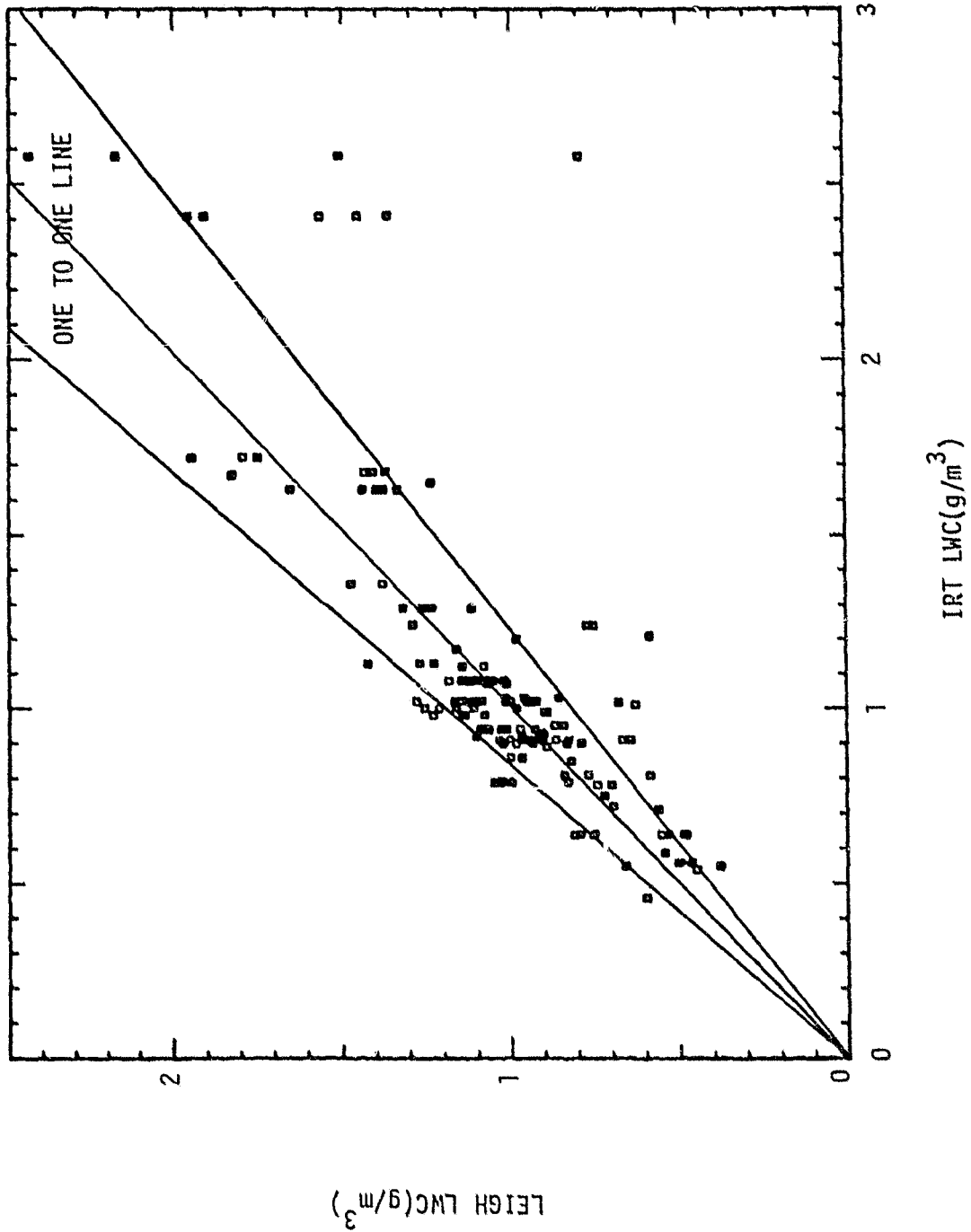


Figure 4-12. SCATTER DIAGRAM OF LEIGH LWC VERSUS IRT LWC

ORIGINAL PAGE IS
OF POOR QUALITY

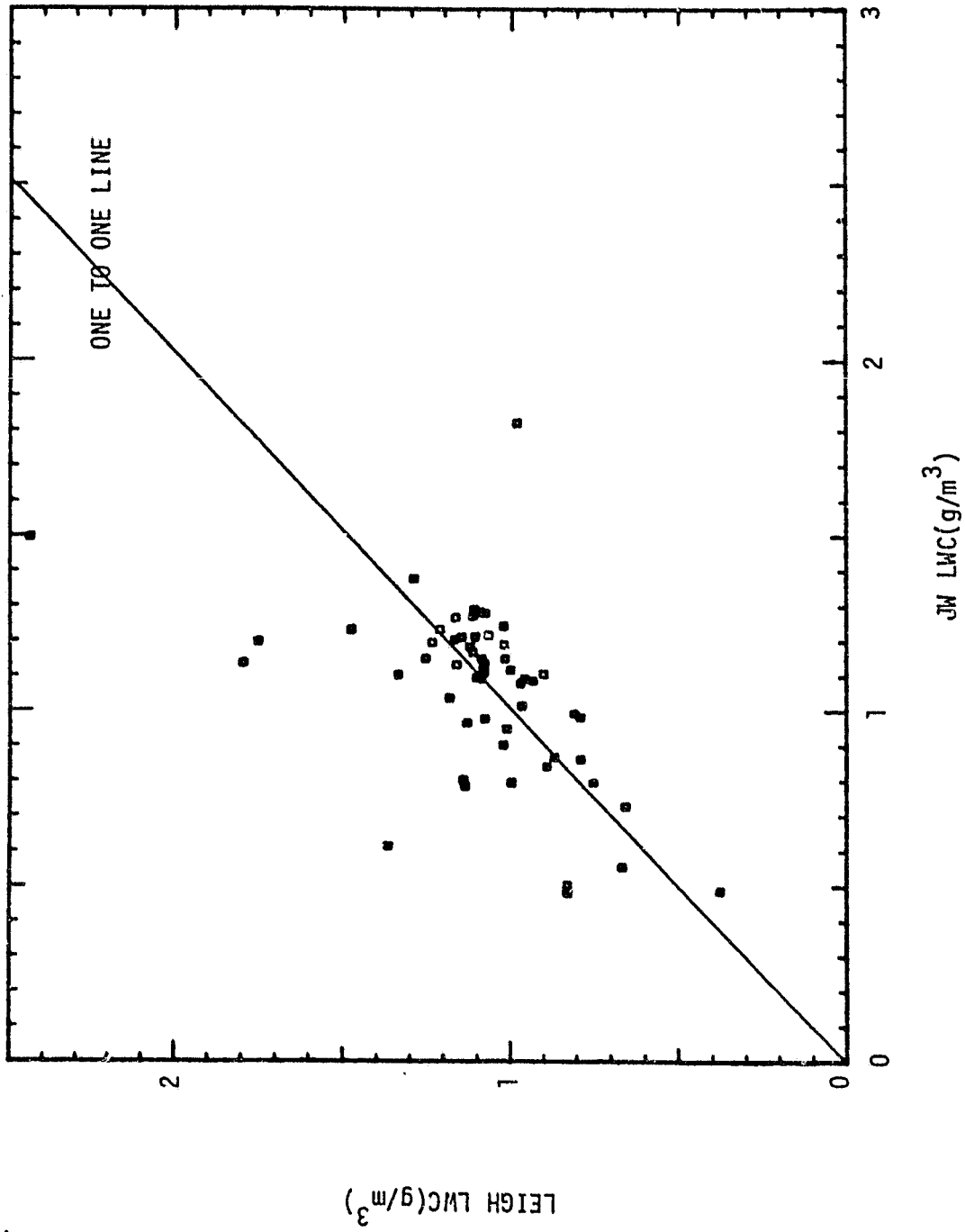


Figure 4-13. SCATTER DIAGRAM OF LEIGH LWC VERSUS J-W LWC

the one-to-one line. For the Leigh measurements plotted at the IRT LWC of 2.58 g/m^3 , the two lowest estimates were taken at a tunnel velocity of 50 mph where the device consistently underestimated the tunnel values. At the IRT LWC setting of 2.41 g/m^3 , the underestimations from the Leigh device is considered to have been caused by incomplete droplet freezing. Although not consistent with the total data set, the decrease with temperature increase (from 4 to 16°F) at this relatively high LWC condition suggests that the Ludlam Limit was reached at temperatures much colder than observed in the earlier program. This inference is not inconsistent with the observations made at the higher IRT LWC setting of 2.58 g/m^3 and the identical tunnel velocity of 100 mph since the tunnel temperatures were much colder (-12°F). Studies are currently being actively pursued by NASA LeRC personnel on the heat balance of the Leigh device and should provide more definite answers on the various causal relationships associated with the Ludlam Limit. For the J-W measurements taken at these two higher LWC settings, it is found that the clouds were characterized by relatively large particles ($\text{MVD} \sim 25 \mu\text{m}$) and, therefore, the device would be expected to underestimate the true LWC. It is also noted that the instrument performed rather intermittently ($\text{CV} \sim 20\%$) at the 2.41 g/m^3 tunnel setting and hence the test point estimate (or mean) would also be low.

As compared to the tunnel estimates, the reduced scatter of the J-W points from the line of equality in the comparison diagram with the Leigh device suggests that part of the scatter results from the uncertainty of the operating equations. This observation is reflected in the higher correlation coefficient listed for the comparisons between the two instruments. It is further noted that the J-W measurements were generally lower than those of the Leigh device.

The comparisons of the LWC estimates between the scattering probes and the tunnel are less encouraging as indicated by the wide range of values listed for the intercept and slope of the regression equation and by the corresponding scatter diagrams presented in Figures 4-14 to 4-18. The estimates from the individual probes either systematically overestimated or underestimated the the tunnel values and strongly suggests that in all but the estimates from FSSP 1, the discrepancies resulted primarily from uncertainties in their effective sampling areas. It is noted that at the two highest tunnel settings

ORIGINAL PAGE IS
OF POOR QUALITY

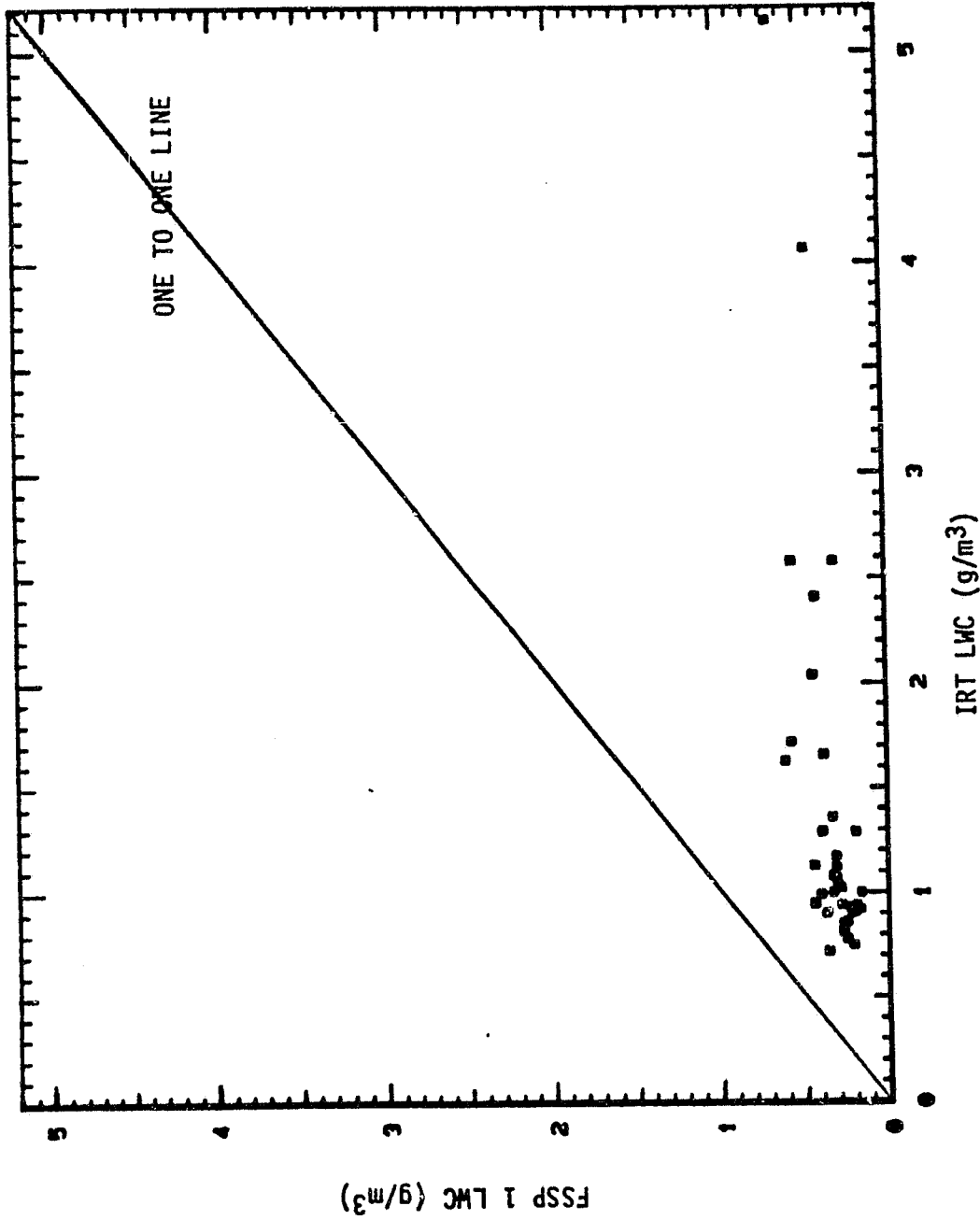


Figure 4-14. SCATTER DIAGRAM OF FSSP 1 LWC VERSUS IRT LWC

ORIGINAL PAGE IS
OF POOR QUALITY

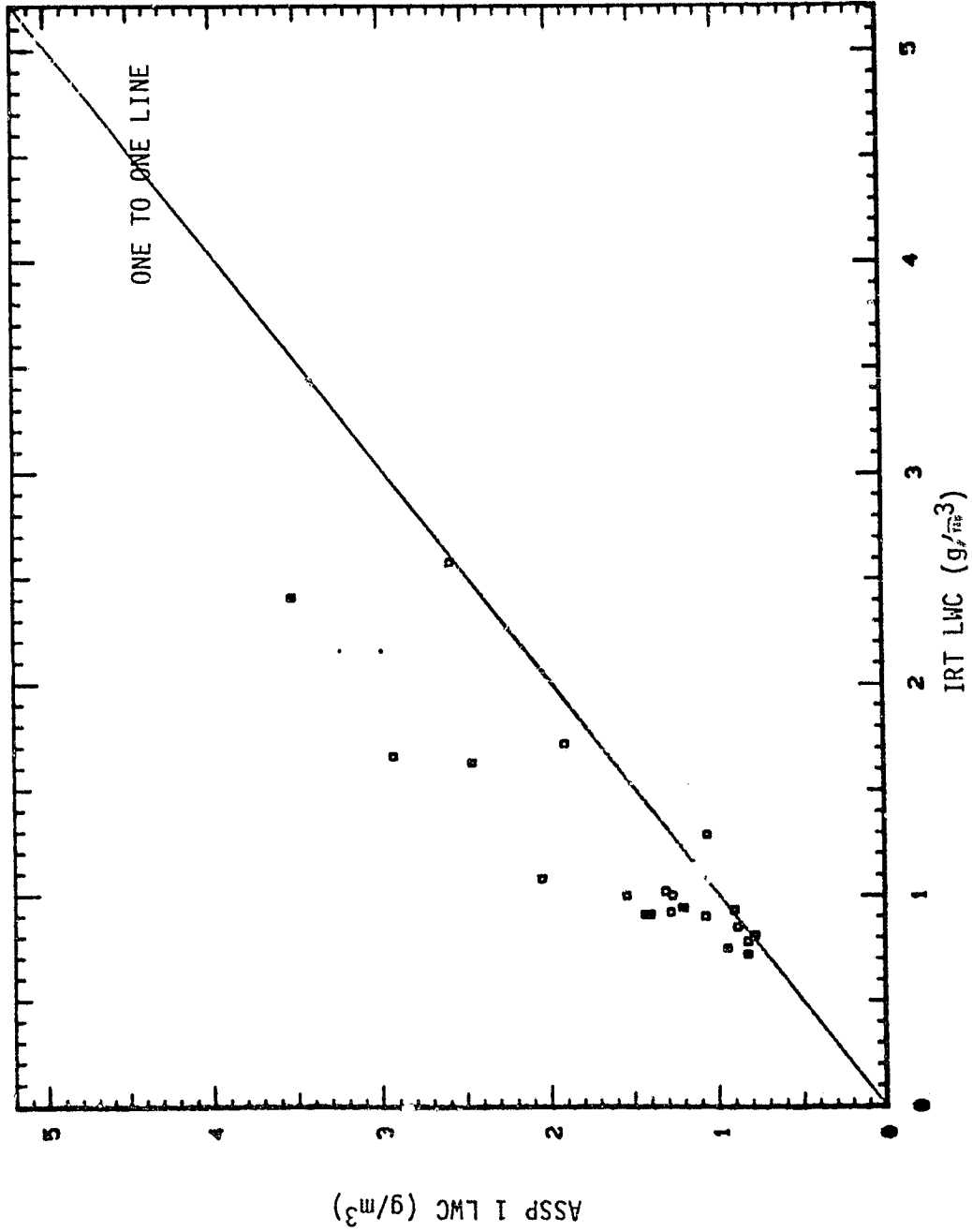


Figure 4-15. SCATTER DIAGRAM OF ASSP 1 LWC VERSUS IRT LWC

ORIGINAL PAGE IS
OF POOR QUALITY

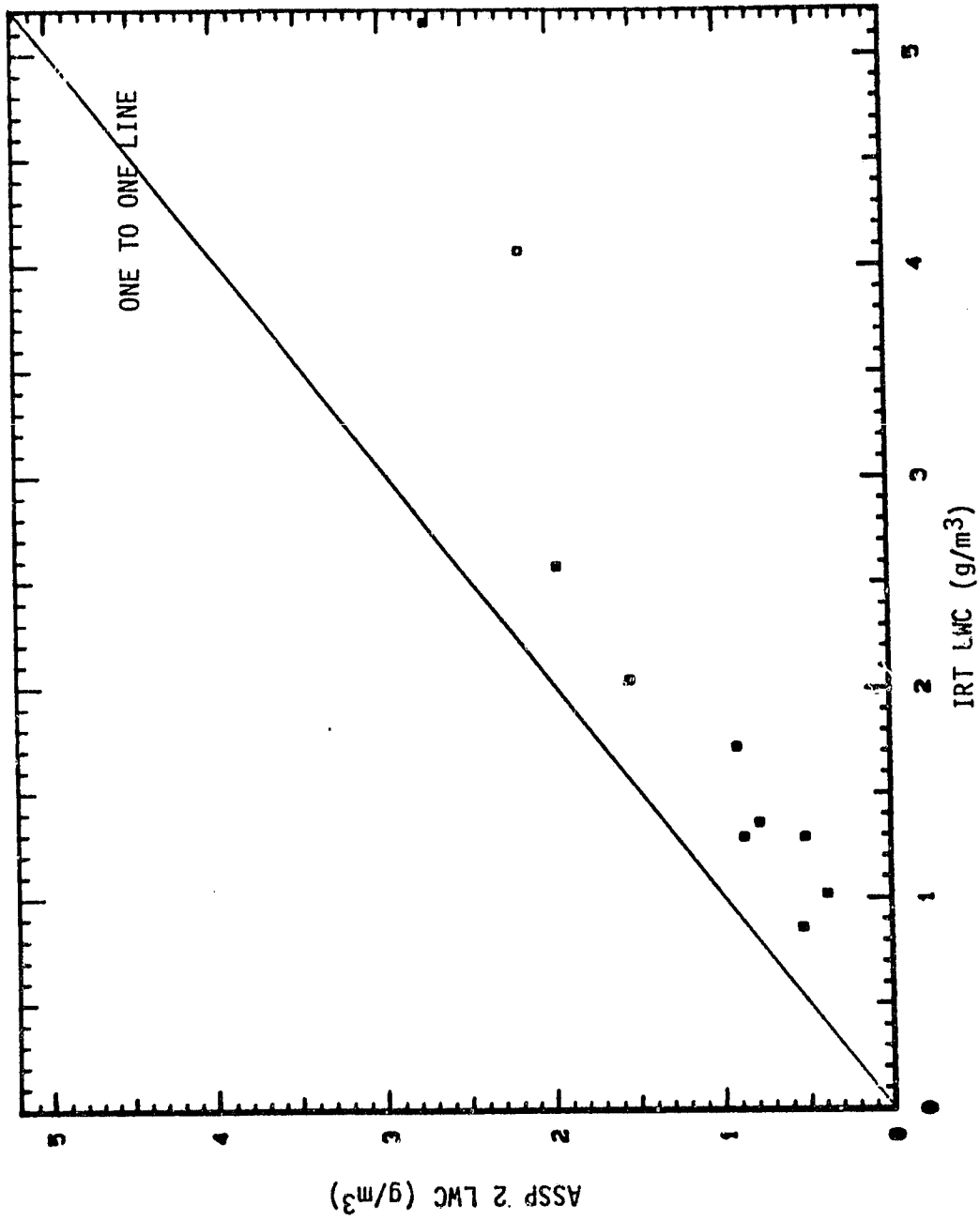


Figure 4-16. SCATTER DIAGRAM OF ASSP 2 LWC VERSUS IRT LWC

ORIGINAL PAGE IS
OF POOR QUALITY

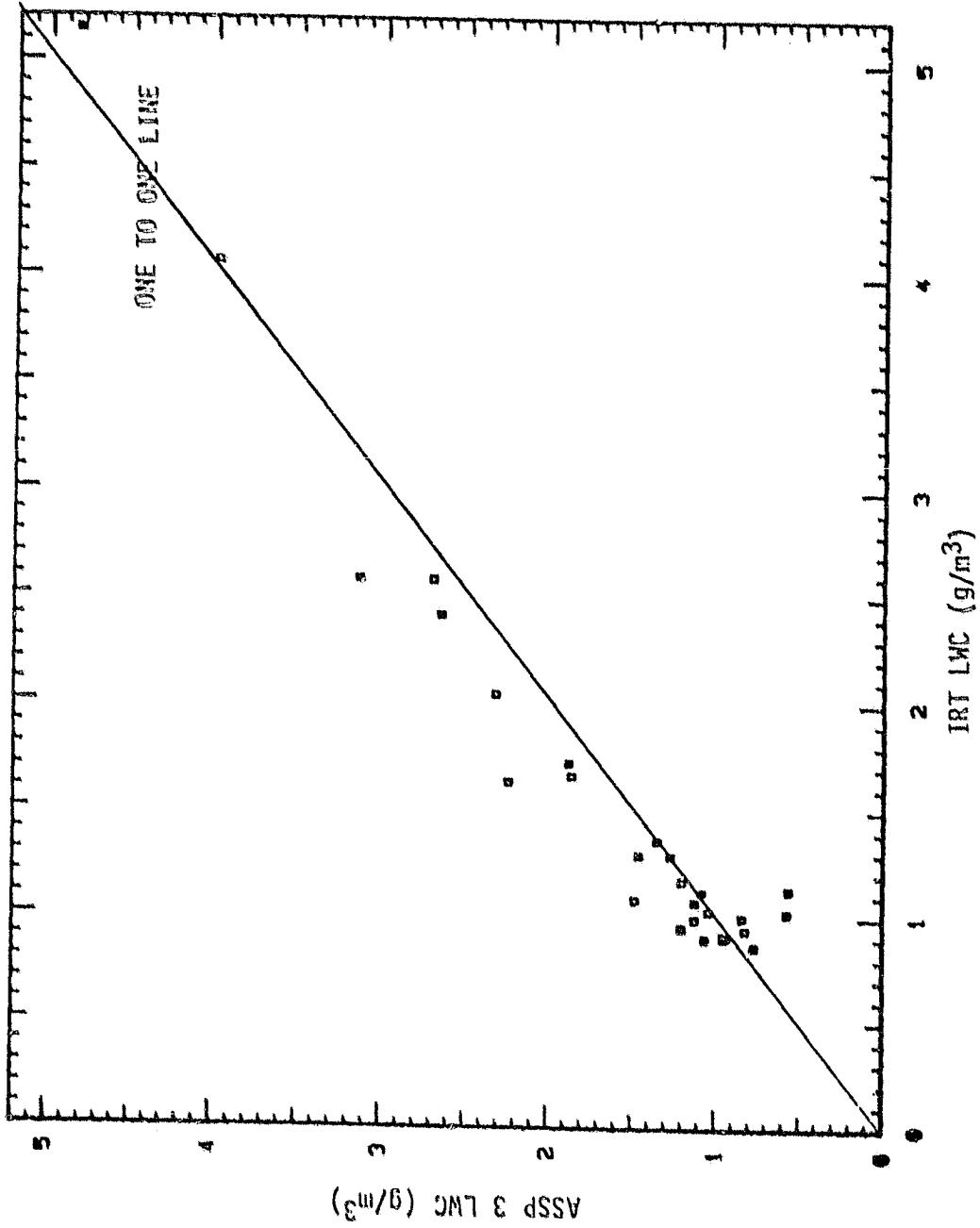


Figure 4-17. SCATTER DIAGRAM OF ASSP 3 LWC VERSUS IRT LWC

ORIGINAL PAGE IS
OF POOR QUALITY

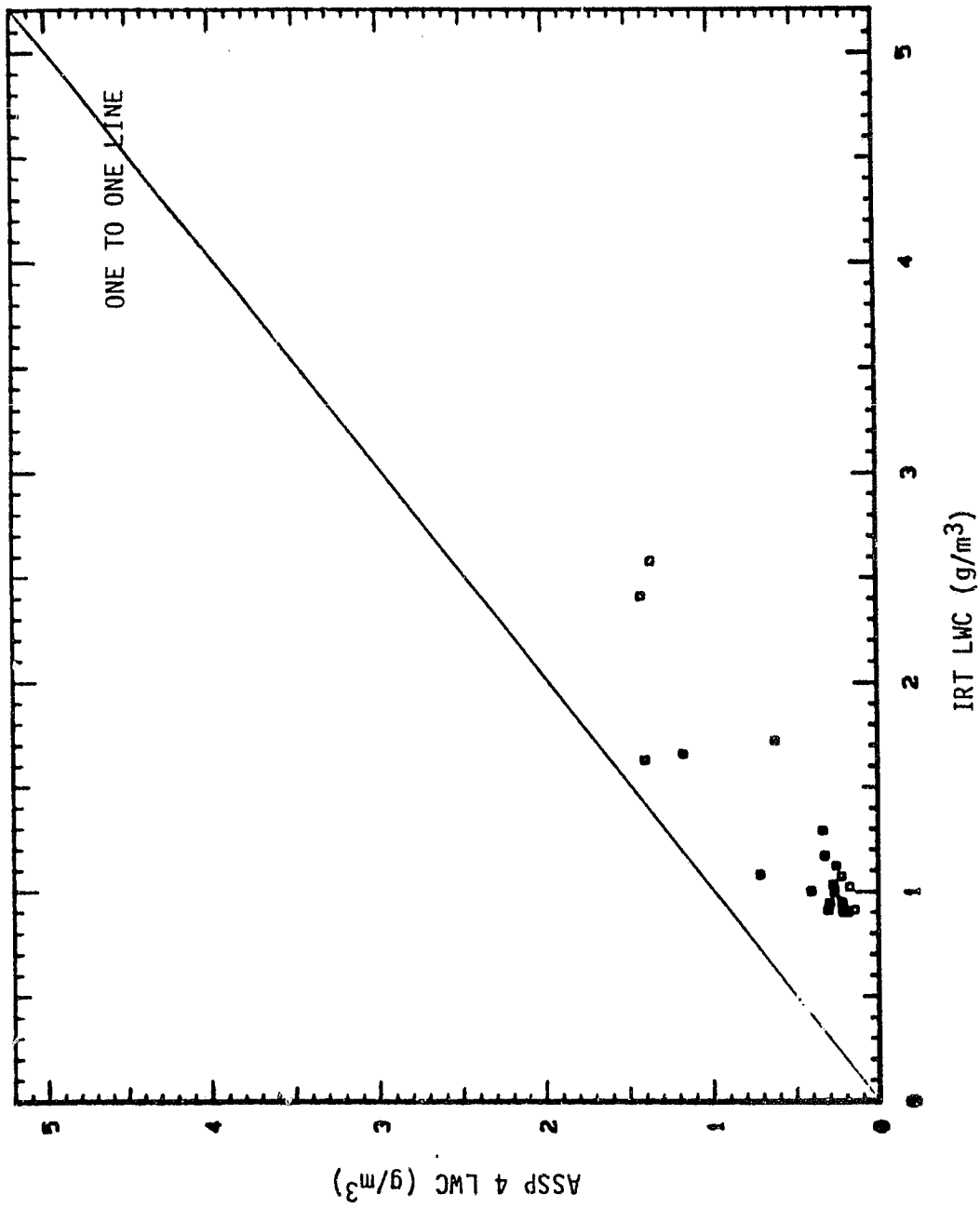


Figure 4-18. SCATTER DIAGRAM OF ASSP 4 LWC VERSUS IRT LWC

(LWC >4 g/m³), significant amounts of water existed in particles having sizes much larger than the upper size limit of these probes and therefore the probe estimates should be considered invalid. The weak dependency exhibited between the estimates of FSSP 1 and the tunnel may have perhaps resulted from a malfunction in its velocity reject circuit which was discovered during the program. When viewed (Figure 4-19) collectively, it is found that the individual probe estimates vary by large amounts. Although part of the scatter may be due to uncertainties in the absolute calibrations of the spray clouds, the variations between the individual probe estimates at given tunnel settings still remains large as shown in Figure 4-20. In this plot, the probe values are plotted against the means of the individual probe estimates for given tunnel settings.

Although the data can be shown to be compatible to the tunnel values by applying appropriate correction factors, these results which were based upon use of the manufacturer's specifications, clearly indicate that if the size-distribution measurements are used to estimate their bulk parameters (e.g., LWC), the probes should be calibrated against known standards. Also, due primarily to possible deterioration in measurement precision due to probe icing, it is further indicated that instruments such as the Leigh IDS or J-W device which make direct measurements of the integrated spectrum be used to complement the measurements. The relatively higher measurement precision offered by these accretion devices is indicated in Figures 4-21 and 4-22 which show that the average test point values for the given tunnel settings fall on the one-to-one line with a minimal amount of scatter. Of these two comparisons, the average measurements from the Leigh IDS shows greater precision and reliability.

The average MVD estimates for the given tunnel settings for each of the probes are plotted against the corresponding tunnel estimates in Figure 4-23. Wide deviations appear in the tunnel size range of from about 10 to 20 μm where the measured estimates are shown to be significantly larger. A closer correspondence is exhibited at the larger tunnel sizes. These observations are reflected in the best fit values given for the coefficients of the individual probe comparison equations in Table 4-6 which shows large intercept values (8-15) and relatively small slope estimates of between 0.4 to 0.7. When the

ORIGINAL PAGE IS
OF POOR QUALITY

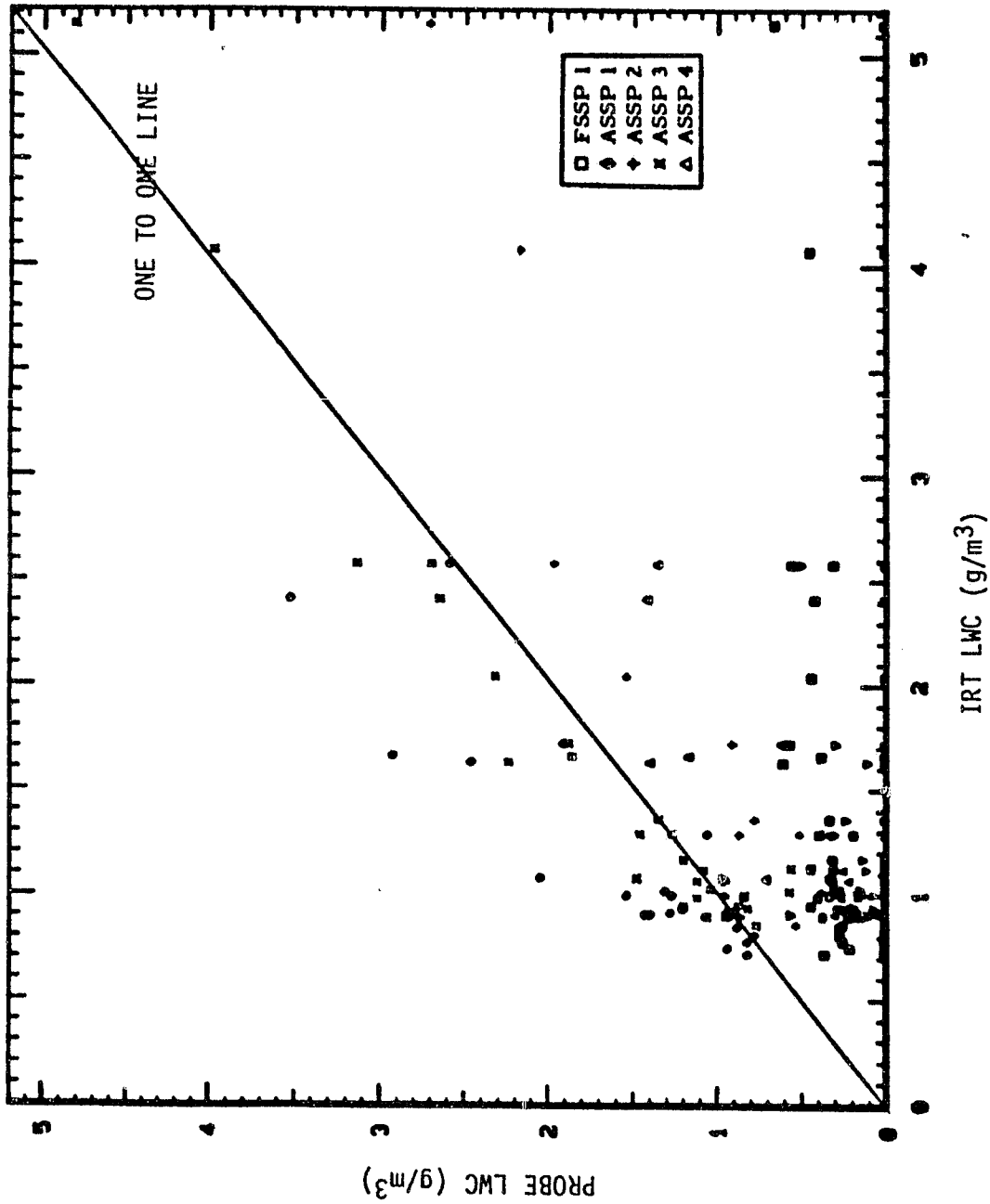


Figure 4-19. SCATTER DIAGRAM OF INDICATED PROBE LWC VERSUS IRT LWC

ORIGINAL PAGE IS
OF POOR QUALITY

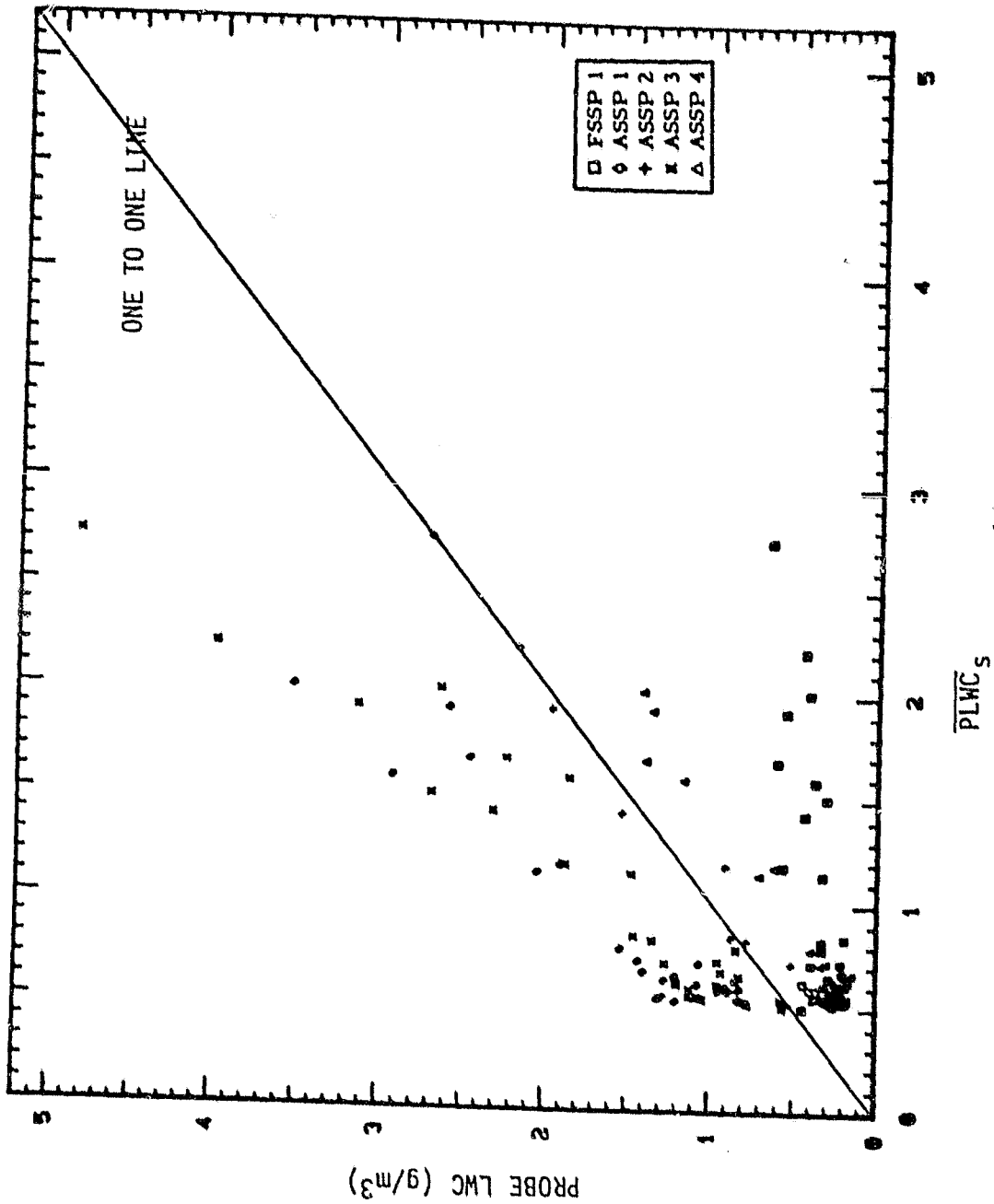


Figure 4-20. SCATTER DIAGRAM OF INDICATED PROBE LWC VERSUS
AVERAGE PROBE LWC FOR GIVEN TUNNEL SETTINGS

ORIGINAL PAGE IS
OF POOR QUALITY

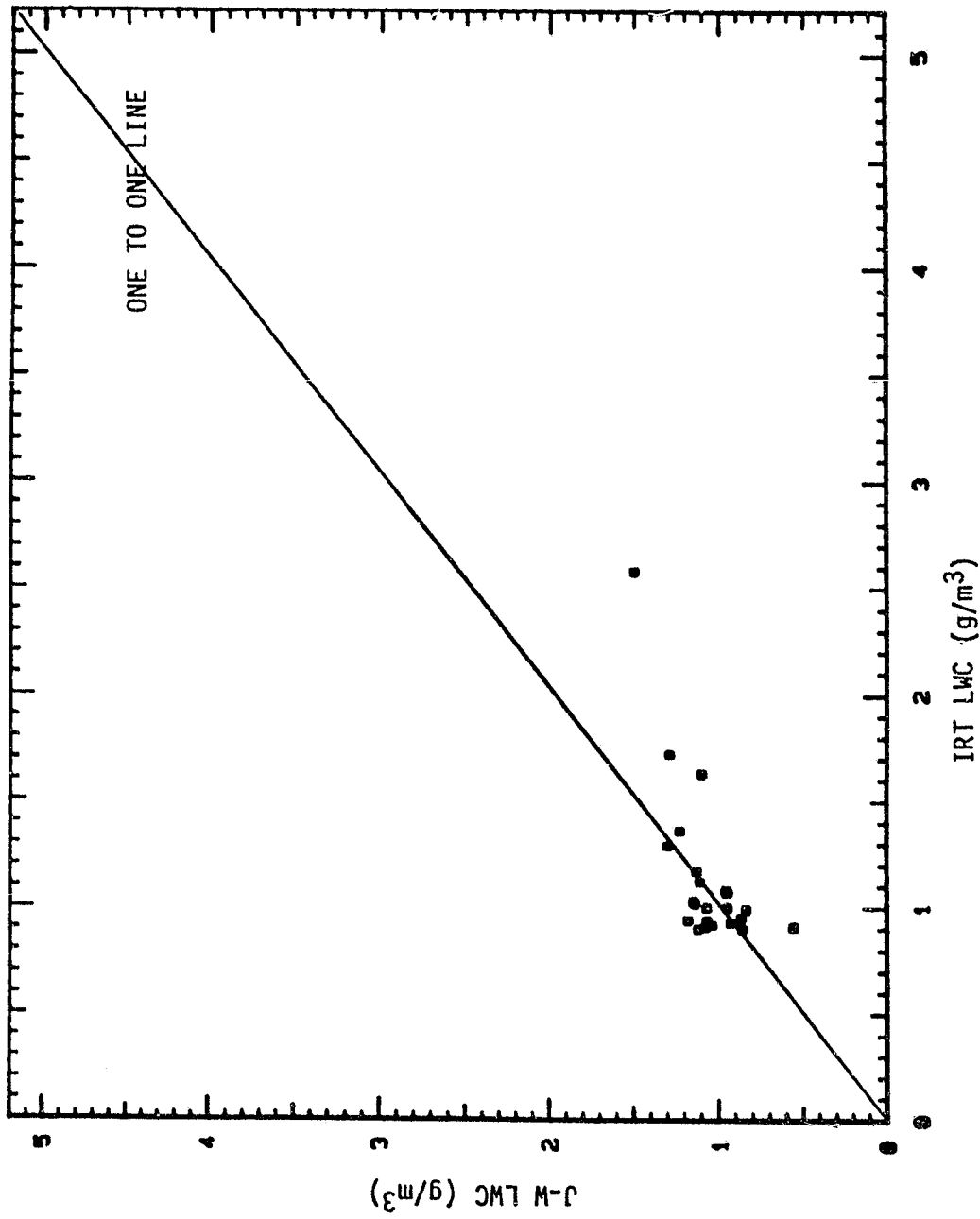


Figure 4-21. SCATTER DIAGRAM OF AVERAGE J-W LWC VERSUS
IRT LWC FOR GIVEN TUNNEL SETTINGS

ORIGINAL PAGE IS
OF POOR QUALITY

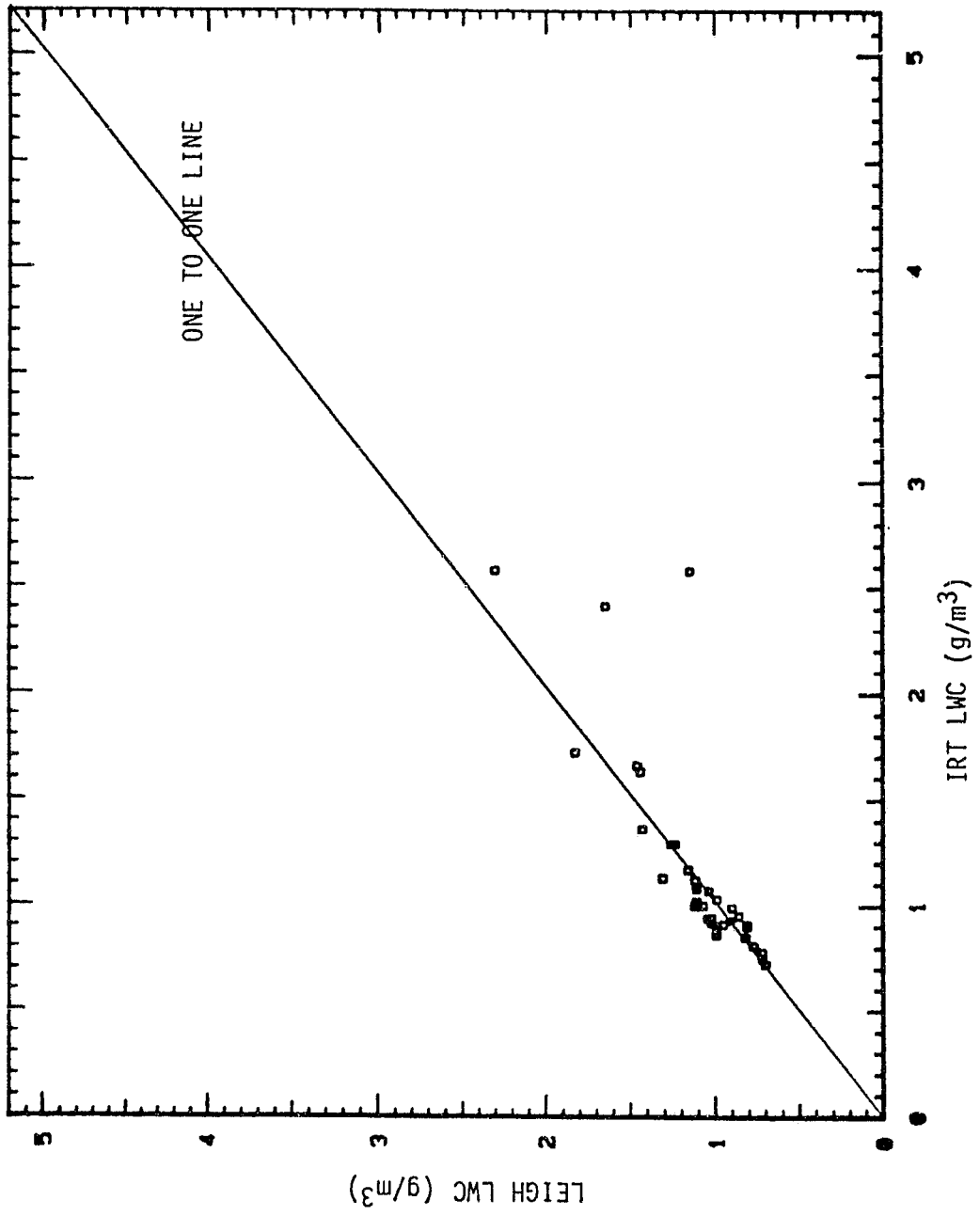
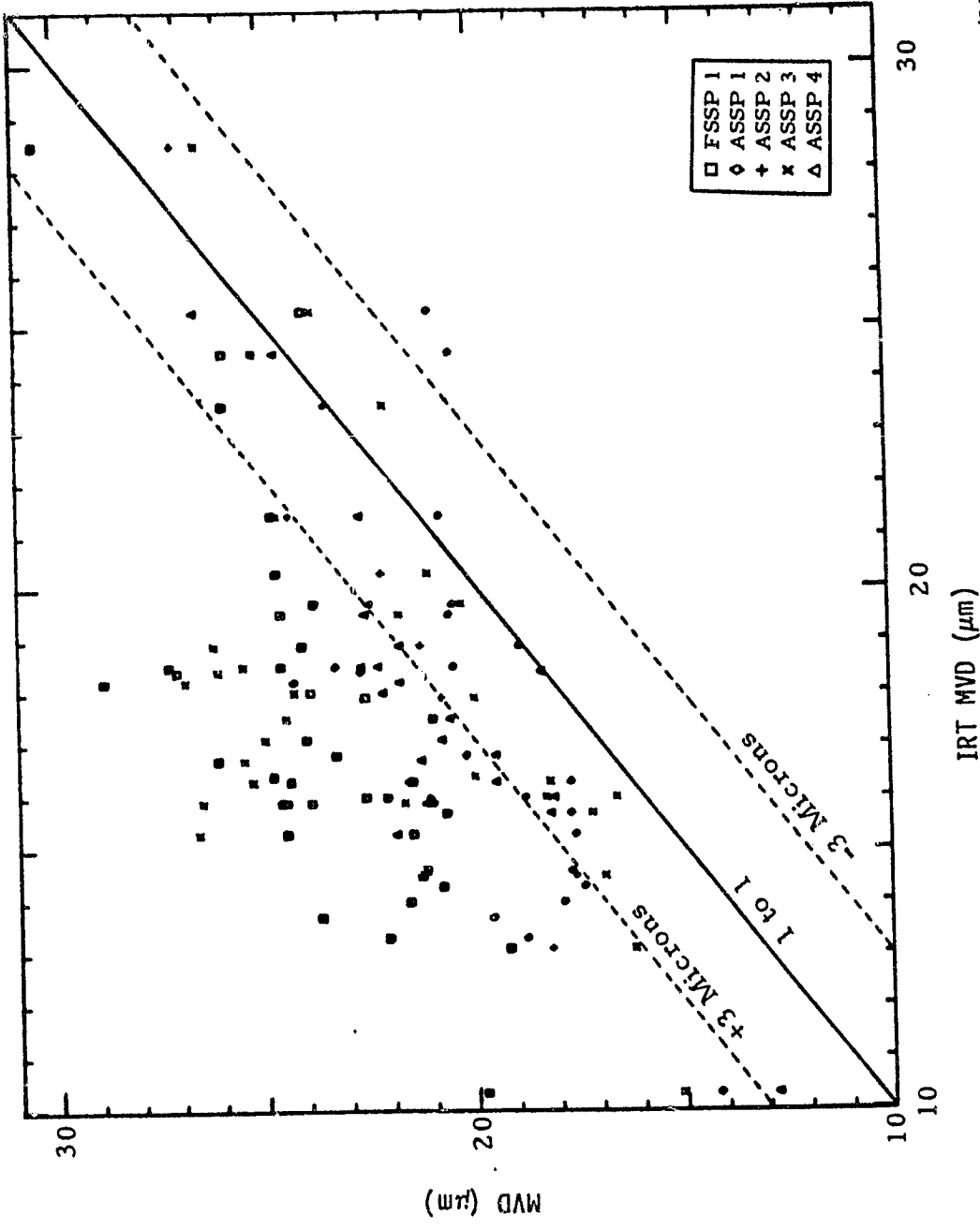


Figure 4-22. SCATTER DIAGRAM OF AVERAGE LEIGH LWC VERSUS
IRT LWC FOR GIVEN TUNNEL SETTINGS

ORIGINAL PAGE IS
OF POOR QUALITY



81/216

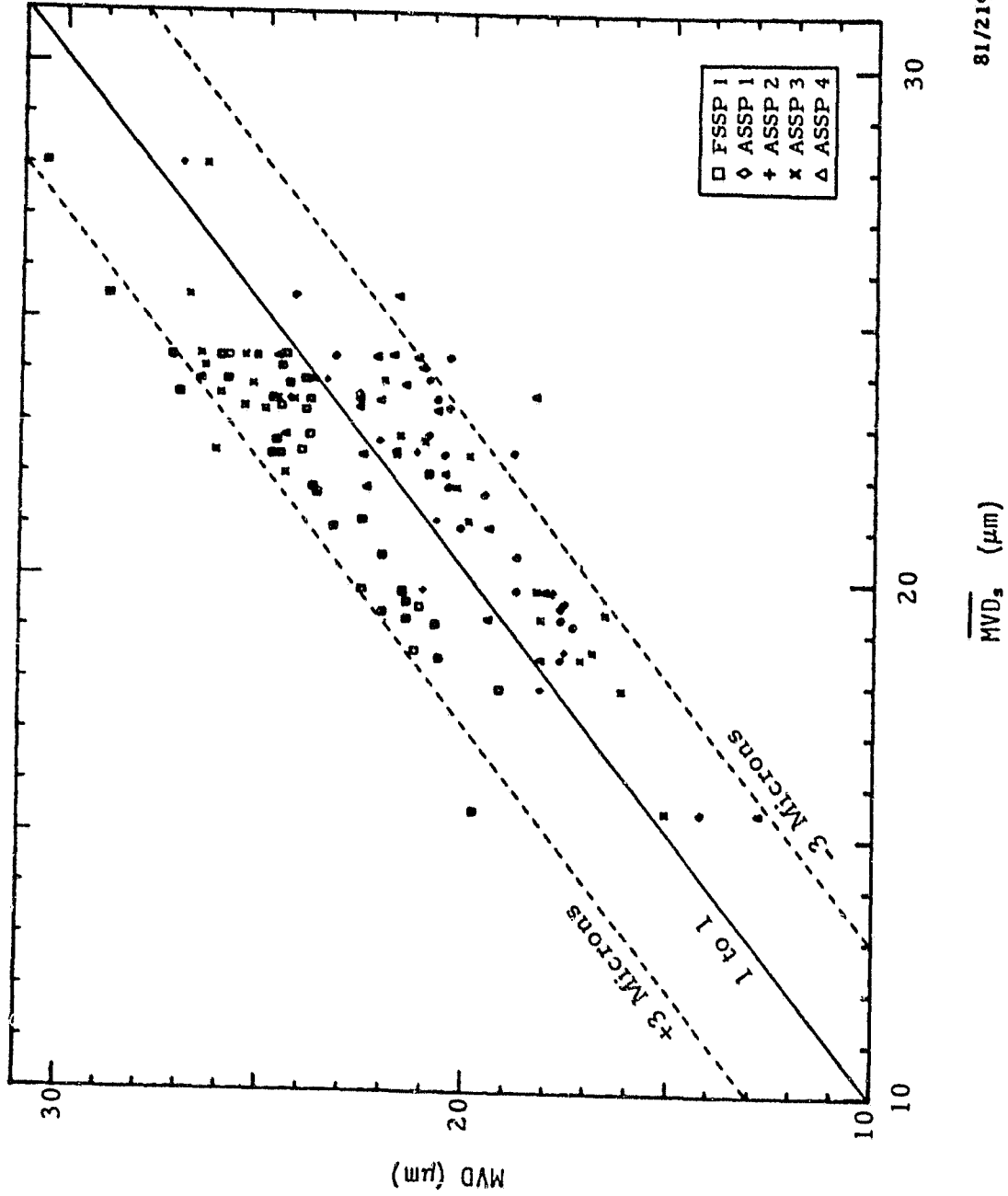
Figure 4-23. SCATTER DIAGRAM OF INDICATED PROBE MVD VERSUS
IRT MVD FOR GIVEN TUNNEL SETTINGS

probe estimates are collectively compared against the tunnel estimates (PMS vs Tunnel), it is shown that not only does the correlation decrease but that the scatter (e) also increases significantly.

Figure 4-24 presents comparisons of the probe estimates against their averages for given tunnel settings (PMS vs $\overline{\text{PMS}}$) and shows that the estimates were in most cases (112 of 121 or 93 percent) within $\pm 3 \mu\text{m}$ of each other. This error is consistent with the accuracy claimed by the manufacturer of the glass bead calibrations of \pm one channel band width, which for these probes were between 3 to 3.5 μm . It is noted that part of LWC variations between the probe estimates can be attributed to these differences although not to the large extent shown in the LWC comparison plot against the tunnel values. Thus, although the measurement accuracy of the probes may be questioned from the comparisons presented in Figure 4-23, the good agreement found between the individual probes suggests that the MVD calibrations performed by the rotating cylinders may perhaps have been in error for some of the tunnel settings. Part of the disagreement between the probe and rotating cylinder estimates results from the fact that the probe MVD estimates did not decrease with tunnel velocity increase as indicated by the operating equations. Unfortunately, the documentation of the procedures used in determining the MVD from the rotating cylinders was not available for this study and, therefore, further evaluations of the disagreement cannot be pursued.

Figure 4-25 presents examples of measurements taken at a given tunnel setting by all five of the scattering probes. The volume or mass distributions have been modified to account for measurement differences in LWC and in MVD by plotting the percentage mass in each of the channels against the scaled particle diameter, D/MVD . Although the individual probe measurements have been normalized for these differences, it is shown that significant measurement differences can still exist. Whereas the distributions from probes ASSP 1, ASSP 2, and ASSP 3 can be considered as being comparable to each other, those from FSSP 1 and ASSP 4 are not. Hence it is strongly suggested that calibration procedures be upgraded to also include means to evaluate the shape or form of the size distribution measurements.

ORIGINAL PAGE IS
OF POOR QUALITY



81/219

Figure 4-24. SCATTER DIAGRAM OF INDICATED PROBE MVD VERSUS
AVERAGE PROBE MVD FOR GIVEN TUNNEL SETTINGS

ORIGINAL PAGE IS
OF POOR QUALITY.

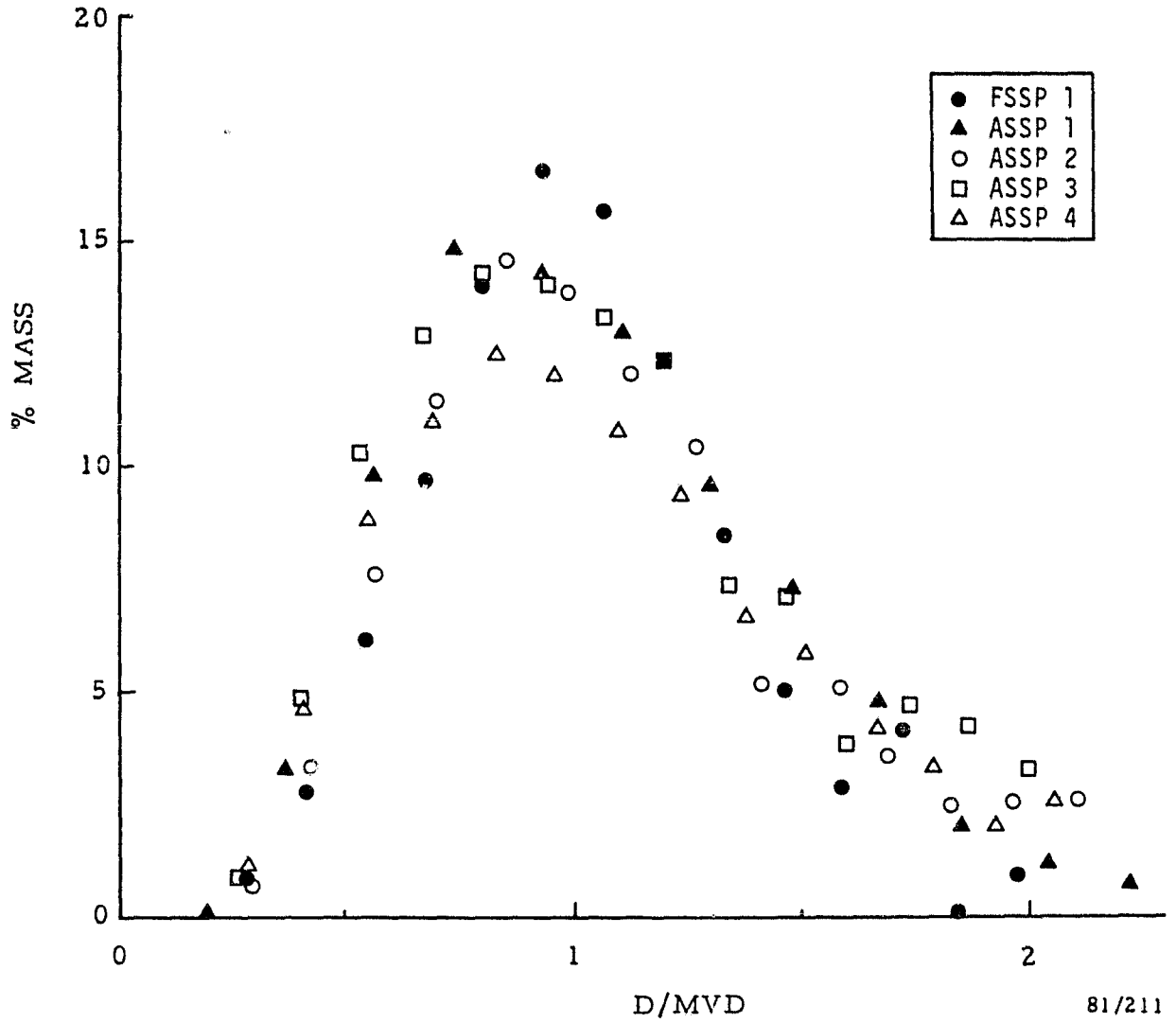


Figure 4-25. NORMALIZED MASS DENSITY VERSUS SCALED PARTICLE DIAMETER DISTRIBUTIONS TAKEN AT A GIVEN TUNNEL SETTING BY INDICATED PROBES

4.6 Drop Size Distribution Form

Of general interest to this study was the determination of a distribution function which best described the droplet size distribution measurements. For this purpose, the applicability of the gamma, log-normal, and Langmuir distribution functions were investigated. The approach consisted of evaluating the goodness of fit of the PMS probe measurements with the assumption that the given distribution functions were valid. The following presents brief descriptions of these functions and procedures used in their evaluation.

4.6.1 Gamma Distribution Function (GD)

The gamma distribution function is described by three parameters and is given as:

$$\begin{aligned} N_D &= N_0 \left(\frac{D}{D_*} \right)^\alpha \exp(-\lambda D) && \text{for } D > 0 \\ &= 0 && \text{for } D \leq 0 \end{aligned} \quad (1)$$

where

- $N_D \Delta D$ = number density between D and $D + \Delta D$
- D = droplet diameter
- N_0 = displacement parameter, $N_0 > 0$
- α = curvature parameter, $\alpha > -1$
- λ = scale parameter, $\lambda > 0$
- D_* = unit constant

A desirable feature of the GD is the ease at which moment related bulk parameters of the distributions can through simple integration be resolved. Some of these parameters include:

- a. Total number density, N_T

$$\begin{aligned} N_T &= \int_0^\infty N_D dD = N \int_0^\infty D^\alpha \exp(-\lambda D) dD \\ &= \frac{N \Gamma(\alpha + 1)}{\lambda^{\alpha+1}} \end{aligned}$$

where Γ represents the gamma function and N for mathematical convenience represents N_0/D_*^α .

b. Total volume density, M

$$M = \int_0^{\infty} N_D D^3 dD = N \int_0^{\infty} D^{\alpha+3} \exp(-\lambda D) dD$$

$$= N \frac{\Gamma(\alpha+4)}{\lambda^{\alpha+4}}$$

c. Liquid water content, LWC

$$LWC = \frac{\pi}{6} \rho_w M$$

d. Reflectivity factor, Z

$$Z = \int_0^{\infty} N_D D^6 dD$$

$$= N \frac{\Gamma(\alpha+7)}{\lambda^{\alpha+7}}$$

Another feature of the GD is that the MVD (or D_0) of a given droplet size distribution is uniquely defined by the curvature and scale coefficients as follows:

$$MVD = D_0 \equiv (\alpha + 3.67)/\lambda \quad (2)$$

Since the GD is described by three parameters any three moment related bulk parameters of a given DSD may be used to estimate their values (Takeuchi, 1978). However, this method commonly referred to as the moment technique may also be inefficient and therefore iteration techniques which minimize the variance of the data points about their estimates can also be used.

The GD can also be normalized to account for sample to sample variations in the values of the descriptive coefficients by the following algebraic manipulations to Eq. 1 and use of the identity given by Eq. 2.

ORIGINAL PAGE IS
OF POOR QUALITY

$$\frac{N_D}{D^\alpha} = N \exp(-\lambda D) \quad (3)$$

$$\frac{N_D}{D^\alpha N} = \exp(-(\alpha+3.67) D/D_0)$$

$$\ln\left(\frac{N_D}{D^\alpha N}\right) / (\alpha+3.67) = -D/D_0 \quad (4)$$

or

$$Y = -D/D_0 \quad (4)$$

It is indicated by Eq. 4 that if the DSD measurements (N_D) adhere to the GD, then plots on a linear graph between the unitless expressions given to the left of the equal sign and the scaled particle diameter D/D_0 will result in data points falling along a straight line having intercept and slope values of 0 and -1, respectively.

For each DSD measurement, the descriptive coefficients of the GD were determined by the two different techniques mentioned earlier. Hence, two separate evaluations on the applicability of the GD were performed. To improve upon the efficiency of the moment technique (Gamma I), four moment related parameters were employed and consisted of the following computational procedures.

$$\alpha = \frac{-b - \sqrt{b^2 - 4ac}}{2a} \quad (5)$$

where

$$a = 1 - Q$$

$$b = 11 - 5Q$$

$$c = 30 - 6Q$$

$$Q = \frac{LZ}{MF}$$

$$L = \sum_{i=1}^{15} N_i D_i$$

$$M = \sum_{i=1}^{15} N_i D_i^3$$

$$F = \sum_{i=1}^{15} N_i D_i^4$$

$$Z = \sum_{i=1}^{15} N_i D_i^6$$

$$\lambda = [(\alpha+6)(\alpha+5)(\alpha+4)(\alpha+3)(\alpha+2) L/Z]^{1/5} \quad (6)$$

$$N_0 = \frac{M \lambda^{\alpha+4}}{\Gamma(\alpha+4)} \quad (7)$$

The second method (Gamma II) consisted of performing iterations on the linearized form of the GD given by Eq. 3.

$$\frac{N_D}{D^\alpha} = N \exp(-\lambda D) \quad (3)$$

or

$$y = N' - \lambda D \quad (3a)$$

where

$$y = \ln N_D - \alpha \ln D$$

$$N' = \ln N_0$$

Equation 3a serves as the basis from which simple linear regression analyses (method of least squares) resolves unbiased estimates of the descriptive coefficients. The iterative technique (see Takeuchi and Chein, 1979 for further details) basically seeks a value of α for which the standard deviation of regression is minimized. Once minimized, values for N_0 and λ are determined from the "best fit" estimates of the intercept ($N_0 = \exp(N')$) and slope, respectively. In this study, α computed from Eq. 5 served as the initial value in the iteration process. The MVD is defined by Eq. 2 in both techniques.

4.6.2 Log-normal Distribution, LN

If the volume (or mass) distributions are assumed to be log-normal, then the probability density function $p(D)$ is given as:

$$p(D) = \frac{1}{\sigma\sqrt{2\pi}} \exp \left[- \left(\frac{\ln D - \ln D_g}{\sqrt{2} \sigma} \right)^2 \right] \quad (8)$$

where

- $p(D) \cdot \ln \left(\frac{D+\Delta D}{D} \right)$ = normalized volume density between D and $D+\Delta D$,
 D_g = geometric mean diameter or antilog of average $\ln D$
 σ = standard deviation of $\ln D$

In order to objectively compare the goodness of fit of the measurements against that of the GD it is mandatory that Eq. 8 be linearized as follows:

$$\begin{aligned} \ln (\sigma\sqrt{2\pi} p(D)) &= - \left(\frac{\ln D - \ln D_g}{\sqrt{2} \sigma} \right)^2 \\ -2 \sigma^2 \ln (\sigma\sqrt{2\pi} p(D)) &= \left(\ln \frac{D}{D_g} \right)^2 \\ \pm [-2 \sigma^2 \ln (\sigma\sqrt{2\pi} p(D))]^{1/2} &= \ln \frac{D}{D_g} \end{aligned}$$

or

$$\pm Y' = \ln \frac{D}{D_g}$$

$$\exp (-Y') = D/D_g \text{ for } D/D_g \leq 1$$

and

$$\exp (Y') = D/D_g \text{ for } D/D_g > 1$$

$$Y = D/D_g = D/D_0 \quad (9)$$

It is so indicated by Eq. 9 that if the volume distributions are in fact log-normal, the plots on a linear graph between the unitless expression given to the left of the equal sign and the scaled particle diameter D/D_g will result in data points falling along a straight line having intercept and slope values of 0 and 1, respectively. Also, since the volume frequency distribution is symmetrical about its geometric mean, the MVD is also identified by D_g .

It is further indicated that except for the difference in the sign of the slope, the values for both the intercept and slope and the expression, D/D_0 , given to the right of the equal sign in both linearized forms of the GD and LN equations are identical. Hence, the goodness of fit of given measurements can be evaluated and objectively compared between the two assumed distribution functions by evaluating the root mean square (RMS) error of the data points from the straight lines.

The coefficients of the LN and normalized volume density (V_i) were determined from each of the probe measurements by the following equations:

$$V_i = \frac{N_i D_i^3}{\sum_{i=1}^{15} N_i D_i^3} \quad (10)$$

$$\ln D_g = \sum_{i=1}^{15} V_i \ln D_i \quad (11)$$

$$\sigma = \left[\sum_{i=1}^{15} (V_i \ln D_i - \ln D_g)^2 \right]^{1/2} \quad (12)$$

4.6.3 Langmuir Distributions

The Langmuir distributions are assumed normalized volume density distributions about the scaled particle diameters D/D_0 as given (Langmuir and Blodgett, 1945) below:

ORIGINAL PAGE IS
OF POOR QUALITY

Table 4-7
FOUR ASSUMED DSD

LWC (%)	B D/D_0	C $(D/D_0)^{1.5}$	D $(D/D_0)^{2.0}$	E $(D/D_0)^{2.5}$
5	0.56	0.42	0.31	0.23
10	0.72	0.62	0.52	0.44
20	0.84	0.77	0.71	0.65
30	1.00	1.00	1.00	1.00
20	1.17	1.26	1.37	1.48
10	1.32	1.51	1.74	2.00
5	1.49	1.81	2.22	2.71

Common to these distributions is the given normalized volume density versus scaled midpoint diameter relationship of the B distribution. The remaining distributions are defined by different power values to which D/D_0 of the B distribution is raised. Hence the Langmuir distributions are defined as a single parameter distribution function.

Based on these considerations, the evaluation of the goodness of fit consisted of first determining the power values along given points of the normalized cumulative mass distribution of a given DSD measurement and second, computing the normalized RMS error of these values. The points along the normalized cumulative mass distribution were chosen to be at the midpoints as well as the intermediate points of the normalized volume distributions given in Table 4-7 and are listed in Table 4-8 along with the corresponding scaled diameters (D_B) of the B distribution. Given D_0 , the determination of the power values at each of base 12 points (K) consisted of the following procedures:

- a. Determine through linear interpolation, the diameter, D_K , at which the given percentage was found.
- b. Establish a scaled diameter, $DS_K = D_K/D_0$.

Table 4-8

CUMULATIVE VOLUME DISTRIBUTION OF
LANGMUIR B DISTRIBUTION

Cumulative LWC (%)	DB (D/D ₀)	Cumulative LWC (%)	DB (D/D ₀)
2.5	0.56	65	1.085
5	0.64	75	1.17
10	0.72	85	1.245
15	0.78	90	1.32
25	0.84	95	1.405
35	0.92	97.5	1.49

- c. From the corresponding scaled diameter (DB_k) of the B distribution given in Table 4-8 determine the power value (E_k) by the following equation:

$$E_k = \frac{\log_{10}(DS_k)}{\log_{10}(DB_k)} \quad (13)$$

Given a number of DSD measurements, the normalized RMS error as defined by the following equation:

$$RMS = \left[\frac{\sum_{k=1}^n \left(\frac{E_k - \bar{E}}{\bar{E}} \right)^2}{n} \right]^{1/2} \quad (14)$$

Since the Langmuir distributions are characterized by a single parameter, the deviations of the power values from their mean value at the given frequencies essentially provide a measure of the goodness of fit. In Eq. 14, the deviations are also normalized to their parameter estimates (or mean power values) as done in the RMS error determinations of the linearized forms of the gamma and lognormal distribution functions. Hence, the applicability of the three distribution functions can be objectively evaluated by comparing their RMS error estimates from a given set of DSD measurements.

4.6.4 Normalized DSD

Figures 4-26 to 4-32 present plots of the DSD measurements normalized to the three distribution functions. For the mere purpose of having the normalized measurements be inversely related to the scaled particle diameters as in the linearized GD plots, negative values of the normalized measurements (Y) of the LN are plotted against the scaled diameters. The normalized deviations of the power values of the Langmuir distributions are also plotted with respect to the normalized line of the GD and at the corresponding scaled diameters found for the given cumulative volume frequencies.

Based on the least amount of scatter shown of the points about its straight line, it is indicated that the gamma distribution function best describes the measurements. These observations are reflected in the RMS errors listed in Table 4-9 for each of the assumed distribution functions. For the evaluations based on the entire spectra, it is shown that the RMS errors associated with the GD are lower than those of the LN by a factor of about 2. Also, of the two techniques used in estimating values for the descriptive coefficients of the GD, the estimates based on the iterative method resulted in slightly smaller errors as would be expected. In comparing the resulting errors between the three distribution functions for the mid-channel measurements, the average error resulting from the GD (Gamma I) approximation is shown to be lower than those associated with the Langmuir and LN assumptions by factors of 2 and 3, respectively. Although a slightly larger average RMS error is indicated from use of the Gamma II estimations of the descriptive coefficients, the difference is considered to be negligible.

4.6.5 Comparisons with DSD from Natural Clouds

Based on the close adherence shown of the measurements to the GD, it can be stated that the GD adequately describes the probe measurements taken in the IRT. Hence given DSD may be compared through their coefficient values provided that they all confirm to the GD. Figure 4-33 presents plots of measurements taken in natural clouds which have been normalized to the three assumed distributions and shows that these measurements are also best described by the GD. Characteristics of the ten DSD are summarized in Table 4-10 which also includes evaluations of the goodness of fit. Since it has been

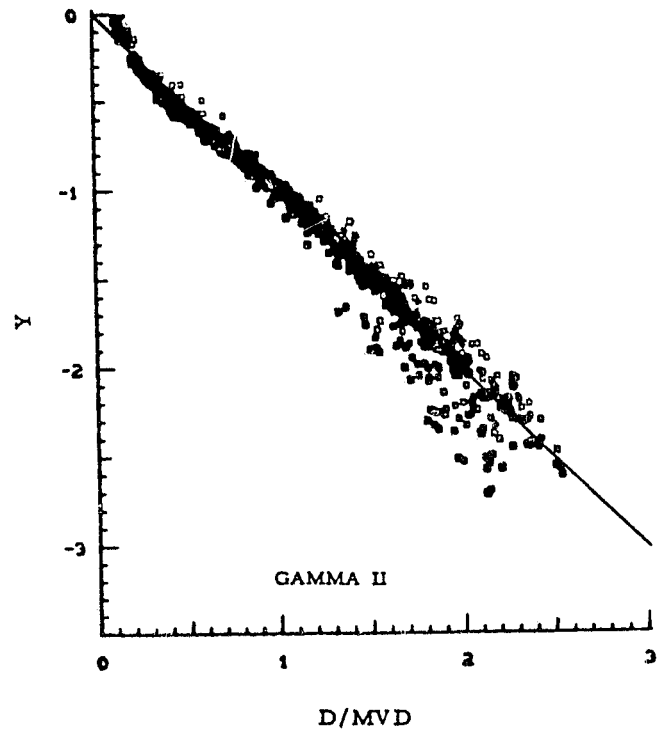
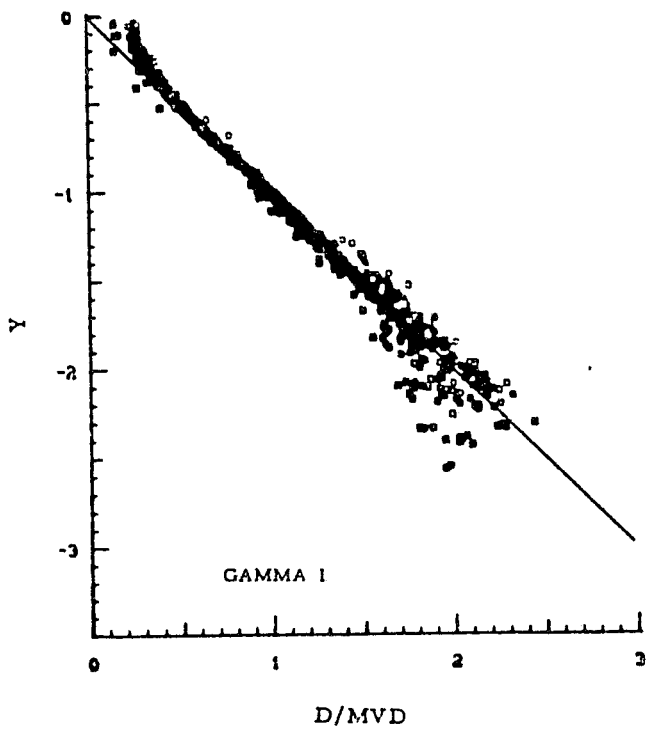
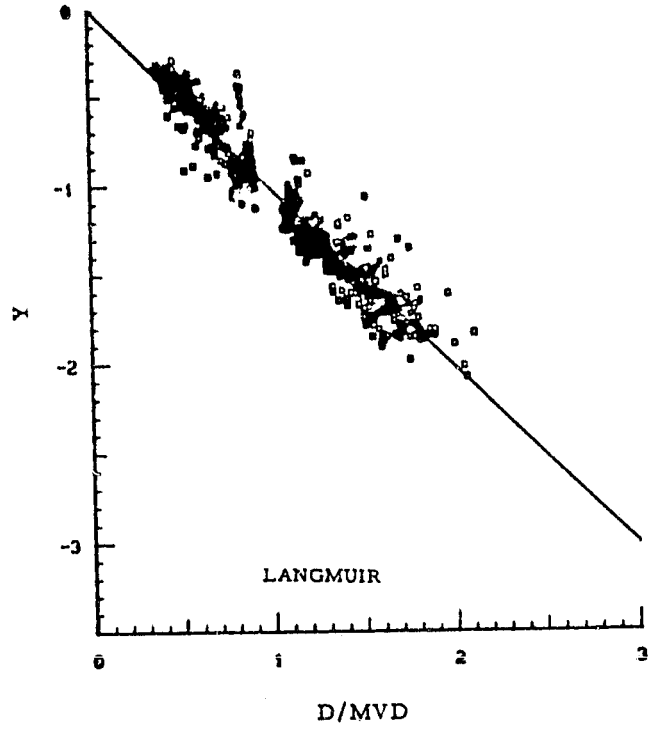
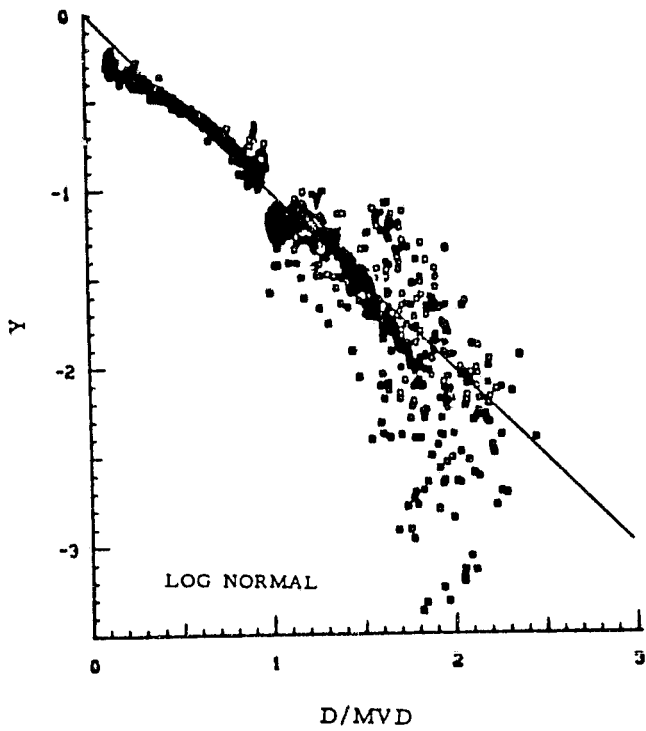


Figure 4-26. NORMALIZED DSD FROM FSSP 1

ORIGINAL PAGE IS
OF POOR QUALITY

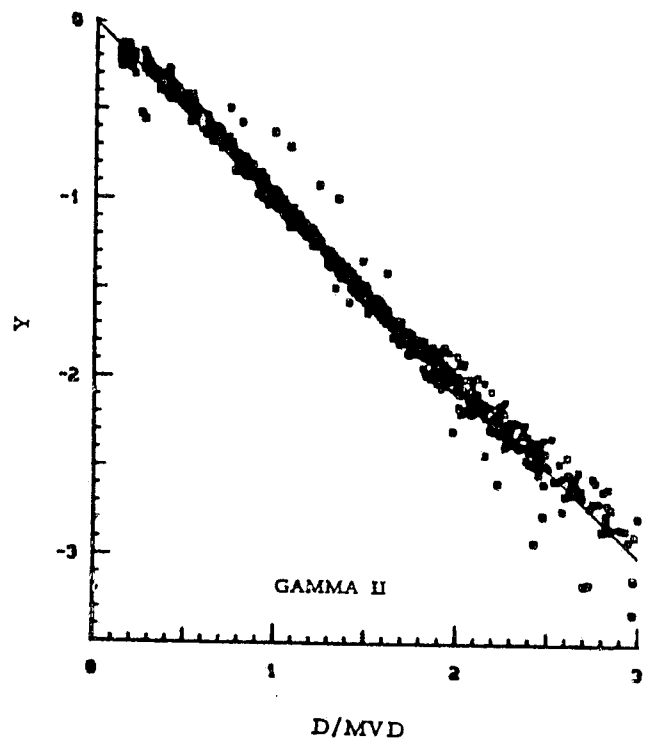
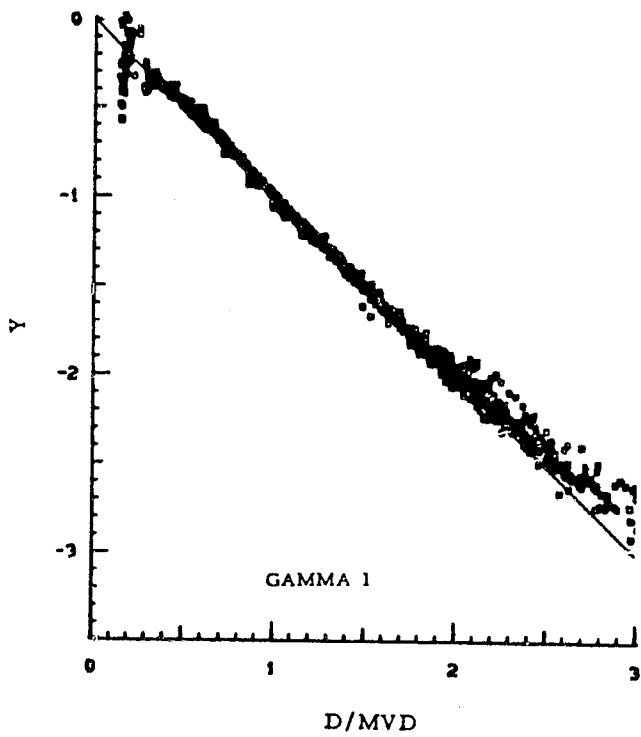
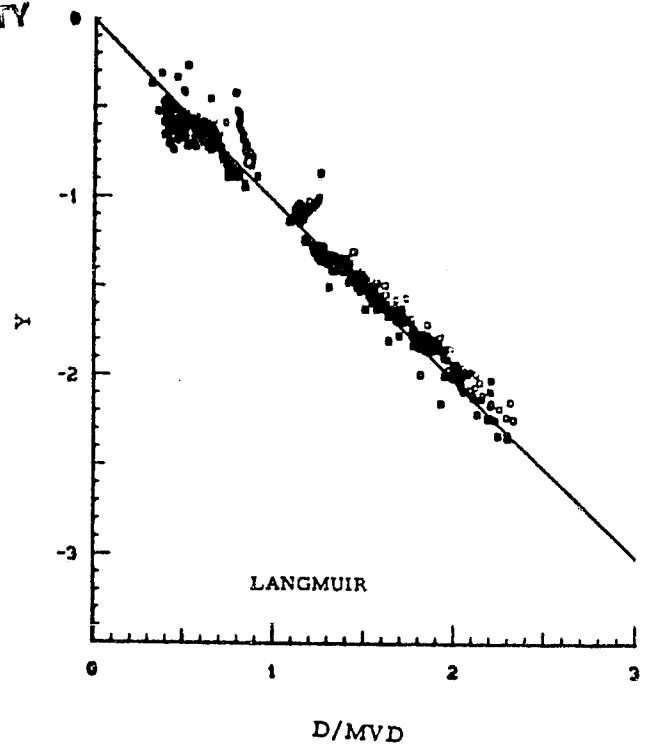
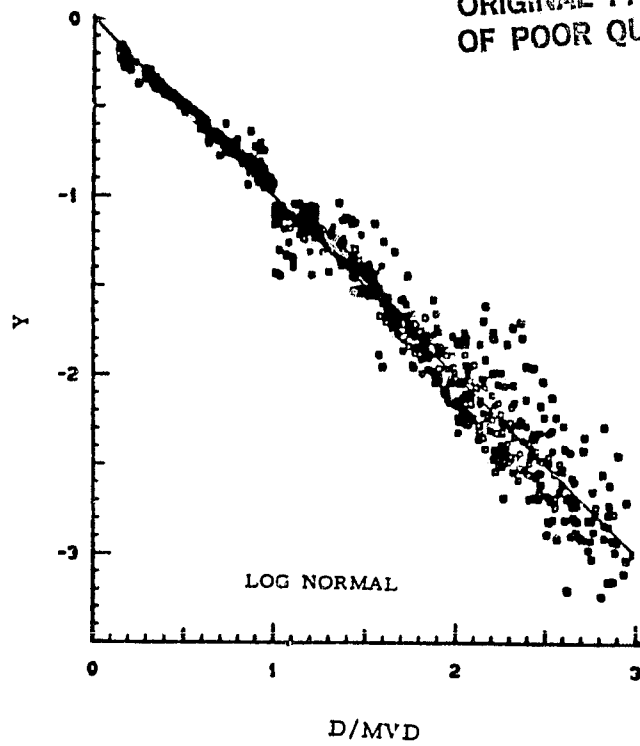


Figure 4-27. NORMALIZED DSD FROM ASSP 1

ORIGINAL PAGE IS
OF POOR QUALITY

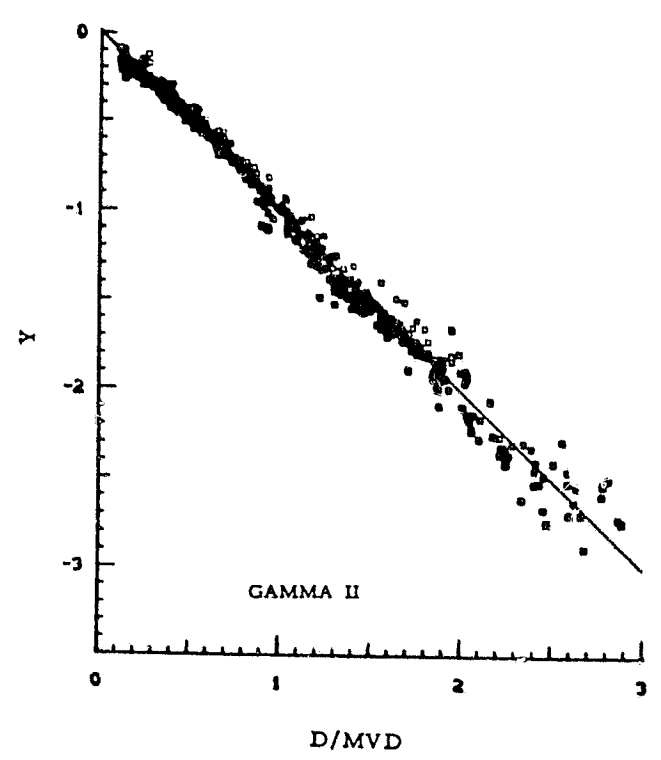
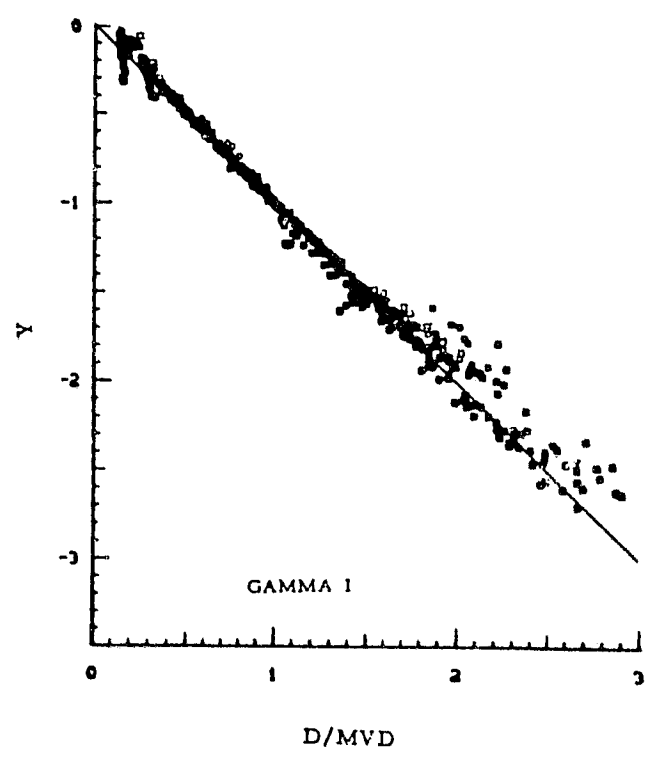
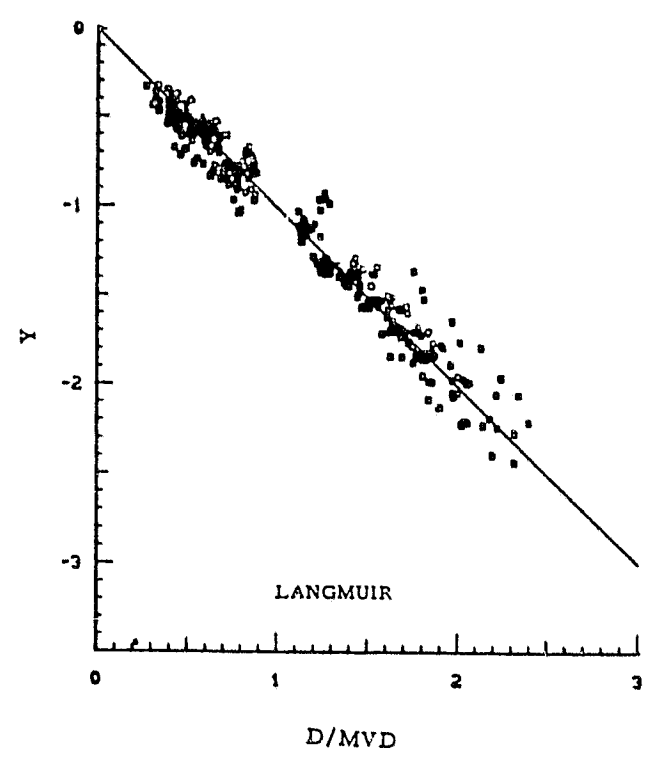
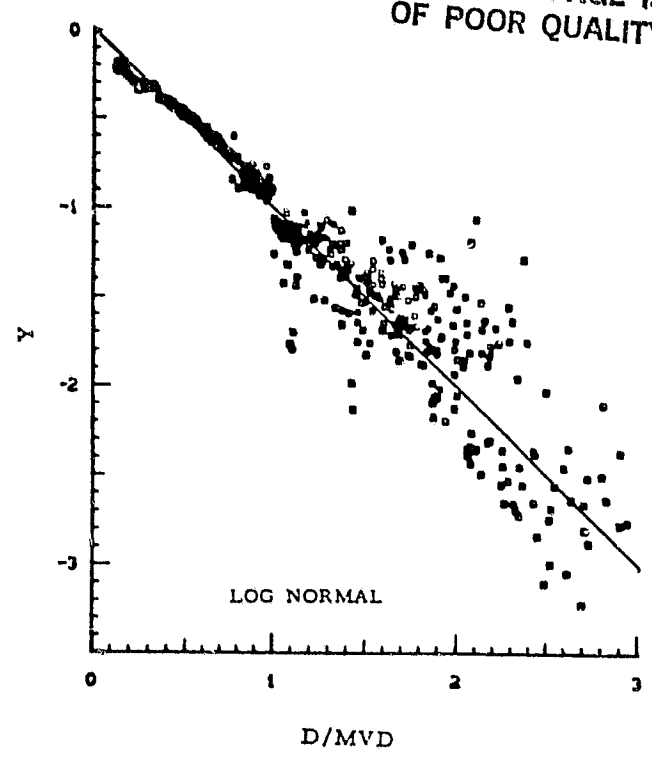


Figure 4-28. NORMALIZED DSD FROM ASSP 2

ORIGINAL PAGE IS
OF POOR QUALITY

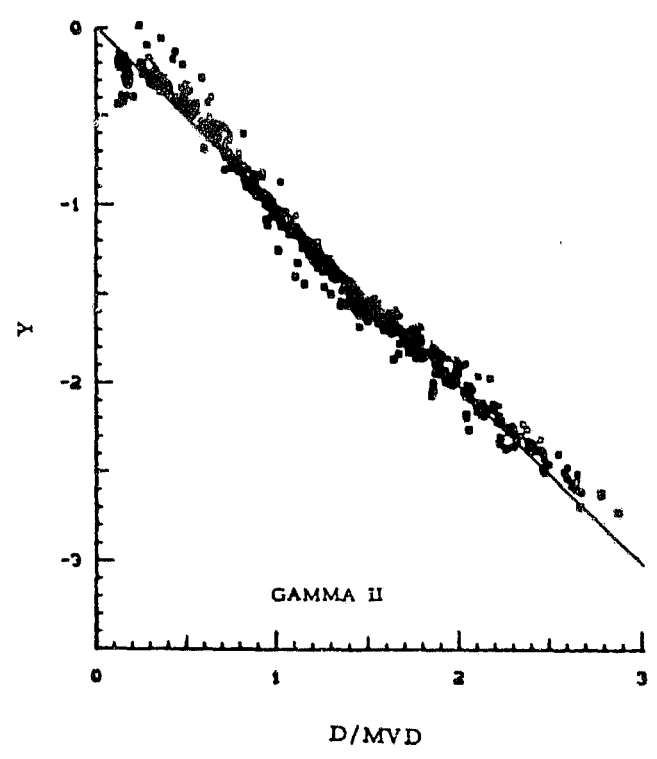
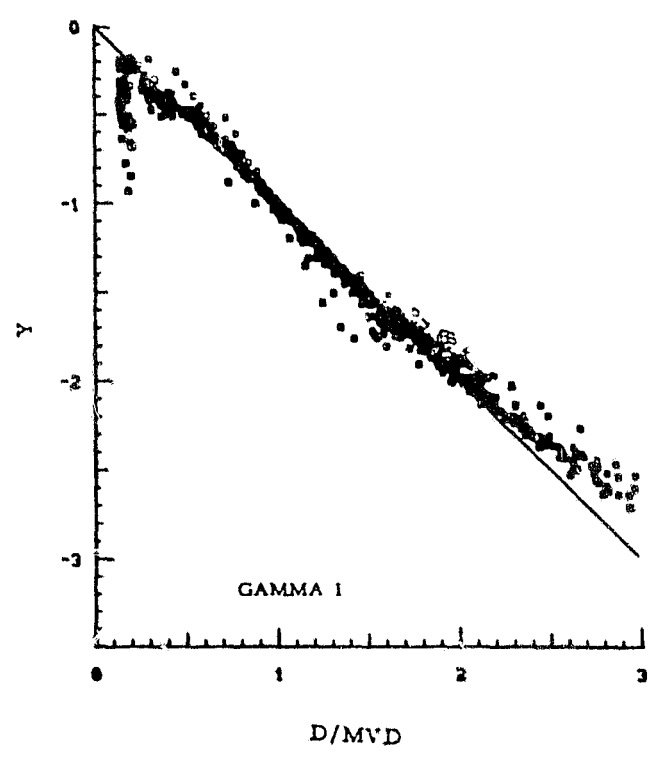
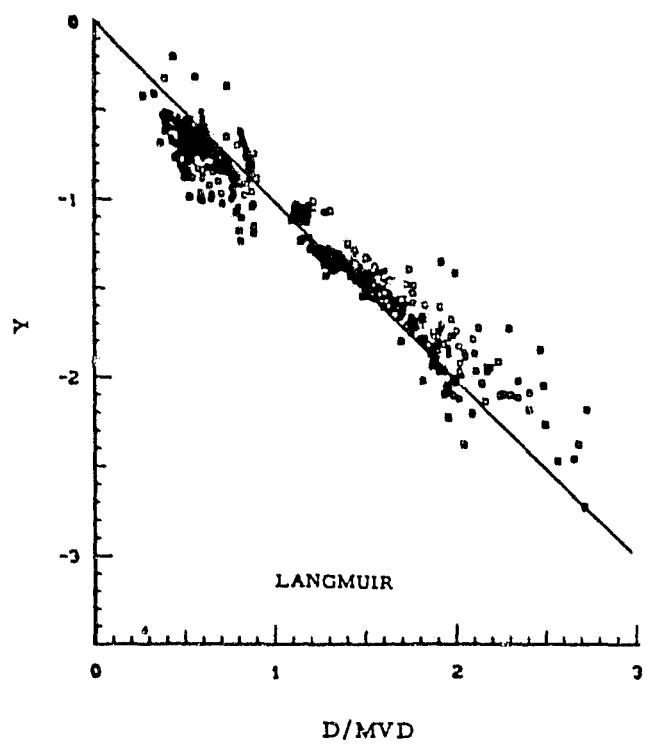
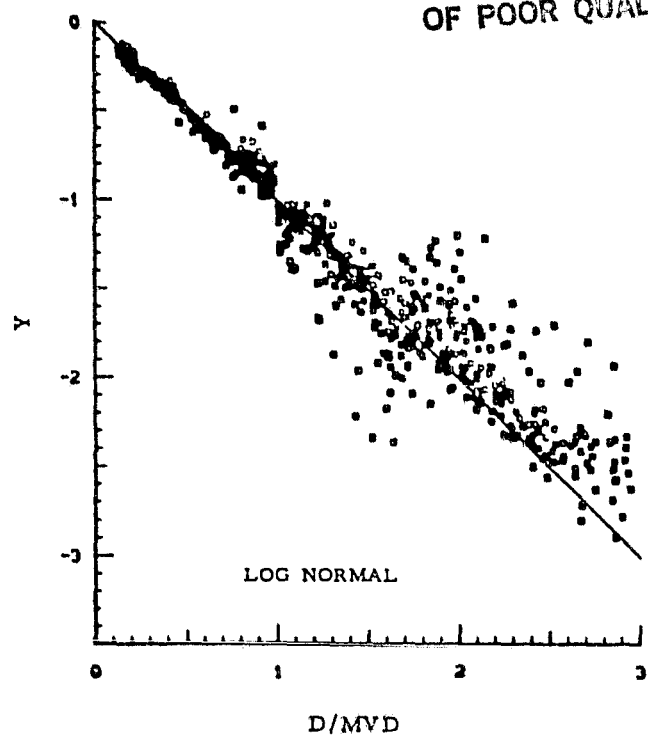


Figure 4-29. NORMALIZED DSD FROM ASSP 3

ORIGINAL PAGE IS
OF POOR QUALITY

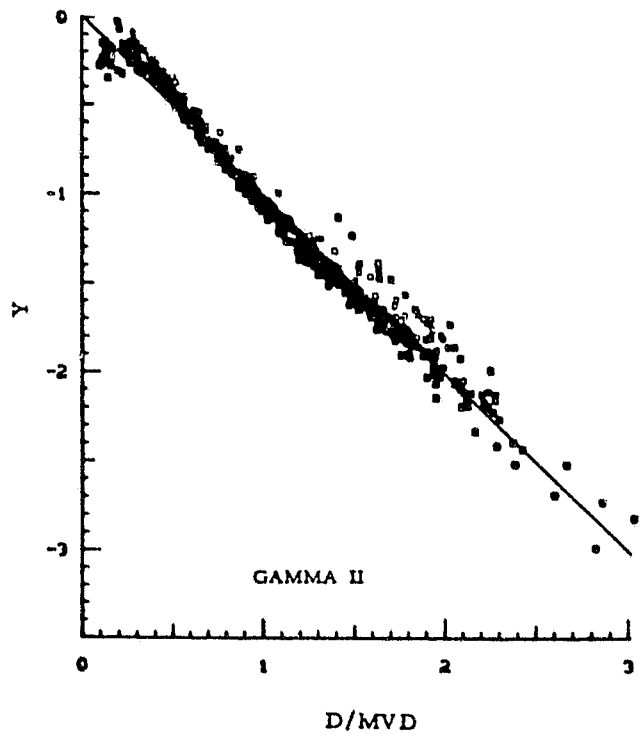
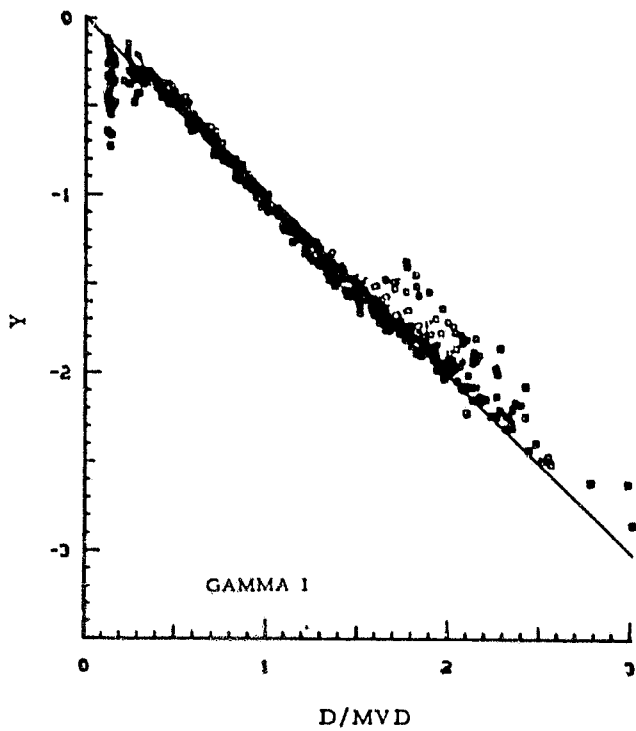
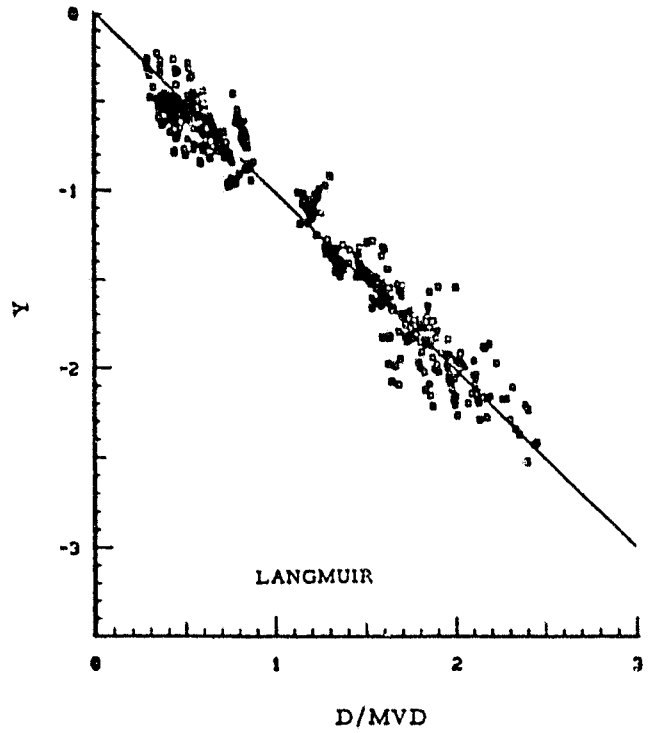
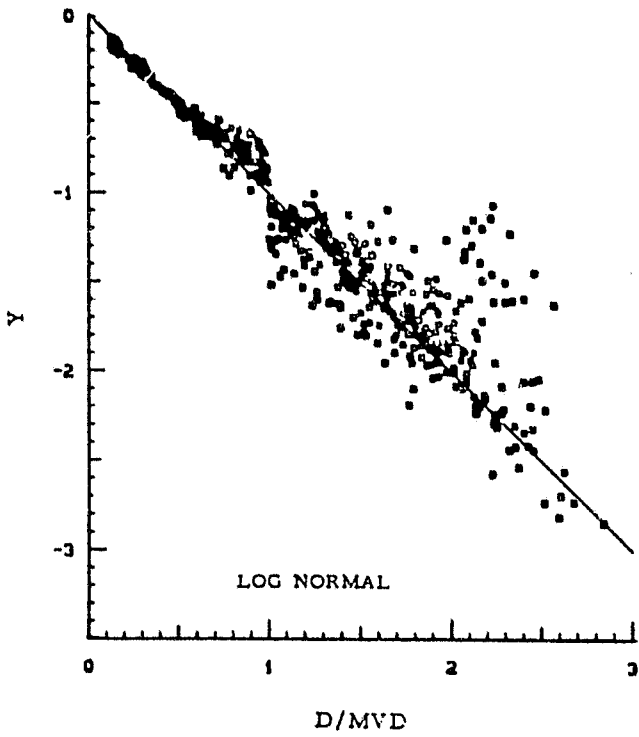


Figure 4-30. NORMALIZED DSD FROM ASSP 4

ORIGINAL PAGE IS
OF POOR QUALITY

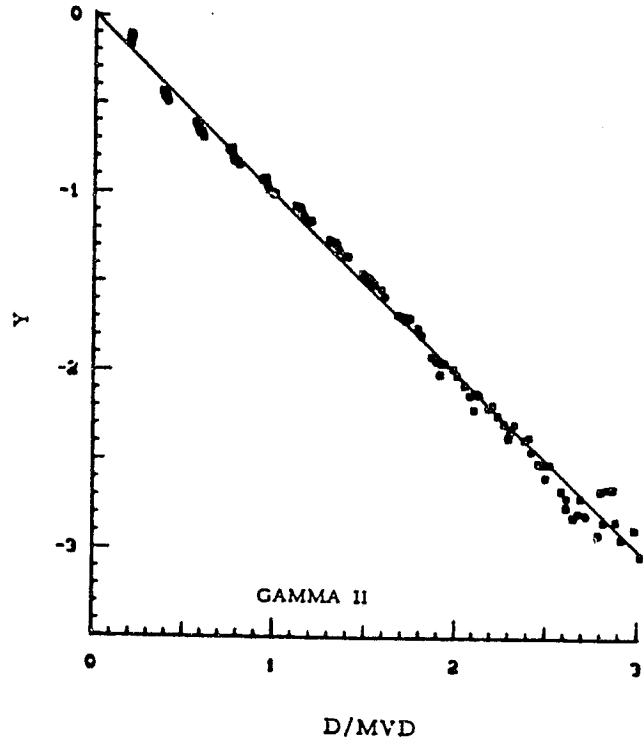
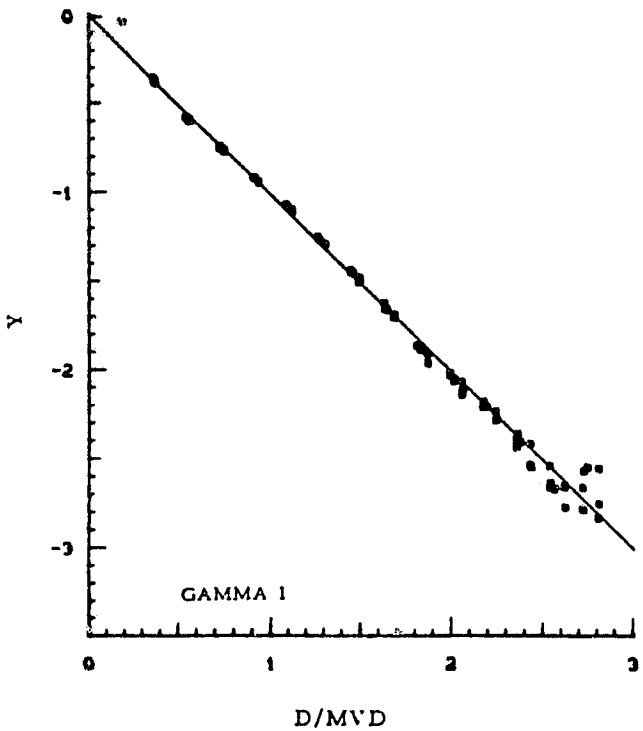
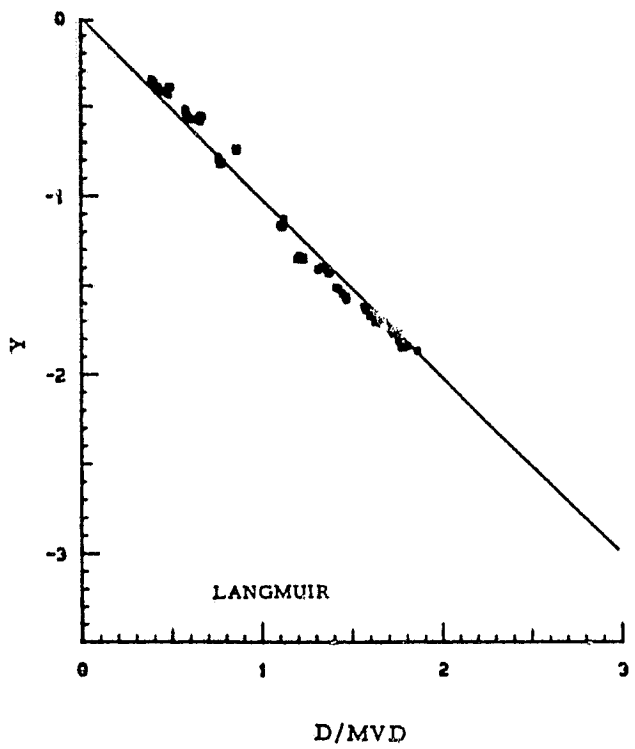
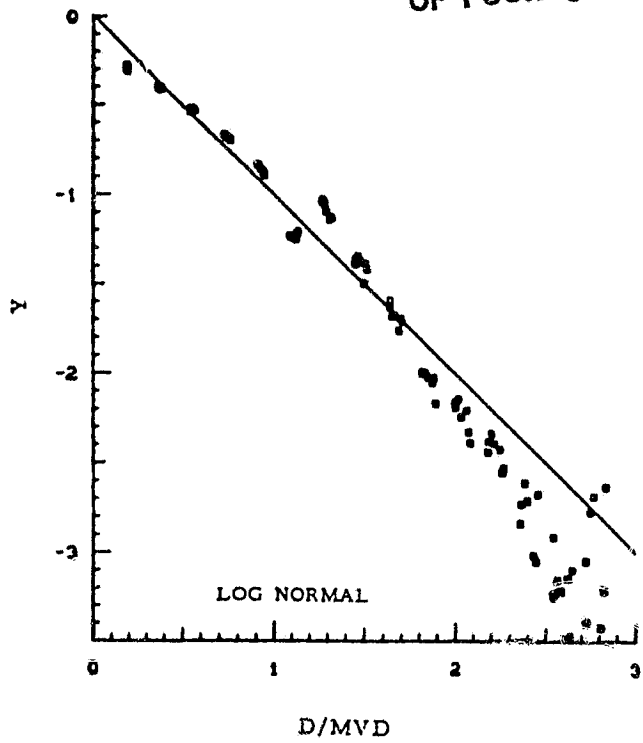


Figure 4-31. NORMALIZED DSD FROM FSSP 1'

ORIGINAL PAGE IS
OF POOR QUALITY

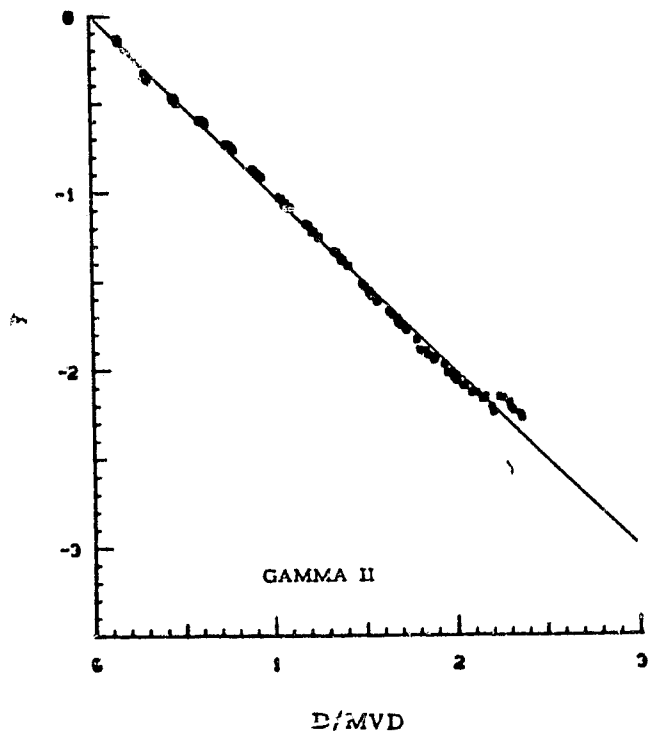
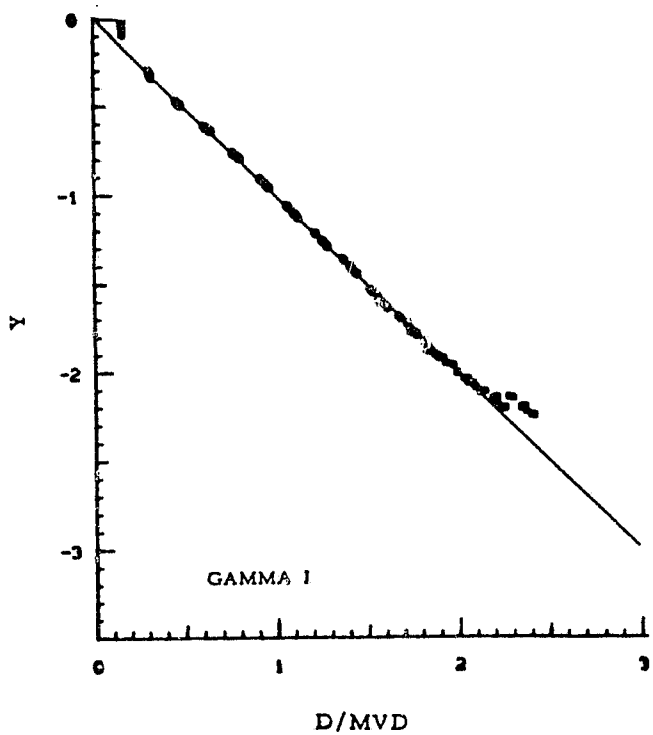
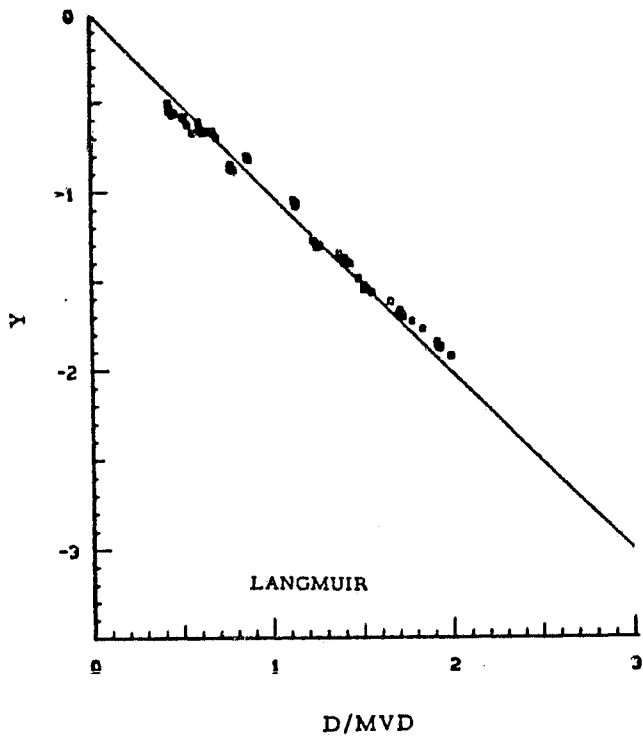
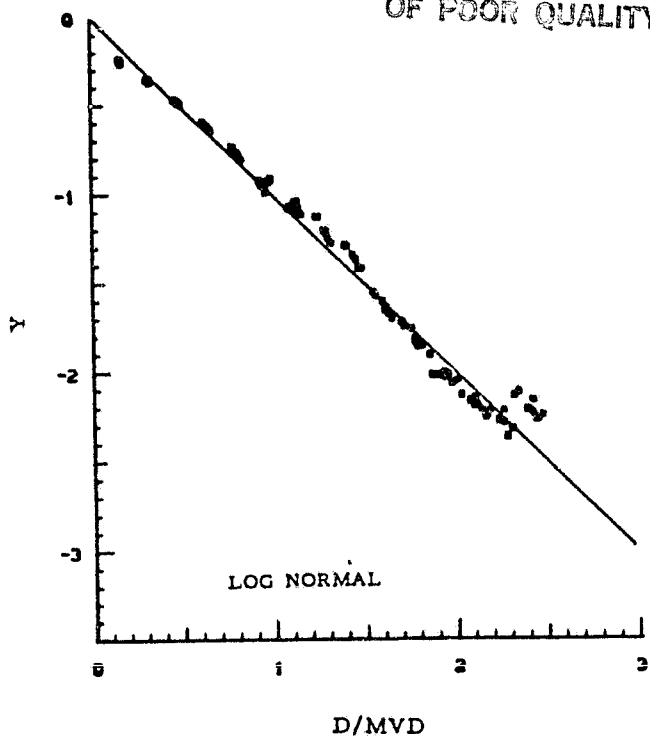


Figure 4-32. NORMALIZED DSD FROM ASSP 2'

ORIGINAL PAGE IS
OF POOR QUALITY

Table 4-9

IRT CLOUD DSD FORM EVALUATION

Probe ID	No. of DSD	<u>RMS Error (100% LWC) for Given DSD Form</u>			
		<u>Langmuir</u>	<u>Log Normal</u>	<u>Gamma I</u>	<u>Gamma II</u>
FSSP 1	83		0.230	0.117	0.098
ASSP 1	54		0.158	0.099	0.079
ASSP 2	32		0.217	0.091	0.076
ASSP 3	48		0.217	0.126	0.078
ASSP 4	41		0.210	0.112	0.079
FSSP 1'	7		0.248	0.072	0.063
ASSP 2'	7		0.078	0.051	0.038
		Average	0.194	0.095	0.073

Probe ID	<u>RMS Error (95% LWC) For Given DSD Form</u>			
	<u>Langmuir</u>	<u>Log Normal</u>	<u>Gamma I</u>	<u>Gamma II</u>
FSSP 1	0.101	0.175	0.052	0.072
ASSP 1	0.087	0.105	0.035	0.060
ASSP 2	0.103	0.186	0.061	0.066
ASSP 3	0.156	0.200	0.075	0.073
ASSP 4	0.127	0.179	0.079	0.076
FSSP 1'	0.074	0.107	0.020	0.046
ASSP 2'	0.059	0.055	0.012	0.028
Average	0.101	0.144	0.048	0.060

C-2

ORIGINAL PAGE IS
OF POOR QUALITY

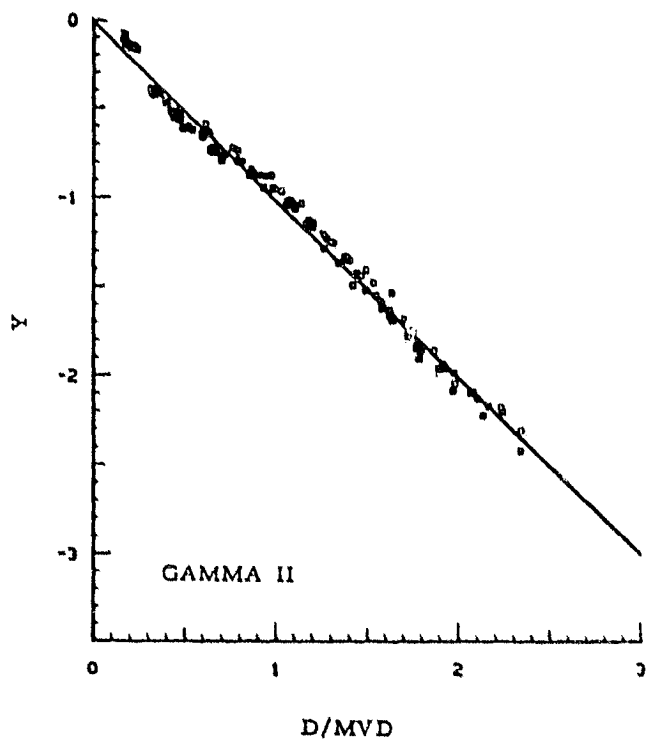
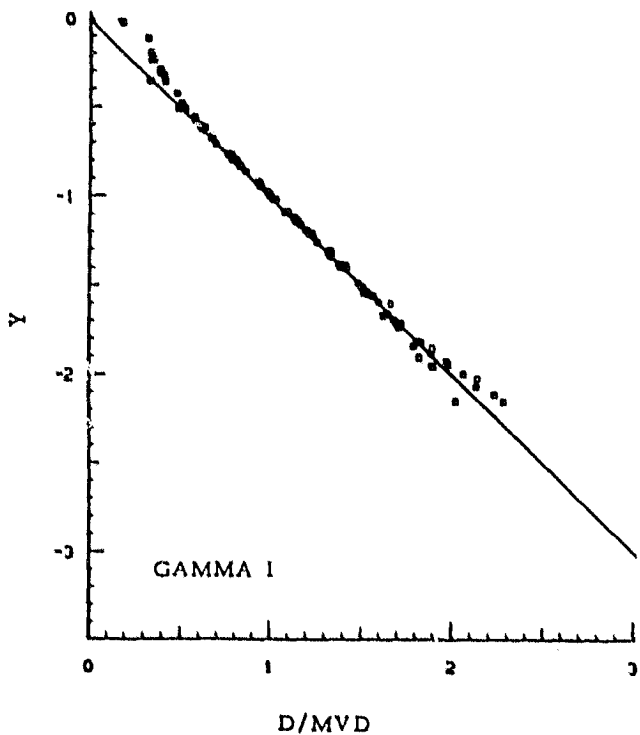
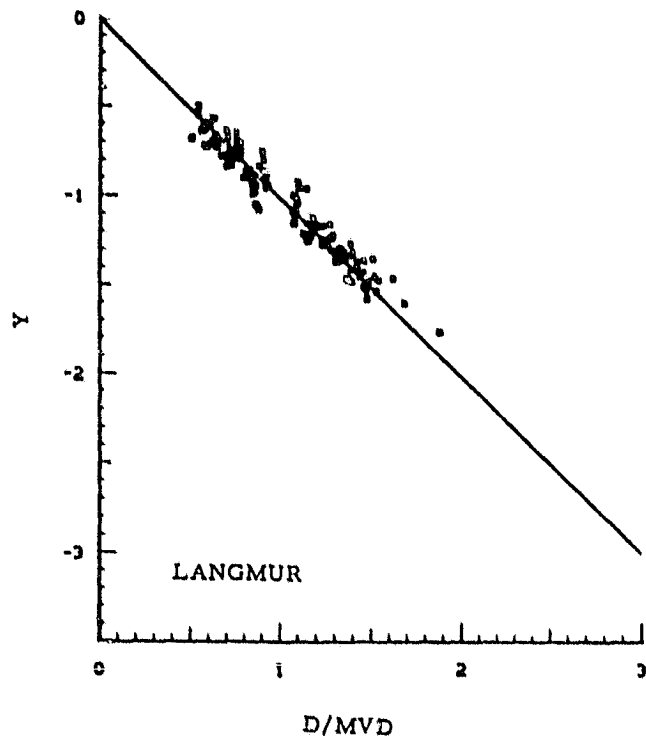
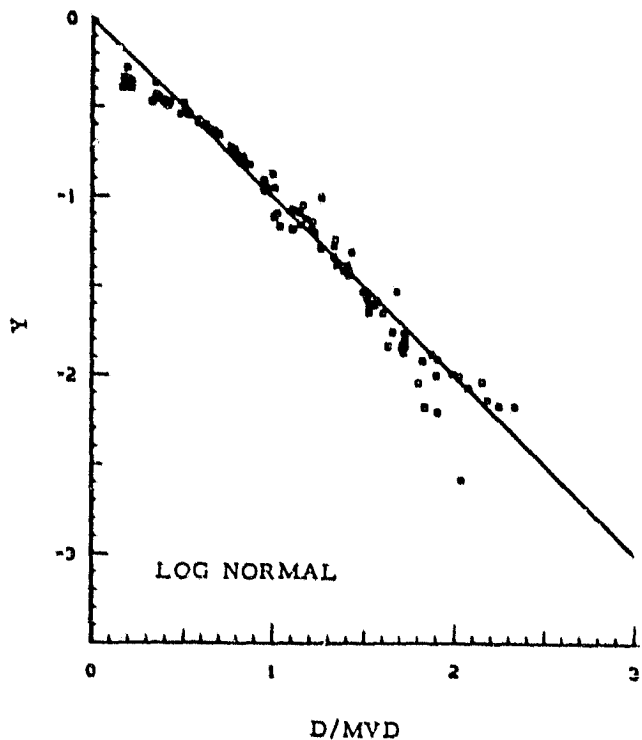


Figure 4-33. NORMALIZED DSD OF NATURAL CLOUDS

ORIGINAL PAGE IS
OF POOR QUALITY.

Table 4-10

NATURAL CLOUD DSD SUMMARY

DSD ID	LWC G/M3	MVD U	NMAX	EXP	ERR	LANGMUIR		LOG NORMAL		GAMMA I		GAMMA II	
						U	U	MVD	SIGN	MVD	ALPHA	MVD	ALPHA
1	.20	19.6	2.32	1.42	.15	19.5	.327	20.0	5.58	20.3	3.95		
2	.96	15.9	1.89	1.00	.09	15.8	.232	15.8	15.34	14.0	8.27		
3	.74	14.9	2.01	1.09	.08	14.8	.246	14.8	13.25	12.8	9.37		
4	.99	16.0	1.87	1.07	.08	15.8	.253	15.9	12.24	15.1	6.51		
5	1.47	17.8	2.19	1.02	.05	17.4	.253	17.5	12.02	16.6	6.02		
6	2.02	18.5	2.11	.98	.05	18.2	.246	18.3	12.82	17.4	6.11		
7	.32	15.2	1.78	.92	.06	15.0	.212	15.1	18.81	13.6	9.24		
8	.35	19.3	1.71	.87	.08	19.1	.210	19.2	19.00	18.4	5.93		
9	.26	16.3	1.66	1.03	.08	15.9	.241	15.9	14.14	15.2	7.30		
10	.34	18.1	1.66	1.05	.09	17.9	.249	18.1	12.53	19.0	5.38		

NATURAL CLOUD DSD FORM EVALUATION

RMS ERROR	LANGMUIR	LOG NORMAL	DSD FORM	
			GAMMA I	GAMMA II
100% LWC	.1137	.1255	.0576	
95% LWC	.0766	.0112	.0522	

shown that the estimates of LWC and MVD from the individual probe measurements differ under given cloud conditions, it is indeed difficult to compare the tunnel measurements against those made through the natural clouds. Nevertheless, since absolute differences in the absolute mass distributions can be appropriately normalized and since the displacement coefficient, N_0 , is essentially removed in the volume frequency versus scaled particle diameter distributions, it may be appropriate to compare the values found for the curvature (α) and scale (λ) parameters between these measurements.

Table 4-11 presents a computer generated summary of the curvature (α) and scale (λ) values of the GD for measurements taken at the various tunnel settings. It is shown that these DSD were characterized by α values ranging from about 1 to 5 and by λ values between 0.2 to 0.5/ μm . Also, for a given tunnel setting, variations in α and λ between probes are indicated to be within about ± 1 and $\pm 0.07/\mu\text{m}$, respectively. In contrast, most of the DSD from the natural clouds shown in Table 4-10 had curvature values (Γ_{II}) of between 5 to 10 and λ values ($\lambda = \frac{\alpha + 3.6}{MVD}$) between 0.5 to 1.0/ μm . These differences are further exemplified in Table 4-12 which presents the mean and standard deviations of the data sets. Where the IRT clouds show average α values of about 2.3 to 3.5, the natural clouds were characterized by an of 6.8. It is noted that the range of α values from the natural cloud DSD are also consistent with the mean value of 8 found from approximately 500 samples taken with oil slides from natural clouds in Russia (Khrigian, 1963). Figures 4-34 and 4-35 present examples of the measurements used in the comparisons and basically show that except for Test Point 42, the normalized mass of the IRT clouds is distributed over a broader scaled size range. This observation is consistent with the fact that the IRT clouds were generally characterized by smaller curvature and scale values. In any event, the somewhat broader irt drop size spectrum will not have a measurable effect upon the ice accretion, relative to the accretion in natural clouds.

Table 4-11

AVERAGE SPECTRA CHARACTERISTICS
FOR INDICATED IRT SETTINGS AND PROBES

IRT SET	TMVD	*****PROBE MVD(U)*****				*****GAMMA II MVD(U)*****				*****GAMMA II ALPHA*****				*****GAMMA II LAMDA(/U)*****			
		FSP1	ASP1	ASP2	ASP3 ASP4	FSP1	ASP1	ASP2	ASP3 ASP4	FSP1	ASP1	ASP2	ASP3 ASP4	FSP1	ASP1	ASP2	ASP3 ASP4
4	25.3	24.0	21.0	23.8	26.6	23.9	23.2	26.9	27.8	2.5	1.4	2.9	2.4	.26	.41	.29	.22
8	16.3	21.5	17.7	18.2	19.5	19.2	17.6	20.3	20.5	5.6	3.5	4.1	3.3	.48	.34	.25	.34
10	18.4	24.6	20.5	25.5	22.7	24.5	22.4	28.2	24.8	2.3	2.2	3.0	1.9	.24	.26	.26	.23
11	16.4	27.1	22.7	26.1	18.4	27.1	24.6	28.6	23.3	1.9	2.6	2.2	2.2	.21	.23	.27	.25
12	18.5	27.3	23.3	26.9	22.3	26.6	26.3	29.4	25.5	1.9	2.6	3.1	2.3	.21	.24	.27	.24
13	16.2	28.9	24.3	26.9	21.8	29.1	26.4	29.4	25.8	1.8	2.1	3.7	2.1	.19	.22	.27	.22
14	19.7	23.8	20.5	20.3	22.5	21.8	20.9	22.9	23.5	5.0	3.2	3.7	3.0	.40	.33	.26	.28
15	15.7	20.7	17.7	17.2	18.2	18.5	17.7	19.8	18.9	4.7	3.7	3.7	3.5	.45	.41	.27	.38
16	16.8	23.3	20.2	17.2	19.5	21.8	21.5	19.8	22.7	3.2	3.0	4.3	2.4	.31	.31	.40	.27
17	16.4	24.8	20.0	20.0	20.0	22.9	20.0	20.0	20.0	4.9	3.0	4.3	2.4	.37	.40	.29	.40
18	14.5	21.3	17.6	17.6	16.9	20.1	20.0	18.8	18.8	5.1	2.4	3.9	2.4	.44	.40	.25	.38
18C	13.1	19.2	18.2	18.2	18.2	18.1	20.0	22.1	18.8	3.9	1.8	3.4	3.4	.42	.38	.26	.36
19A	23.5	25.9	22.1	23.5	22.1	23.3	22.4	23.4	22.8	5.3	2.4	4.4	2.4	.38	.36	.27	.35
19B	20.3	24.7	22.2	22.2	21.1	22.4	22.4	23.6	22.4	4.1	2.8	4.3	2.4	.34	.35	.27	.35
19C	17.9	22.6	20.8	20.8	20.0	20.3	20.0	22.5	21.7	4.5	2.4	4.5	2.4	.40	.37	.27	.38
19D	16.0	22.6	18.8	21.1	18.3	20.7	19.3	22.1	22.6	3.7	3.4	2.7	2.4	.36	.31	.27	.30
19E	15.3	21.5	17.6	18.8	18.1	19.2	18.4	22.1	22.6	3.8	2.1	2.7	2.4	.39	.31	.27	.30
19G	14.6	21.2	17.7	18.8	18.1	20.0	19.1	22.1	22.6	2.6	1.8	2.7	2.4	.31	.29	.27	.30
19H	14.3	20.8	17.4	18.8	18.1	19.2	18.5	22.1	22.6	2.8	1.8	2.7	2.4	.34	.30	.27	.30
19I	14.0	21.6	17.9	18.8	18.1	19.8	18.5	22.1	22.6	2.8	1.8	2.7	2.4	.31	.28	.27	.30
19J	13.7	23.7	19.6	21.3	18.1	21.3	21.2	22.1	22.6	3.0	1.9	2.7	2.4	.31	.26	.27	.30
19K	13.3	22.1	18.8	20.0	18.1	20.0	20.7	22.1	22.6	2.7	1.5	2.7	2.4	.32	.25	.27	.30
20A	28.5	30.5	27.1	26.5	24.7	30.9	29.2	29.2	27.6	3.5	1.8	3.8	2.6	.23	.27	.19	.24
20B	24.5	25.9	25.2	25.2	24.7	24.4	21.8	26.6	26.5	4.1	2.3	3.6	2.6	.32	.27	.23	.27
20C	21.4	24.8	20.8	24.7	22.7	23.8	21.2	25.8	26.3	3.2	2.3	3.6	2.5	.29	.28	.23	.26
20D	18.9	24.1	18.9	26.2	21.8	22.2	19.7	23.1	27.8	3.2	1.9	3.1	2.4	.31	.28	.23	.26
20E	18.0	23.9	24.3	24.3	22.2	22.3	20.0	23.4	26.2	3.1	1.9	3.9	2.3	.30	.27	.23	.26
20F	17.5	21.0	24.5	24.5	20.6	19.7	20.0	26.4	26.4	2.7	1.5	3.4	1.9	.32	.27	.23	.27
20G	17.1	24.0	25.0	25.0	20.8	21.6	20.0	27.2	27.2	2.9	1.5	3.4	1.9	.30	.26	.23	.25
20H	16.7	26.1	25.5	25.5	21.3	23.5	20.0	27.5	27.5	2.9	1.5	3.2	2.3	.28	.25	.23	.26
20I	16.3	24.4	25.3	25.3	21.6	23.1	20.0	27.4	23.8	2.6	1.5	3.3	2.1	.27	.25	.23	.24
20J	15.9	24.6	26.5	26.5	21.2	23.0	20.0	27.9	23.4	2.5	1.5	3.4	1.8	.27	.25	.23	.23
20K	15.3	24.5	26.6	26.6	21.9	22.8	20.0	27.9	24.3	2.5	1.5	3.1	1.5	.27	.24	.21	.21
21	16.0	22.1	16.6	16.6	24.5	19.7	20.0	21.0	21.0	4.2	3.5	3.1	3.9	.40	.31	.27	.32
22	15.9	23.9	21.7	21.7	24.5	21.9	22.7	23.8	27.5	3.2	3.5	4.7	3.9	.31	.31	.25	.20
23	10.3	19.8	15.1	15.1	12.8	20.8	13.5	23.1	13.8	4.6	1.4	1.4	3.2	.40	.38	.25	.50
24	19.5	24.6	21.8	21.8	22.6	24.6	19.9	26.0	23.3	4.1	4.9	3.3	3.3	.32	.43	.27	.30

Table 4-12

SUMMARY STATISTICS OF MEAN
AND STANDARD DEVIATIONS (σ)
OF CURVATURE AND SHAPE PARAMETERS

Probe	α		λ (μm)	
	Mean	σ	Mean	σ
FSSP1	3.4	1.0	0.33	0.07
ASSP1	2.5	0.9	0.30	0.06
ASSP2	2.3	0.3	0.25	0.03
ASSP3	3.2	0.8	0.30	0.06
ASSP4	2.4	0.5	0.27	0.06
Natural Clouds	6.8	1.7	0.67	0.21

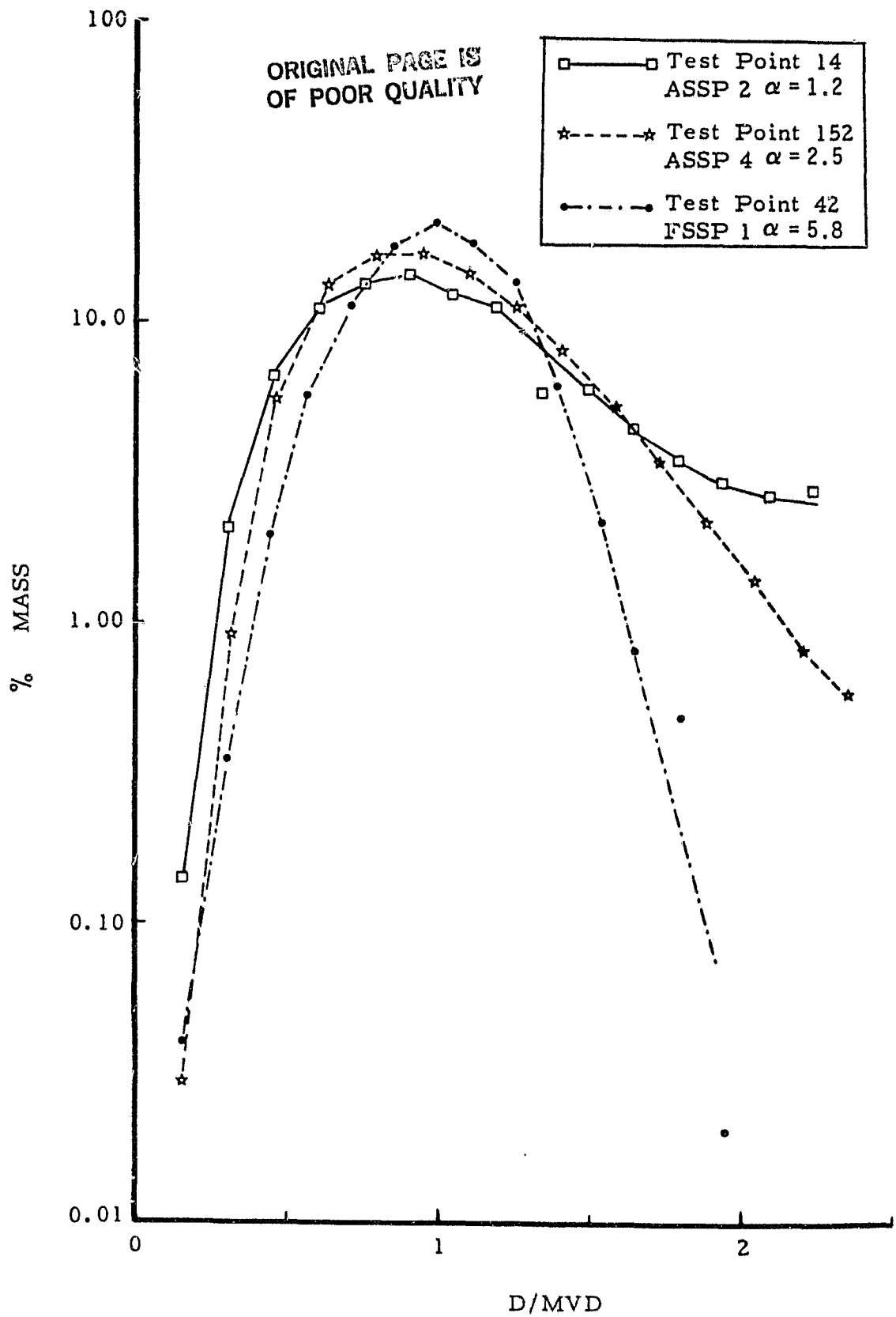


Figure 4-34. EXAMPLES OF NORMALIZED MASS DENSITY VERSUS SCALED PARTICLE DIAMETER DISTRIBUTIONS OF IRT CLOUDS

ORIGINAL PAGE IS
OF POOR QUALITY

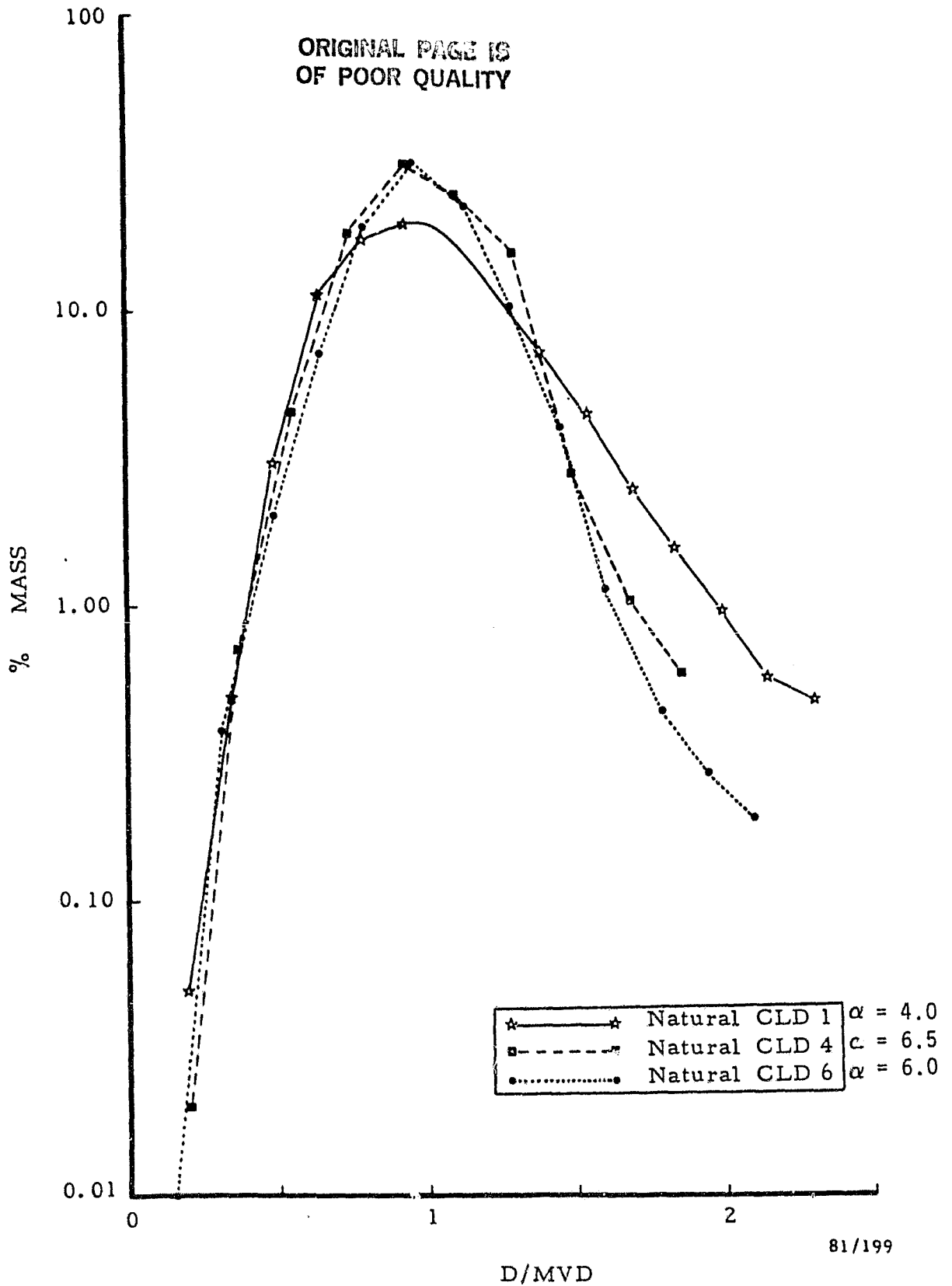


Figure 4-35. EXAMPLES OF NORMALIZED MASS DENSITY VERSUS SCALED PARTICLE DIAMETER DISTRIBUTIONS OF NATURAL CLOUDS

5. CONCLUSIONS

Tests conducted in the NASA LeRC IRT at different air speeds, pressure settings, and temperatures lead to the following conclusions:

A. Instrument Comparisons:

1. There was no apparent velocity effect to the PMS probe measurements at air speeds ranging from 50 to 285 mph.
2. The measurements from the LWC instruments (J-W and Leigh) agreed (little scatter) with each other and with the IRT calibrations.
3. The five PMS probes gave an excessively wide scatter in estimates of LWC (0.2 to 2.0 compared to the IRT setting of 1 g/m³).
4. For given cloud conditions, the estimates of cloud MVD or drop size between the five PMS probes were within $\pm 3 \mu\text{m}$ of each other in 93 percent of the cases.
5. Significant failure rates were observed of these instruments especially when one considers that the instruments were required to be in proper operating condition for testing. Failure rates of 66 percent and 24 percent were observed in the J-W and Leigh devices, respectively. Failure rates ranging from 100 percent to 2 percent were observed at the six scattering probes installed in the tunnel. Some of the failures can be attributed to hardware problems (e.g., J-W and all of the measurements from the FSSP 2), while others were related to measurement determination due to probe icing and perhaps to wetting of the optics.

B. Tunnel Concerns:

1. The cloud conditions produced in the IRT are highly repeatable as indicated by the values of the coefficient of variation determined for the following evaluations.

<u>Source of Variation</u>	<u>CV LWC (%)</u>	<u>CV MVD (%)</u>
During given sprays	± 5	$\pm 2-3$
Between given sprays on given days	± 10	$\pm 3-7$
Between given sprays among days	± 12	$\pm 3-7$
Between given sprays among seasons	± 12	

2. The PMS probe estimates of MVD exceeded those of the tunnel values which were based on rotating cylinder calibrations. The "best fit" regression equation determined between the five PMS probe estimates (PMVD) and the tunnel values (TMVD) is given as:

$$\text{PMVD} = 13.1 + 0.5 \text{ TMVD}$$

3. As compared to the log normal and Langmuir distribution functions, the gamma distribution function best describes the drop size distribution measurements from the IRT and natural clouds. The drop size distributions from the IRT were slightly broader than those of the natural clouds as was also indicated by smaller values for both the curvature and scale parameters of the gamma distribution function.

6. RECOMMENDATIONS

The discrepancies shown between the measurements of the individual probes of given cloud conditions in the IRT strongly set forth the need to establish a test facility (or facilities) where instruments can be calibrated against known cloud standards. Aside from providing means to better define the sample area and band width of individual probes, the resulting calibrations would add credibility to the measurements. An icing tunnel such as the IRT used in this study should be considered as a possible test facility in addition to those operated by the National Research Council (NRC) of Canada and by the Arnold Engineering Development Center (AEDC), Arnold AFS in Tennessee.

Due to possible measurement deterioration from probe icing it is recommended that direct LWC measurement devices (e.g., J-W and Leigh) such as used in this study complement the probe measurements during icing certification flights.

Based on the large differences found between the probe and tunnel estimates of cloud MVD, it is suggested that procedures used in estimating the MVD from the rotating cylinder measurements be reevaluated. Specific emphasis should be placed upon evaluating errors resulting from incorrect assumptions on DSD form. Also, the effects of air speed utilized in the present operating equations of the IRT should be reviewed in view of the discrepancies found in this study.

7. REFERENCES

- Khrgian, A. Kh., Borovikov, A. M., I. I. Gaivoronskii, E. G. Zak, V. V. Kostarev, I. P. Mazin, V. E. Minervin, S. M. Schmeter, 1963: Cloud physics. Published in Israel Program for Scientific Translations. A. Kh. Khrgian, editor.
- Knollenberg, R. G., 1970: The optical array: an alternative to scattering or extinction for airborne particle size determination. J. Appl. Met., pp. 501-508.
- Langmuir, I. and K. B. Blodgett, 1949: Mathematical investigations of water droplet trajectories. General Electric Res. Lab., Rept. No. RL-225, Schenectady, N.Y., 47 pp.
- Stone, J. M., 1963: Radiation and optics. McGraw-Hill Book Co., 544 pp.
- Takeuchi, D. M., 1978: Characterization of raindrop size distributions. From preprints "Conference on Cloud Physics and Atmospheric Electricity," July 31-August 4, 1978. Issaquah, Washington. American Meteorological Society, Boston, Mass.
- Takeuchi, D. M., and P. C. Chen, 1979: A technique for determining parameter estimates of the gamma distribution. From preprints "Sixth Conference on Probability and Statistics in Atmospheric Sciences," October 9-12, 1979. Banff, Alta., Canada. American Meteorological Society, Boston, Mass.

ORIGINAL PAGE IS
OF POOR QUALITY

APPENDIX A - TEST POINT SUMMARY

IRT TEST POINT SUMMARY
JANUARY 1981

PAGE 1

TAPE 3

TEST PT	RUN DA	TIME	DT	TAS	TEM	RH	PAIR	PH20	T-Q	DV	J=0	L=0	PROBE Q	ID	G/M3	U	CC	NT	RCT	ALP	LAM	AC	EFF	REMARKS
1	5858	8 174435	30	200	13	-99	42.0	57.0	.79	15	.48	.85	2	.07	20	139	31	7	31	3.1	435			PROBE OUT OF SPEC
2	5858	8 180615	30	200	14	-99	42.0	57.0	.79	15	.50	.83	2	.07	20	146	33	5	33	3.0	434			PRGBE OUT OF SPEC
3	5858	8 190735	30	200	14	-99	42.0	57.0	.79	15	.80	1.00	2	.08	15	120	42	5	42	4.7	583	75	48	PROBE OUT OF SPEC
4	5858	8 193330	45	200	14	-99	42.0	57.0	.79	15	-.88	1.05	2	.12	24	142	32	8	32	2.7	335			PROBE OUT OF SPEC JW INACTIVE
5	5858	8 194250	45	200	14	-99	42.0	57.0	.79	15	-.88	1.04	2	.11	10	47	10	4	10	4.3	741			PROBE OUT OF SPEC JW INACTIVE
6	5858	8 195230	40	200	14	-99	42.0	57.0	.79	15	-.88	1.03	2	.06	24	82	18	6	18	2.6	342			PROBE OUT OF SPEC JW INACTIVE
7	5858	8 2012 5	30	200	14	-99	30.0	62.5	1.16	24	-.88	-.19	2	.15	29	120	27	3	27	2.2	238			PROBE OUT OF SPEC JW INACTIVE
8	5858	8 204315	30	195	14	-99	30.0	62.5	1.19	24	-.88	-.24	2	.16	22	125	43	4	43	2.8	303	75	48	LEIGH INTERMITTENT PROBE OUT OF SPEC JW INACTIVE
9	5858	8 210125	30	195	14	-99	30.0	62.5	1.19	24	-.88	-.78	2	.17	28	141	31	5	31	2.2	267			LEIGH INTERMITTENT PROBE OUT OF SPEC JW INACTIVE
10	5858	8 210935	20	191	14	-99	30.0	62.5	1.22	24	-.88	-.23	2	.15	24	106	36	8	36	2.7	288	75	48	LEIGH INTERMITTENT PROBE OUT OF SPEC JW INACTIVE
11	5858	8 211645	30	193	14	-99	30.0	62.5	1.20	24	-.88	-.99	2	.21	25	111	37	9	37	3.1	284	76	49	LEIGH INACTIVE PROBE OUT OF SPEC JW INACTIVE
12	5858	8 2136 0	60	195	13	-99	30.0	62.5	1.19	24	-.88	-.20	2	.12	26	150	33	5	33	2.2	284			PROBE OUT OF SPEC JW INACTIVE
																								LEIGH INTERMITTENT

IRT TEST POINT SUMMARY
JANUARY 1981

TEST PT	DA	TIME	DT	TAS	TEM	RH	PAIR	PH2O	T-Q	DV	J-Q	L-Q	PROBE	Q	DV	NT	RCT	ALP	LAM	AC	EFF	REMARKS	
ID		LST	SEC	MPH	F	%	PSIG	PSIG	G/M3	U	G/M3	G/M3	ID	G/M3	U	/CC		/4U	Z	X			
14	5895	9 175350	30	200	14	-99	25.0	32.5	.56	15	-.88	0	.50	DAP	2	.02	75	0	0-10.	0	0	JM INACTIVE	
													ASSP	2	.24	20	179	64	3.8	388	76	49	
15	5895	9 180140	30	198	14	-99	25.0	32.0	.54	15	-.88	0	.45	OAP	2	.00	92	0	0-10.	0	0	JM INACTIVE	
													ASSP	2	.09	18	133	48	3.5	436	73	50	
16	5895	9 183110	60	200	14	-99	31.0	41.0	.64	15	-.88	0	.48	OAP	2	0.00	0	0	0-10.	0	0	JM INACTIVE	
													ASSP	2	.23	18	178	63	5.5	524	81	49	
17	5895	9 185020	45	200	13	-99	31.0	41.0	.64	15	-.88	0	.49	OAP	2	.00	164	0	0-10.	0	0	JM INACTIVE	
													ASSP	2	.20	17	174	61	5.3	536	76	48	
18	5895	9 1854 0	60	200	13	-99	31.0	41.0	.64	15	-.88	0	.53	OAP	2	.01	149	0	0-10.	0	0	JM INACTIVE	
													ASSP	2	.18	17	165	59	5.3	542	77	49	
19	5895	9 185555	45	200	13	-99	31.0	41.0	.64	15	-.88	0	.55	OAP	2	.01	150	0	0-10.	0	0	PROBE ICED OVER?	
													ASSP	2	.09	15	122	42	4.5	547	72	47	
20	5895	9 194155	25	50	-14	-99	50.0	60.0	2.58	16	-.88	0	.79	OAP	2	.00	23	0	0-10.	0	0	JM INACTIVE	
													ASSP	2	.65	13	1044	94	6.9	809	74	49	
21	5895	9 194325	45	100	-14	-99	50.0	60.0	1.29	14	-.88	0	1.26	OAP	2	.23	91	3	2-10.	0	0	JM INACTIVE	
													ASSP	2	.87	18	576	104	6.1	547	84	50	
22	5895	9 194545	30	150	-14	-99	50.0	60.0	.86	13	-.67	.86	.97	OAP	2	.43	114	4	4-10.	0	0	JM INTERMITTENT	
													ASSP	2	.53	18	345	95	5.3	482	81	50	
23	5895	9 194745	45	200	-14	-99	50.0	60.0	.64	12	.99	.81	.81	OAP	2	.30	126	2	4-10.	0	0	JM INACTIVE	
													ASSP	2	.27	19	186	68	4.3	414	71	50	
24	5895	9 195715	30	50	-16	-99	50.0	75.0	4.07	23	-.88	-2.22	.22	OAP	2	.62	37	61	7-10.	0	0	JM INACTIVE	
													ASSP	2	2.18	23	826	75	4.6	362	84	50	
25	5895	9 1959 0	45	100	-18	-99	50.0	75.0	2.04	20	-.88	-.09	.09	OAP	2	.72	102	12	6-10.	0	0	LEIGH OUT OF RANGE	
													ASSP	2	1.54	22	580	102	5.6	423	85	48	
													ASSP	2	3	3	1	1	1	3	3	0	1

ORIGINAL PAGE IS
OF POOR QUALITY

IRI TEST POINT SUMMARY
JANUARY 1981

TAPE 4

TEST PT	RUN DA	TIME	DT	TAS	TEM	RH	PAIR	PH20	T-O	DV	J-O	L-O	PROBE ID	G/M3	U	G/M3	U	CC	PROBE / CV(X)	NT	ALP	LAM	AC	EFF	REMARKS
26	5895	9 200125	35	150	-18	-99	50.0	75.0	1.36	18	1.23	2	2	41	88	7	6-10.	0	7	17	0	0	0	0	JM INTERMITTENT
													ASSP 2	.78	21	377	99	5.2	430	80	48	4	2	1	
27	5895	9 201315	25	200	-11	-99	50.0	75.0	1.02	16-	1.18	40	17	104	2	2-10.	0	2	18	0	0	0	0	JM INTERMITTENT	
													ASSP 2	.38	21	194	69	4.7	405	71	49	4	3	3	
28	5895	9 201755	45	50	-15	-99	50.0	90.0	5.15	29	-.88	0	12	1.65	46	5	16-10.	0	105	16	0	0	0	0	JM INACTIVE
													ASSP 2	2.20	26	636	56	4.2	307	84	49	3	0	7	
29	5895	9 202020	40	100	-15	-99	50.0	90.0	2.58	24	-.88	0	13	1.09	66	2	15-10.	0	11	8	3	0	0	0	LEIGH OUT OF RANGE
													ASSP 2	1.89	25	543	96	5.2	364	86	49	4	0	3	
30	5895	9 202220	20	150	-15	-99	50.0	90.0	1.72	21	1.14	4	5	1.42	87	25	21-10.	0	25	21	0	0	0	0	JM INACTIVE
													ASSP 2	.93	24	301	80	4.8	352	72	49	5	7	0	
31	5895	9 2024 0	20	200	-15	-99	50.0	90.0	1.29	19	-.41	78	8	2.36	106	28	37-10.	0	28	37	0	0	0	0	JM INTERMITTENT
													ASSP 2	.18	20	105	39	4.2	389	62	52	3	7	12	
32	5895	9 2038 5	25	50	-20	-99	50.0	90.0	5.15	29	-.88	0	17	2.56	57	109	20-10.	0	9	0	0	0	0	0	JM INACTIVE
													ASSP 2	3.25	28	813	74	4.4	300	86	50	3	0	5	
33	5895	9 203930	30	100	-20	-99	50.0	90.0	2.58	24	-.88	0	213	1.20	68	37	15-10.	0	5	10	0	0	0	0	LEIGH OUT OF RANGE
													ASSP 2	2.05	25	578	102	5.1	355	86	48	2	0	1	
34	5895	9 204125	30	150	-20	-99	50.0	90.0	1.72	21	1.53	1	122	1.54	90	22	21-10.	0	22	21	0	0	0	0	JM INACTIVE
													ASSP 2	.88	24	340	90	4.3	343	83	48	4	3	3	
35	5895	9 205440	20	200	-11	-99	50.0	90.0	1.29	19	1.40	3	101	.18	95	2	3-10.	0	9	42	25	0	0	0	LEIGH INTERMITTENT
													ASSP 2	.51	21	241	87	4.9	408	74	50	3	5	4	

IRT TEST POINT SUMMARY
JANUARY 1981

TAPE 5

PAGE 1

TEST PT	RUN ID	DA	TIME	DT LST	SEC	MPH	F	X	PSIG	G/M3	U	G/M3	J=0	L=0	PROBE	Q	DI	G/M3	U	/CC	NT	ALP	LAM	AC	EFF	REMARKS	
36	5896	12	185645	30	173	5	-99	52.5	75.5	1.13	16	-0.88	1.43	0	FSSP	1	.37	22	126	23	6.0	435				JM INACTIVE	
															ASSP	3	.83	19	419	148	7.4	586	0	100			
37	5896	12	185915	30	173	5	-99	52.5	75.5	1.13	16	-0.88	1.23	0	FSSP	1	.40	22	142	26	6.1	445				JM INACTIVE	
															ASSP	3	.49	16	373	132	7.7	691	0	100			
38	5896	12	190215	30	173	5	-99	52.5	75.5	1.13	16	-0.88	1.27	0	FSSP	1	.55	22	215	40	5.9	450				JM INACTIVE	
															ASSP	3	.37	15	353	125	7.0	685	0	100			
39	5896	12	191025	30	220	9	-99	36.0	62.0	.94	19	-0.88	.93	0	FSSP	1	.29	24	103	24	4.2	324				JM INACTIVE	
															ASSP	3	.28	25	207	93	3.2	327	0	100			
40	5896	12	191615	30	200	9	-99	50.0	75.0	1.02	16	-0.88	.95	0	FSSP	1	.27	23	91	19	5.6	407				JM INACTIVE	
															ASSP	3	.30	16	257	105	6.0	576	0	100			
41	5896	12	193250	30	150	4	-99	42.0	56.0	1.02	16	-0.88	.68	0	FSSP	1	.25	18	168	27	7.1	619				JM INACTIVE	
															ASSP	3	.54	14	509	156	11.1	1024	0	100			
42	5896	12	193940	40	100	6	-99	32.0	39.0	1.08	16	-0.88	1.07	0	FSSP	1	.37	22	124	13	7.5	522				JM INACTIVE	
															ASSP	3	1.25	17	821	168	7.9	675	0	100			
43	5896	12	194840	30	220	9	-99	36.0	67.0	1.03	20	-0.88	.86	0	FSSP	1	.25	26	74	17	4.2	307				JM INACTIVE	
															ASSP	3	.33	23	219	99	3.8	362	0	100			
44	5896	12	195530	30	200	8	-99	50.0	75.0	1.02	16	-0.88	1.00	0	FSSP	1	.29	22	101	22	5.8	425				JM INACTIVE	
															ASSP	3	.54	18	347	142	6.4	557	0	100			
45	5896	12	204030	30	100	4	-99	65.0	100.0	2.41	20	-0.88	1.96	0	FSSP	1	.39	25	60	8	8.4	486				JM INACTIVE	
															ASSP	3	2.48	21	934	191	6.8	489	0	100			
46	5896	12	204535	30	100	4	-99	64.0	69.0	.91	10	-0.88	.64	0	FSSP	1	.31	19	156	17	6.6	531				JM INACTIVE	
															ASSP	3	.85	15	778	159	7.3	699	0	100			
47	5896	12	205525	30	100	4	-99	41.0	57.5	1.65	20	-0.88	1.24	0	FSSP	1	.35	24	81	8	9.4	554				JM INACTIVE	
															ASSP	3	.91	15	800	164	8.4	783	0	100			

ORIGINAL PAGE IS
OF POOR QUALITY

IRT TEST POINT SUMMARY
 JANUARY 1981

TAPE 5

PAGE 2

TEST PT	RUN DA	TIME	DT	TAS	TEM	RH	PAIR	PH20	T-Q	DV	J-Q	L-Q	PRORE	Q	ID	G/M3	U	G/M3	U	CC	PROBE	/CV(Z)	ALP	LAM	AC	EFF	REMARKS
48	5896	12 210250	30	100	5	-99	26.0	42.0	1.63	25	0	0	1.44	FSSP	1	.70	24	230	25	5.1	371						JW INACTIVE
													ASSP	3	2.48	6	23	833	170	5.6	404						0 100
49	5896	12 212325	30	100	-13	-99	32.0	39.0	1.08	16	0	0	1.15	FSSP	1	.44	23	132	14	7.2	485						JW INACTIVE
													ASSP	3	1.57	9	19	824	169	6.9	556						0 100
50	5896	12 2129 0	30	150	-9	-99	42.0	56.0	1.02	16	0	0	.93	FSSP	1	.52	22	194	31	5.8	434						JW INACTIVE
													ASSP	3	.75	18	477	146	6.9	595							0 100
51	5896	12 213745	30	150	-9	-99	42.0	56.0	1.02	16	0	0	1.02	FSSP	1	.45	21	180	29	6.0	454						JW INACTIVE
													ASSP	3	.91	19	514	158	7.4	607							0 100
52	5896	12 2143 0	30	200	-9	-99	50.0	75.0	1.02	16	0	0	.94	FSSP	1	.36	24	108	23	5.3	373						JW INACTIVE
													ASSP	3	.33	19	269	110	4.4	440							0 100
53	5896	12 214630	30	220	-9	-99	50.0	60.0	.59	12	0	0	.54	FSSP	1	.17	22	73	17	4.8	386						JW INACTIVE
													ASSP	3	.02	26	33	15	2.2	311							PROBE ICED OVER?
															.66	15	93	93	46	29						0 0	

ORIGINAL PAGE IS
 OF POOR QUALITY

IRI TEST POINT SUMMARY
JANUARY 1981

TAPE 6

PAGE 1

TEST PT	RUN DA	TIME	DT LST	TAS SEC	TEM MPH	F	X	PSIG	PSIG	PH20	I-Q	DV	J-Q	L-Q	PRUHE	Q	ID	G/M3	U	/CC	NT	RCT	ALP	LAM	AC	EFF	REMARKS	
54	5861	14 1724	5	30	100	16	-99	32.0	39.0	1.08	16	1.04	1.19	FSSP	1	3	1	30	22	97	10	7.9	536					
															ASSP	3	1.60	19	881	180	7.6	612			0	100		
55	5861	14 173135	30	150	16	-99	43.0	56.0	.98	15	.79	1.14	FSSP	1	2	3	20	21	73	11	7.8	548						
															ASSP	3	1.16	18	587	180	8.8	681			0	100		
56	5861	14 173935	30	200	16	-99	50.0	75.0	1.02	16	1.18	1.12	FSSP	1	3	5	22	7	33	33	22	19						
															ASSP	3	1.12	20	419	172	8.6	601			0	100		
57	5861	14 174740	30	220	16	-99	36.0	62.0	.94	19	1.14	1.08	FSSP	1	3	5	28	25	87	20	4.7	341						
															ASSP	3	1.29	26	342	154	5.6	371			0	100		
58	5861	14 1759	0	30	250	15	-99	53.0	91.0	1.00	16	1.12	-.61	FSSP	1	7	76	17	23	59	16	5.7	418					
															ASSP	3	.91	22	285	146	8.5	558			0	100		
59	5861	14 182145	30	260	15	-99	36.0	70.0	.91	18	-.88	-.18	FSSP	1	0	179	13	4	13	13	7	5						
															ASSP	3	.97	27	248	132	5.1	342			0	100		
60	5861	14 182645	30	285	16	-99	36.0	76.0	.90	18	-.88	-.07	FSSP	1	0	122	32	7	35	35	12	9						
															ASSP	3	.91	27	209	122	5.5	350			0	100		
61	5861	14 185145	30	100	7	-99	65.0	100.0	2.41	20	-.88	1.91	FSSP	1	0	4	14	4	12	12	10	9						
															ASSP	3	2.83	23	915	187	6.3	440			0	100		
62	5861	14 190335	30	100	6	-99	64.0	69.0	.91	10	-.88	1.04	FSSP	1	0	1	27	14	13	13	20	21						
															ASSP	3	1.06	15	848	174	7.0	645			0	100		
63	5861	14 1911	0	30	100	6	-99	41.2	58.0	1.67	20	-.88	1.83	FSSP	1	0	3	10	2	12	12	8	6					
															ASSP	3	1.86	20	842	172	6.5	503			0	100		
64	5861	14 19175	60	100	6	-99	26.0	42.0	1.63	25	-.88	1.65	FSSP	1	0	6	25	7	16	16	22	12						
															ASSP	3	2.01	24	728	149	4.8	359			0	100		
65	5861	14 192735	30	220	6	-99	36.0	62.0	.94	19	-.88	1.03	FSSP	1	0	1	27	25	80	19	4.2	313						
															ASSP	3	.89	26	280	126	4.8	347			0	100		

ORIGINAL PAGE IS
OF POOR QUALITY

LEIGH INTERMITTENT
JM INACTIVE
LEIGH INTERMITTENT
JM INACTIVE
LEIGH INTERMITTENT
JM INACTIVE
JM INACTIVE
JM INACTIVE
JM INACTIVE
JM INACTIVE
JM INACTIVE

IRT TEST POINT SUMMARY
JANUARY 1981

TAPE 6

PAGE 2

TEST PT	RUN DA	TIME	DT	TAS	TEH	PH	PAIR	PH20	T-O	DV	J=0	L=0	PROBE ID	G/M3	U	PROBE / CV (%)	NT	RCT	ALP	LAM	AC	EFF	REMARKS	
			SEC	MPH	F	X	PSIG	G/M3	U	G/M3	G/M3	G/M3				U								
66	5861	14	194030	30	250	5	-99	53.0	91.0	1.00	16	-0.88	0	5	17	24	56	15	4.9	364	5	0	100	JM INACTIVE
													ASSP 3	.78	22	264	135	7.4	514	0	0	0	0	
67	5861	14	1946	0	30	260	6	-99	36.0	70.0	.91	18	-0.88	0	22	28	55	15	4.2	292	4	0	100	JM INACTIVE
													ASSP 3	.89	26	266	142	4.9	349	0	0	0	0	
68	5861	14	195350	30	285	5	-99	36.0	76.0	.90	18	-0.88	-0.42	102	29	29	55	17	4.3	286	4	0	100	JM INACTIVE
													ASSP 3	.99	27	273	159	4.7	324	0	0	0	0	
69	5861	14	201220	30	220	-11	-99	50.0	90.0	1.17	18	-0.88	-1.08	39	24	24	103	24	4.9	362	3	0	100	LEIGH INTERMITTENT
													ASSP 3	1.20	24	338	152	6.2	411	0	0	0	0	
70	5861	14	2016	5	30	230	-10	-99	50.0	90.0	1.12	18	-0.88	1.15	21	21	174	43	4.3	387	4	0	100	JM INACTIVE
													ASSP 3	1.08	25	315	149	5.7	391	0	0	0	0	
71	5861	14	2028	5	30	240	-11	-99	50.0	90.0	1.07	17	-0.88	1.07	24	24	113	29	4.3	336	4	0	100	JM INACTIVE
													ASSP 3	1.12	25	306	150	5.7	380	0	0	0	0	
72	5861	14	203135	30	250	-9	-99	50.0	90.0	1.03	17	-0.88	.96	4	26	26	79	21	4.7	325	4	0	100	JM INACTIVE
													ASSP 3	1.04	25	288	148	5.3	361	0	0	0	0	
73	5861	14	203510	30	260	-9	-99	50.0	90.0	.99	16	-0.88	.90	4	24	24	126	35	4.6	338	3	0	100	JM INACTIVE
													ASSP 3	1.12	25	303	161	5.5	369	0	0	0	0	
74	5861	14	204530	30	270	-12	-99	50.0	90.0	.95	16	-0.88	.84	5	25	25	137	40	4.4	326	3	0	100	JM INACTIVE
													ASSP 3	1.20	26	285	158	5.6	358	0	0	0	0	
75	5861	14	204835	30	285	-8	-99	50.0	90.0	.90	15	-0.88	.83	4	24	24	122	38	4.3	325	2	0	100	JM INACTIVE
													ASSP 3	1.06	27	266	155	5.2	343	0	0	0	0	
76	5861	14	2056	5	30	50	-13	-99	50.0	60.0	2.58	16	-0.88	1.51	25	25	53	3	9.7	547	8	0	100	JM INACTIVE
													ASSP 3	2.70	18	1491	153	8.1	646	0	0	0	0	
77	5861	14	2101	0	30	100	-13	-99	50.0	60.0	1.29	14	-0.28	0	21	21	59	6	9.8	639	8	0	100	JM INACTIVE
													ASSP 3	1.46	17	953	195	9.3	774	0	0	0	0	
																								LEIGH INTERMITTENT

ORIGINAL PAGE IS
OF POOR QUALITY

IRT TEST POINT SUMMARY
JANUARY 1981

TAPE 6

PAGE 3

TEST PT	RUN DA	TIME	DT	IAS	TEM	RH	PAIR	PH20	T-Q	DV	J=0	L=0	PROBE	Q	DV	NT	RCT	ALP	LAM	AC	EFF	REMARKS	
	ID	LST	SEC	MPH	F	%	PSIG	G/M3	U	G/M3	G/M3	G/M3	U	/CC	U				/MU	Z	Z		
78	5861 14	210920	30	150	-11	-99	50.0	60.0	.86	13	-.88	1.00	FSSP 1	.25	19	131	21	6.5	539				JW INACTIVE
													ASSP 3	.77	16	562	173	9.6	821				
79	5861 14	211645	30	150	-11	-99	50.0	75.0	1.36	18	-.88	1.38	FSSP 1	.33	23	107	17	6.5	455				JW INACTIVE
													ASSP 3	1.35	20	590	181	7.4	557				
80	5861 14	212115	30	100	-11	-99	59.0	75.0	2.04	20	-.88	-.04	FSSP 1	.44	25	96	10	7.8	467				JW INACTIVE
													ASSP 3	2.32	21	914	187	7.0	512				LEIGH INACTIVE
81	5861 14	212845	30	50	-11	-99	50.0	75.0	4.07	23	-.88	-2.06	FSSP 1	.45	27	73	4	9.3	490				JW INACTIVE
													ASSP 3	3.99	22	1402	143	6.7	476				LEIGH OUT OF RANGE
82	5861 14	213315	30	50	-11	-99	50.0	90.0	5.15	29	-.88	-2.27	FSSP 1	.66	30	80	4	7.8	381				JW INACTIVE
													ASSP 3	4.84	26	1098	112	5.9	372				LEIGH OUT OF RANGE
83	5861 14	213720	20	100	-13	-99	50.0	90.0	2.58	24	-.88	2.18	FSSP 1	.50	26	94	10	7.5	424				JW INACTIVE
													ASSP 3	3.14	25	849	174	5.7	379				JW INACTIVE
84	5861 14	214055	30	150	-11	-99	50.0	90.0	1.72	21	-.88	-1.05	FSSP 1	.51	25	134	21	5.7	382				JW INACTIVE
													ASSP 3	1.88	25	551	169	5.6	387				LEIGH INTERMITTENT
85	5861 14	214420	30	200	-9	-99	50.0	90.0	1.29	19	-.88	1.32	FSSP 1	.44	25	123	26	5.0	349				JW INACTIVE
													ASSP 3	1.27	26	358	147	5.0	344				JW INACTIVE

ORIGINAL PAGE IS
OF POOR QUALITY

IRT TEST POINT SUMMARY
JANUARY 1981

TAPE 7

TEST PT	RUN DA	TIME	DT	TAS	TEM	RH	PAIR	PH2O	T-Q	DV	J-Q	L-Q	PROBE Q	ID	G/M3	U	G/M3	U	CC	PROBE / CV (%)	NT	RCT	ALP	LAM	AC	EFF	REMARKS					
86	5862 15	165555	30	100	16	-99	65.0	100.0	2.41	20	-0.88	1.57	FSSP 1	.38	24	85	9	9.0	531	2	11	11	7	6	542	29	45	JW INACTIVE				
													ASSP 1	3.59	21	1414	192	7.5	542	29	45	3	7	1								
87	5862 15	170140	30	100	13	-99	64.0	69.0	.91	10	-0.88	.83	FSSP 1	.12	18	56	611.9	858	2	9	9	13	13	937	0	45	JW INACTIVE					
													ASSP 1	1.42	14	1528	210	9.5	937	0	45	2	0	2	18	0						
88	5862 15	170745	60	100	14	-99	41.0	58.0	1.68	20	-0.88	1.41	FSSP 1	.38	24	96	10	7.8	486	2	9	9	6	6	496	25	47	JW INACTIVE				
													ASSP 1	2.85	20	1435	203	6.1	496	25	47	3	1	1	3	2	11	1				
89	5862 15	171315	60	100	14	-99	26.0	42.0	1.63	25	-0.88	1.38	FSSP 1	.67	23	236	25	5.6	412	3	28	28	11	9	9	393	23	47	JW INACTIVE			
													ASSP 1	2.32	20	1396	200	4.3	393	23	47	4	3	1	1	8	7	2	1			
90	5862 15	172130	30	100	13	93	32.0	39.0	1.08	16	-0.88	1.06	FSSP 1	.25	21	90	9	8.9	614	5	14	14	11	11	590	23	47	JW INACTIVE				
													ASSP 1	2.03	17	1471	209	6.5	590	23	47	9	4	1	1	8	10	1	0			
91	5862 15	173655	60	150	14	81	43.0	56.0	.98	15	-0.88	1.23	FSSP 1	.29	21	114	18	6.7	500	5	19	19	12	8	591	25	34	JW INACTIVE				
													ASSP 1	1.46	17	1061	167	6.5	591	25	34	16	2	1	1	3	2	1	1			
92	5862 15	174325	60	200	15	73	50.0	75.0	1.02	16	-0.88	1.17	FSSP 1	.34	22	122	26	6.2	453	14	3	10	10	5	4	582	20	33	JW INACTIVE			
													ASSP 1	1.53	19	776	157	7.4	582	20	33	5	6	2	1	3	4	0	1			
93	5862 15	174930	30	220	13	75	36.0	62.0	.94	19	-0.88	1.02	FSSP 1	.34	25	94	22	5.2	361	16	2	12	6	4	462	32	32	JW INACTIVE				
													ASSP 1	1.58	21	669	144	6.0	462	32	32	4	1	2	1	2	0	2				
94	5862 15	175540	60	240	14	76	44.0	75.0	.94	17	-0.88	1.02	FSSP 1	.19	24	61	15	5.5	392	12	3	11	11	8	7	545	34	28	JW INACTIVE			
													ASSP 1	1.56	20	662	137	7.3	545	34	28	3	2	3	2	3	0	1				
95	5862 15	180035	60	250	14	76	53.0	91.0	1.00	16	-0.88	.69	FSSP 1	.12	26	39	10	4.3	330	21	5	15	15	6	6	513	36	31	JW INACTIVE			
													ASSP 1	1.63	22	579	135	7.3	513	36	31	3	2	7	2	3	4	0	4			
96	5862 15	1822 0	30	260	14	-99	36.0	70.0	.91	18	-0.88	.94	FSSP 1	.17	25	55	15	4.4	331	4	4	10	10	6	6	441	31	32	LEIGH INTERMITTENT			
													ASSP 1	1.48	22	565	143	5.9	441	31	32	4	3	1	2	5	5	0	1			
97	5862 15	182715	30	270	14	-99	36.0	73.0	.92	18	-0.88	.49	FSSP 1	.17	26	52	15	4.2	314	3	12	12	5	3	3	408	33	32	JW INACTIVE			
													ASSP 1	1.61	24	493	129	5.9	408	33	32	4	3	3	3	2	4	0	1			

IRT TEST POINT SUMMARY
 JANUARY 1981

TAPE 7

TEST PT	RUN DA	TIME	DT LSY	TAS MPH	TEM F	RH %	PAIR X	PH20	T-O	DV	J-Q	L-Q	PROBE ID	G/M3	PSIG	G/M3	U	PROBE / CV(X)	NT RCT	ALP	LAM	AC	EFF	REMARKS
110	5862	15 202850	25 200	-11	90	50.0	90.0	1.29	15	-0.88	0	17	FSSP 1	.34	23	130	28	4.9	380	9	31	19	31	JM INACTIVE
111	5862	15 203955	30 200	-12	-99	50.0	75.0	1.02	16	-0.88	0	4	FSSP 1	.27	22	118	25	5.5	435	11	2	2	2	JM INACTIVE
112	5862	15 204435	25 220	-11	100	50.0	75.0	.93	15	-0.88	0	2	FSSP 1	.23	22	105	25	5.1	415	1	2	1	1	JM INACTIVE
113	5862	15 2049 0	30 230	-10	85	50.0	75.0	.89	15	-0.88	0	5	FSSP 1	.23	22	93	23	4.8	385	2	1	1	1	JM INACTIVE
114	5862	15 205955	25 240	-10	-99	50.0	75.0	.85	15	-0.88	0	8	FSSP 1	.27	21	139	36	4.4	384	4	4	4	4	JM INACTIVE
115	5862	15 210230	30 250	-11	-99	50.0	75.0	.81	14	-0.88	0	2	FSSP 1	.27	21	150	40	4.4	395	2	1	1	1	JM INACTIVE
116	5862	15 210540	20 260	-10	-99	50.0	75.0	.78	14	-0.88	0	4	FSSP 1	.24	21	127	36	4.3	379	2	2	2	1	JM INACTIVE
117	5862	15 210650	30 260	-10	-99	50.0	75.0	.78	14	-0.88	0	3	FSSP 1	.26	22	125	35	4.3	370	2	2	1	1	JM INACTIVE
118	5862	15 210930	45 270	-10	-99	50.0	75.0	.75	14	-0.88	0	5	FSSP 1	.21	24	75	22	4.5	346	4	4	4	4	JM INACTIVE
119	5862	15 212140	40 283	-10	-99	50.0	75.0	.72	13	-0.88	0	3	FSSP 1	.36	22	177	54	4.0	353	2	2	2	2	JM INACTIVE

ORIGINAL PAGE IS
 OF POOR QUALITY

IRT TEST POINT SUMMARY
JANUARY 1981

TAPE 8

PAGE 1

TEST PT	RUN ID	DA TIME	DT LST	TAS SEC	TEM HPH	RH F	PAIR X	PH20 PSIG	I-U DV G/M3	DV J-Q	PROBE L-0	G ID G/M3	U /CC	APPRORE / CY(X)	NT RCT ALP	LAM AC EFF	REMARKS
120	5863 16 181435	60 100	14 -99	65.0	100.0	2.41	20 -0.88	1.46	0.10	150	1	0-10	0	0	0	0	JM INACTIVE
				ASSP 1	3.37	20	1428	193	7.6	564	0	44	1	2	9	1	
121	5863 16 181835	60 100	14 -99	64.0	69.0	.91	10 -0.88	.87	0.02	228	0	0-10	0	0	0	0	JM INACTIVE
				ASSP 1	1.45	14	1568	204	9.6	943	12	43	0	0	0	0	
122	5863 16 182245	60 100	13 -99	41.0	58.0	1.68	20 -0.88	1.44	0.16	53	3	2-10	0	0	0	0	JM INACTIVE
				ASSP 1	3.01	21	1482	203	5.0	422	45	45	0	0	0	0	
123	5863 16 1827 5	60 100	13 -99	26.0	42.0	1.63	25 -0.88	1.40	0.33	66	4	3-10	0	0	0	0	JM INACTIVE
				ASSP 1	2.61	22	1468	206	4.1	369	0	46	0	0	0	0	
124	5863 16 1832 0	60 100	13 -99	32.0	39.0	1.08	16 -0.88	-.02	0.04	54	0	0-10	0	0	0	0	JM INACTIVE
				ASSP 1	2.14	18	1512	205	5.5	512	11	45	0	0	0	0	
125	5863 16 1839 0	60 150	14 -99	43.0	56.0	.98	15 -0.88	-.02	0.01	131	1	0-10	0	0	0	0	LEIGH INACTIVE
				ASSP 1	1.60	18	1101	176	6.7	598	37	35	0	0	0	0	
126	5863 16 1844 5	60 200	14 -99	50.0	75.0	1.02	16 -0.88	-.01	0.04	124	0	0-10	0	0	0	0	JM INACTIVE
				ASSP 1	1.30	19	771	158	6.4	546	36	34	0	0	0	0	
127	5863 16 185435	30 220	14 -99	36.0	62.0	.94	19 -0.88	-.01	0.05	86	0	0-10	0	0	0	0	JM INACTIVE
				ASSP 1	1.53	21	749	156	5.3	439	32	31	0	0	0	0	
128	5863 16 1900 0	30 240	15 -99	44.0	75.0	.94	17 -0.88	-.27	0.03	98	0	0-10	0	0	0	0	JM INACTIVE
				ASSP 1	1.51	21	675	157	5.6	446	29	32	0	0	0	0	
129	5863 16 190455	30 250	14 -99	53.0	91.0	1.00	16 -0.88	-.01	0.05	139	0	0-10	0	0	0	0	JM INACTIVE
				ASSP 1	.92	20	510	114	5.0	436	26	29	0	0	0	0	

ORIGINAL PAGE IS
OF POOR QUALITY

120

IRT TEST POINT SUMMARY
JANUARY 1981

PAGE 1

TAPE 9

TEST PT	RUN DA	TIME	DT LST	TAS MPH	F	X	PSIG	G/M3	U	G/M3	J-Q	L-Q	PROBE ID	G/M3	DV U	NT RCT	ALP	LAM	AC	EFF	REMARKS
130	5863 16	1935 5	30 260	13 86	36.0	70.0	.91	18	-.88	0	0	0	FSSP 2	.22	25	128	37	2.8	275		PROBE OUT OF SPEC JW INACTIVE
131	5863 16	1939 10	60 260	13 84	36.0	70.0	.91	18	-.88	0	0	0	FSSP 2	.17	25	92	27	3.0	283		LEIGH INACTIVE PROBE OUT OF SPEC JW INACTIVE
132	5863 16	1959 0	30 260	13 99	36.0	70.0	.91	18	1.03	13	0	0	FSSP 2	.14	25	164	48	2.6	316		LEIGH INACTIVE PROBE OUT OF SPEC
133	5863 16	2004 0	30 270	14 70	36.0	73.0	.92	18	-.92	13	94	0	FSSP 2	.12	25	157	48	2.6	326		LEIGH INACTIVE PROBE OUT OF SPEC
134	5863 16	2008 45	25 285	14 99	36.0	76.0	.90	18	.99	10	33	0	FSSP 2	.16	24	185	59	2.6	319		LEIGH INTERMITTENT PROBE OUT OF SPEC
135	5863 16	2021 45	30 285	13 66	36.0	76.0	.90	18	1.82	10	3	0	FSSP 2	.11	25	143	46	2.5	318		LEIGH INTERMITTENT PROBE OUT OF SPEC
136	5863 16	2032 45	60 100	4 99	32.0	39.0	1.08	16	-.88	0	4	0	FSSP 2	.57	23	420	47	3.5	356		PROBE OUT OF SPEC JW INACTIVE
137	5863 16	2042 20	30 150	4 89	42.5	56.0	1.00	16	1.23	5	3	0	FSSP 2	.47	22	449	76	3.3	369		PROBE OUT OF SPEC
138	5863 16	2048 30	30 200	5 89	50.0	75.0	1.02	16	-.88	0	2	0	FSSP 2	.15	24	205	46	2.6	333		PROBE OUT OF SPEC JW INACTIVE
139	5863 16	2053 40	50 220	5 99	36.0	62.0	.94	19	-.88	0	3	0	FSSP 2	.15	24	183	45	2.7	325		PROBE OUT OF SPEC JW INACTIVE
140	5863 16	2100 20	30 240	5 99	44.0	75.0	.94	17	-.88	0	2	0	FSSP 2	.20	4	11	11	7	5		PROBE OUT OF SPEC JW INACTIVE

ORIGINAL PAGE IS
OF POOR QUALITY

IRT TEST POINT SUMMARY
JANUARY 1981

PAGE 1

TAPE 10

TEST PT	RUN DA	TIME	DT	TAS	TEM	RH	PAIR	PH20	T-U	DV	J=0	L=0	PROBE ID	G/M3	U	G/M3	U	/CC	NT RCT	ALP	LAM AC	EFF	REMARKS
141	5864	19 165420	40	100	15	-99	65.0	100.0	2.41	20	2	2	1.37	FSSP	1	.17	13	400	43	5.0	730	2	PROBE OUT OF SPEC
142	5864	19 1659 5	40	100	15	-99	64.0	69.0	.91	10	10	11	.67	FSSP	1	.04	7	424	46	7.1	1510	2	PROBE OUT OF SPEC
143	5864	19 170520	40	100	15	-99	41.0	58.0	1.68	20	0	4	1.37	FSSP	1	.01	4	332	36	18.9	5404	2	PROBE OUT OF SPEC JM INACTIVE
144	5864	19 1711 5	60	100	15	-99	26.0	42.0	1.63	25	4	6	1.34	FSSP	1	.01	5	368	39	7.7	2185	21	PROBE OUT OF SPEC
145	5864	19 171915	35	285	17	-99	36.0	76.0	.90	18	2	3	1.02	FSSP	1	.01	7	121	37	5.2	1382	2	PROBE OUT OF SPEC
146	5864	19 172845	30	270	16	-99	36.0	73.0	.92	18	2	5	1.10	FSSP	1	.01	7	135	39	5.5	1501	13	PROBE OUT OF SPEC

IRT TEST POINT SUMMARY
JANUARY 1981

TAPE 11

TEST PT	RUN DA	TIME	DI TAS	TEM	RH	PAIR	PH20	T-D	DV	J=0	L=0	PROBE ID	G/M3	U	/CC	DV	NT	RCT	ALP	LAM	AC	EFF	REMARKS	
159	5864 19	195530	20	200	7	-99	50.0	75.0	1.02	16	1.17	1.12	FSSP 1	.01	7	179	38	6.3	1629				PROBE OUT OF SPEC	
160	5864 19	2002 0	30	150	7	75	42.5	56.0	1.00	16	-.08	-.02	FSSP 1	.00	4	19	3105	29971					PROBE OUT OF SPEC	
161	5864 19	200645	30	100	7	-99	32.0	39.0	1.08	16	.90	1.03	FSSP 1	.01	4	259	2A15	.7	4448				PROBE OUT OF SPEC	
162	5864 19	203030	40	285	-11	-99	50.0	90.0	.90	15	.86	.79	FSSP 1	.03	13	126	39	3.1	555				PROBE OUT OF SPEC	
163	5864 19	203355	25	270	-8	-99	50.0	90.0	.95	16	.87	.87	FSSP 1	.03	13	150	44	3.2	603				PROBE OUT OF SPEC	
164	5864 19	203710	40	260	-9	-99	50.0	90.0	.99	16	.64	.89	FSSP 1	.04	13	159	45	3.1	556				PROBE OUT OF SPEC	
165	5864 19	203925	20	250	-11	-99	50.0	90.0	1.03	17	1.15	1.02	FSSP 1	.11	4	157	42	3.1	551				PROBE OUT OF SPEC	
166	5864 19	205140	40	240	-11	-99	50.0	90.0	1.07	17	.95	1.02	FSSP 1	.02	12	151	39	3.3	687				PROBE OUT OF SPEC	
167	5864 19	205415	25	230	-11	-99	50.0	90.0	1.12	18	1.11	1.08	FSSP 1	0.00	0	0	0	0	0	0				PROBE OUT OF SPEC
168	5864 19	2056 0	20	220	-11	-99	50.0	90.0	1.17	18	1.13	1.16	FSSP 1	0.00	0	0	0	0	0	0				PROBE OUT OF SPEC
169	5864 19	2058 0	25	200	-11	-99	50.0	90.0	1.29	19	1.20	1.24	FSSP 1	0.00	0	0	0	0	0	0				PROBE OUT OF SPEC
170	5864 19	210935	25	150	-11	-99	50.0	90.0	1.72	21	1.20	1.75	FSSP 1	0.00	0	0	0	0	0	0				PROBE OUT OF SPEC

IRT TEST POINT SUMMARY
JANUARY 1981

TAPE 13

PAGE 1

TEST PT	RUN ID	DA	TIME	DT LST	TAS MPH	F	TEM	RH	PAIR	PH20	T-U	DV	J-D	L-Q	PROBE ID	G/M3	U	CC	PROBE / CV(X)	ALP	LAM	AC	EFF	REMARKS		
177	5665	20	212830	60	235	16	-99	35.0	57.0	.81	17	-.88	0	1	ASSP	4	.07	18	82	53	3.5	424	0	100	PROBE OUT OF SPEC JW INACTIVE	
178	5665	20	213540	25	235	16	-99	24.0	75.0	1.24	29	-.88	0	4	FSSP	1	.02	14	121	31	2.7	603	0	0	PROBE OUT OF SPEC JW INACTIVE	
179	5665	20	220035	30	235	16	-99	24.0	75.0	1.24	29	-.88	0	2	FSSP	1	.01	12	115	29	2.9	649	0	100	PROBE OUT OF SPEC JW INACTIVE	
180	5665	20	230050	30	228	-11	-99	21.0	31.0	.56	17	-.88	0	1	FSSP	1	.02	11	191	47	3.2	719	0	100	PROBE OUT OF SPEC JW INACTIVE	
181	5665	20	233555	40	228	-11	-99	30.0	46.0	.71	17	-.88	0	1	FSSP	1	.03	13	195	48	2.9	615	0	100	PROBE OUT OF SPEC JW INACTIVE	
182	5665	20	235755	35	228	-11	-99	46.0	78.0	1.01	17	-.88	0	2	FSSP	1	.07	15	191	47	2.9	480	0	100	PROBE OUT OF SPEC JW INACTIVE	
183	5665	20	25	0	40	228	-11	-99	46.0	78.0	1.01	17	-.88	0	4	FSSP	1	.07	15	193	47	2.9	470	0	100	PROBE OUT OF SPEC JW INACTIVE
184	5665	20	4725	30	228	-11	-99	21.0	31.0	.56	17	-.88	0	6	FSSP	1	.03	14	194	48	2.8	556	0	100	PROBE OUT OF SPEC JW INACTIVE	
185	5665	20	10655	30	228	-11	-99	23.0	69.0	1.21	29	-.88	0	7	FSSP	1	.16	25	170	42	2.1	259	0	100	PROBE OUT OF SPEC JW INACTIVE	

IRT TEST POINT SUMMARY
JANUARY 1981

TAPE 14

TEST PT	RUN DA	TIME	DT LST	TAS MPH	F	DTAS	TEM	RH	PAIR	PH20	T-Q	DV	J=0	L=0	PROBE	Q	DV	NT	RCT	ALP	LAM	AC	EFF	REMARKS	
	ID		SEC	G/M3	PSIG	G/M3	U	G/M3	U	G/M3	U	G/M3	U	G/M3	U	G/M3	U	G/M3	U	G/M3	U	G/M3	U	%	%
186	5866	21	1656	0	45	100	54	59	32.0	39.0	1.08	16	-.88	0	FSSP	1	.17	13	554	60	4.0	653			PROBE OUT OF SPEC JW INACTIVE
187	5866	21	170020	30	150	53	54	43.0	56.0	.98	15	.58	-.00	7	FSSP	1	.14	14	266	43	4.1	554			LEIGH INACTIVE PROBE OUT OF SPEC
188	5866	21	170350	30	200	56	59	50.0	75.0	1.02	16	.75	-.00	15	FSSP	1	.11	15	252	54	3.4	502			LEIGH INACTIVE PROBE OUT OF SPEC
189	5866	21	170630	30	220	58	73	36.0	62.0	.94	19	.61	-.00	11	FSSP	1	.08	16	228	54	2.7	441			LEIGH INACTIVE PROBE OUT OF SPEC
190	5866	21	170935	30	250	60	78	53.0	91.0	1.00	16	.71	-.00	15	FSSP	1	.08	16	205	55	2.8	447			LEIGH INACTIVE PROBE OUT OF SPEC
191	5866	21	171155	35	260	62	105	36.0	70.0	.91	18	.49	-.00	13	FSSP	1	.04	15	157	44	2.6	479			LEIGH INACTIVE PROBE OUT OF SPEC
192	5866	21	171425	25	285	68	69	36.0	76.0	.90	18	.41	-.00	9	FSSP	1	.02	14	112	34	2.7	538			LEIGH INACTIVE PROBE OUT OF SPEC
193	5866	21	174740	30	235	16	61	20.0	30.0	.55	17	.73	.66	8	FSSP	1	.17	20	167	42	3.3	376			LEIGH INACTIVE PROBE OUT OF SPEC
194	5866	21	175040	40	235	16	55	35.0	57.0	.81	17	-.34	-.68	88	FSSP	1	.12	20	174	44	2.4	332			PROBE OUT OF SPEC JW INTERMITTENT
195	5866	21	175235	30	235	16	49	35.0	57.0	.81	17	-.88	.84	0	FSSP	1	.05	23	30	20	3.6	347			LEIGH INTERMITTENT PROBE OUT OF SPEC JW INACTIVE
196	5866	21	180535	30	235	16	64	24.0	75.0	1.24	29	1.38	1.29	3	FSSP	1	.25	24	149	38	3.0	292			PROBE OUT OF SPEC
197	5866	21	182350	30	100	15	69	32.0	39.0	1.08	16	.97	1.13	6	FSSP	1	.50	19	345	37	4.8	459			PROBE OUT OF SPEC

IRT TEST POINT SUMMARY
JANUARY 1981

TAPE 14

TEST PT	RUN DA	TIME	DT	TAS	TEM	RH	PAIR	PH2O	T-Q	DV	J-Q	L-Q	PROBE ID	G/M3	U	/CC	PROBE / CV(X)	ALP	LAM	AC	EFF	REMARKS	
198	5866	21 183045	40	150	15	76	43.0	56.0	.98	15	.80	1.14	FSSP 1	.21	18	168	27	5.0	501			PROBE OUT OF SPEC	
													ASSP 4	.12	18	88	36	5.6	532			0 100	
																						0 0	PROBE OUT OF SPEC
199	5866	21 183510	30	200	15	92	50.0	75.0	1.02	16	1.27	1.11	FSSP 1	.22	19	141	30	5.2	470			PROBE OUT OF SPEC	
													ASSP 4	.09	17	76	42	5.2	518			0 100	
																						0 0	PROBE OUT OF SPEC
200	5866	21 183930	30	220	16	92	36.0	62.0	.94	19	1.28	1.08	FSSP 1	.21	20	149	35	3.9	394			PROBE OUT OF SPEC	
													ASSP 4	.12	22	68	41	4.0	363			0 100	
																						0 0	PROBE OUT OF SPEC
201	5866	21 184225	30	250	16	79	53.0	91.0	1.00	16	1.29	1.11	FSSP 1	.16	20	111	30	3.8	382			PROBE OUT OF SPEC	
													ASSP 4	.10	20	48	33	7.0	537			0 100	
																						0 0	PROBE OUT OF SPEC
202	5866	21 185510	40	260	16	77	36.0	70.0	.91	18	1.12	1.00	FSSP 1	.20	22	132	37	3.3	331			PROBE OUT OF SPEC	
													ASSP 4	.12	2	8	8	4	3			0 100	
																						0 0	PROBE OUT OF SPEC
203	5866	21 185835	30	285	16	76	36.0	76.0	.90	18	1.19	1.02	FSSP 1	.16	22	112	34	3.1	323			PROBE OUT OF SPEC	
													ASSP 4	.11	23	39	30	5.9	424			0 100	
																						0 0	PROBE OUT OF SPEC
204	5866	21 1913	5	540	200	16	71	50.0	.64	12	.80	.75	FSSP 1	.10	15	125	27	5.5	610			PROBE OUT OF SPEC	
													ASSP 4	.04	13	60	33	6.3	750			0 100	
																						0 0	PROBE OUT OF SPEC
205	5866	21 192935	360	200	16	65	50.0	75.0	1.02	16	1.21	1.11	FSSP 1	.20	19	135	29	5.0	469			PROBE OUT OF SPEC	
													ASSP 4	.22	5	26	26	11	10			0 100	
																						0 0	PROBE OUT OF SPEC
206	5866	21 194640	60	200	16	-99	30.0	55.0	1.02	21	1.15	1.09	FSSP 1	.04	18	62	13	3.2	422			PROBE OUT OF SPEC	
													ASSP 4	.15	29	63	35	3.1	263			0 100	
																						0 0	PROBE OUT OF SPEC
207	5866	21 202425	60	200	16	-99	30.0	55.0	1.02	21	1.21	1.15	FSSP 1	0.00	0	0	0	0	0			PROBE OUT OF SPEC	
													ASSP 4	.16	25	68	37	3.8	312			0 100	
																						0 0	PROBE OUT OF SPEC
208	5866	21 2039	0	300	200	16	-99	50.0	.64	12	.98	.79	FSSP 1	.00	4	0	0	0	0			PROBE OUT OF SPEC	
													ASSP 4	.02	13	43	23	6.8	835			0 100	
																						0 0	PROBE OUT OF SPEC
209	5866	21 205815	120	200	16	-99	50.0	75.0	1.02	16	1.27	1.17	FSSP 1	.00	4	1	0	0	0			PROBE OUT OF SPEC	
													ASSP 4	.07	17	64	35	5.7	564			0 100	
																						0 0	PROBE OUT OF SPEC

IRT TEST POINT SUMMARY
JUNE 1981

TAPE 15

TEST PT	RUN DA	TIME	DT	TAS	TEM	RH	PAIR	PH20	T-Q	DV	J-Q	L-R	PROHE	Q	ID	G/M3	U	G/M3	U	CC	DV	NT	RCT	ALP	LAM	AC	EFF	REMARKS
210	5931	8 181025	55	150	29	-99	42.5	56.0	1.00	16	.71	-.88	FSSP	1	.71	0	.71	0	.71	22	356	62	4.3	373	93	52	LEIGH INACTIVE	
211	5931	8 184110	40	150	23	-99	42.5	56.0	1.00	16	.77	-.88	FSSP	1	.82	5	.82	5	.82	22	385	68	4.2	358	92	53	LEIGH INACTIVE	
212	5931	8 191920	50	150	-8	-99	42.5	56.0	1.00	16	.77	-.88	FSSP	1	.78	6	.78	6	.78	22	390	69	4.0	350	91	53	LEIGH INACTIVE	
213	5931	8 1936 0	30	150	-4	-99	42.5	56.0	1.00	16	.80	-.88	FSSP	1	.77	5	.77	5	.77	22	408	73	3.9	355	90	54	LEIGH INACTIVE	
214	5931	8 201945	30	150	-4	-99	42.5	56.0	1.00	16	.83	-.88	FSSP	1	.76	6	.76	6	.76	22	404	72	3.9	350	90	53	LEIGH INACTIVE	
215	5931	8 211010	40	150	-3	-99	42.5	56.0	1.00	16	.77	-.88	FSSP	1	.73	6	.73	6	.73	22	411	74	4.0	364	90	54	LEIGH INACTIVE	
216	5931	8 213625	30	150	-4	-99	42.5	56.0	1.00	16	.75	-.88	FSSP	1	.72	7	.72	7	.72	22	408	74	4.0	368	90	54	LEIGH INACTIVE	
217	5931	8 221410	30	150	29	-99	42.5	56.0	1.00	16	.87	-.88	FSSP	1	.81	5	.81	5	.81	22	1042	93	5.3	423	80	20	LEIGH INACTIVE	